


Phylogeny of *Riama* (Squamata: Gymnophthalmidae), impact of phenotypic evidence on molecular datasets, and the origin of the Sierra Nevada de Santa Marta endemic fauna

Santiago J. Sánchez-Pacheco^{a,b,c,*} , Omar Torres-Carvajal^d, Vanessa Aguirre-Peñafliel^d, Pedro M. Sales Nunes^{e,f}, Laura Verrastro^c, Gilson A. Rivas^g, Miguel T. Rodrigues^e, Taran Grant^e and Robert W. Murphy^{a,b}

^aDepartment of Ecology and Evolutionary Biology, University of Toronto, 25 Willcocks Street, Toronto, ON M5S 3B2, Canada; ^bDepartment of Natural History, Royal Ontario Museum, 100 Queen's Park, Toronto, ON M5S 2C6, Canada; ^cLaboratorio de Herpetologia, Departamento de Zoologia, Instituto de Biociências, Universidade Federal do Rio Grande do Sul, Av. Bento Gonçalves 9500, Porto Alegre, RS 91540-000, Brazil; ^dMuseo de Zoología, Escuela de Biología, Pontificia Universidad Católica del Ecuador, Av. 12 de Octubre y Roca apartado 17-01-2184, Quito, Ecuador; ^eDepartamento de Zoologia, Instituto de Biociências, Universidade de São Paulo, São Paulo, SP, Brazil; ^fDepartamento de Zoologia, Centro de Biociências, Universidade Federal de Pernambuco, Av. Professor Moraes Rego S/n, Cidade Universitaria 50670-901, Recife, PE, Brazil; ^gMuseo de Biología, Facultad Experimental de Ciencias, Universidad del Zulia, Apartado Postal 526, Maracaibo, 4011 Estado Zulia, Venezuela

Accepted 17 March 2017

Abstract

Riama is the most speciose genus of the Neotropical lizard family Gymnophthalmidae. Its more than 30 montane species occur throughout the northern Andes, the Cordillera de la Costa (CC) in Venezuela, and Trinidad. We present the most comprehensive phylogenetic analysis of *Riama* to date based on a total evidence (TE) approach and direct optimization of molecular and morphological evidence. Analyses use DNA sequences from four loci and 35 phenotypic characters. The dataset consists of 55 ingroup terminals representing 25 of the 30 currently recognized species of *Riama* plus five undescribed taxa, including an endemic species from the Sierra Nevada de Santa Marta (SNSM) in Colombia, and 66 outgroup terminals of 47 species. Analysis results in a well-supported hypothesis in which *Riama* is polyphyletic, with its species falling into three clades. The Tepuian *Anadia mediamidi* nests within one clade of *Riama*, and the recently resurrected *Pantodactylus* nests within *Cercosaura*. Accordingly, we propose a monophyletic taxonomy that reflects historical relationships. Analysis of character evolution indicates that the presence/absence of prefrontals—a cornerstone of the early genus-level taxonomy of cercosaurines—is optimally explained as having been plesiomorphically present in the most recent common ancestor of Cercosaurinae and lost in that of the immediately less inclusive clade. Multiple independent reversals to present and subsequent returns to absent occur within this clade. To evaluate the impact of phenotypic evidence on our results, we compare our TE results with results obtained from analyses using only molecular data. Although phenotypic evidence comprises only 1.2% of the TE matrix, its inclusion alters both the topology and support values of the clades that do not differ. Finally, current phylogenetic evidence reveals a SNSM–CC–Trinidad–tepuis biogeographical link. We hypothesize that an ancient connection facilitated the exchange of species between the SNSM and the CC.

© The Willi Hennig Society 2017.

Introduction

Gymnophthalmidae Fitzinger, 1826 is a species-rich family of small to medium Neotropical lizards. With

236 named species divided into 46 genera (Uetz and Hošek, 2017) and distributed throughout South America (with relatively few representatives in Middle America), Gymnophthalmidae is one of the most important components of the lizard fauna in the Neotropics. Although multiple molecular-based phylogenetic analyses in the 21st Century have led to great

*Corresponding author.

E-mail address: santiago.sanchezpacheco@mail.utoronto.ca

improvement in gymnophthalmid systematics (e.g. Pelleggrino et al., 2001; Castoe et al., 2004; Pyron et al., 2013; Colli et al., 2015; Kok, 2015; Goicoechea et al., 2016), much of the current genus-level taxonomy still relies on early phenetic clusterings. This is particularly true for the Cercosaurinae Gray, 1838¹, which holds for over 50% of gymnophthalmid diversity. Despite considerable progress in unravelling the phylogenetic relationships of cercosaurines (e.g. Torres-Carvajal et al., 2016), compelling evidence for the monophyly of some genera is lacking. Many species were never included in phylogenetic analyses, and, thus, their placement in one genus or another is based mainly on overall similarity. The questionable generic placement of some species (e.g. based on geographical proximity) and the lack of rigorous tests of monophyly of genera exacerbate the problem.

This study focuses on *Riama* Gray, 1858 (Cercosaurinae). With 30 recognized species, it is by far the largest genus of gymnophthalmids and additional species are awaiting description (S.J.S-P. pers. obs.; present study). Although the molecular studies by Castoe et al. (2004; see also Doan and Castoe, 2005), Aguirre-Peñafiel et al. (2014) and Torres-Carvajal et al. (2016) advanced understanding of the phylogeny of *Riama*, the current delimitation of this genus is suspect. As recognized by Doan and Castoe (2005), Castoe et al. (2004) sampled five of the 24 species of *Riama* only. Torres-Carvajal et al. (2016) added seven species and analyses nested one of them within *Proctoporus* Tschudi, 1845 s.s. Thus, neither the monophyly of *Riama* nor the relationships within the genus have been tested rigorously. Furthermore, the trees from Castoe et al. (2004) and subsequent authors differ from the morphological assessment of Doan (2003a), which was limited to pholidosis. Finally, all nominal and undescribed species of *Riama* have narrow, montane ranges with strikingly disjunct distributions. Most species occur along the tropical Andes from 1100 to 3340 m above sea level (a.s.l.) and expansive geographical barriers (e.g. depressions) separate them from species occurring from 650 to 2165 m a.s.l. on the Cordillera de la Costa in Venezuela, the Sierra Nevada de Santa Marta (SNSM) in Colombia, and northern Trinidad. Thus, we test the monophyly of *Riama* and explore the phylogenetic relationships among its species. Our phylogenetic analysis of cercosaurine lizards uses nuclear and mitochondrial DNA sequences as well as morphological data. Furthermore, the high degree of endemism of *Riama* species offers an exceptional opportunity to test historical biogeographical hypotheses involving different Neotropical montane

regions. Accordingly, analyses test hypotheses on the origin of the montane SNSM endemic vertebrate fauna. Phylogenetic analyses also explore the evolution of prefrontal scales in Cercosaurinae—a cornerstone of the early genus-level taxonomy of this group (see below)—as well as the relationships of *Cercosaura* Wagler, 1830, *Pantodactylus* Dumeril and Bibron, 1839 and *Proctoporus*.

Impact of phenotypic evidence on molecular datasets

Technological advances in DNA sequencing and molecular phylogenetics facilitate analyses based on genotypic evidence. In contrast, analyses of phenotypic evidence suffer stagnation due to (i) the ease of obtaining large molecular datasets and (ii) the time-consuming coding of morphological characters requiring expertise with a group of organisms and yielding far fewer characters than molecular procedures for analysis (de Sá et al., 2014). Furthermore, given the relative sizes of the phenotypic and genotypic matrices (tens or hundreds of characters vs. thousands of sites, respectively), the notoriously disproportional quantity of molecular data may overwhelm phenotypic data in total evidence (TE) analyses (Kluge, 1983). To test this prediction, we explore the impact of a modest morphological dataset on an analysis dominated by a larger DNA sequence matrix, a phenomenon that has received recent attention (e.g. de Sá et al., 2014; Mirande, 2016).

Systematics background

External head morphology has played an important role in the systematics of Cercosaurinae. For example, some cercosaurine genera were traditionally grouped by the presence or absence of prefrontal scales. However, compelling phylogenetic evidence for that grouping is lacking, because molecular-based phylogenetic analyses (e.g. Castoe et al., 2004; Goicoechea et al., 2012) have shown that these genera do not correspond to monophyletic groups.

The former *Proctoporus* s.l. (i.e. *Petracola* + *Proctoporus* + *Riama*) and several of its traditionally assumed relatives (e.g. *Euspondylus* and *Opipheuter xestus*) exemplify this scenario. The absence of prefrontals served to diagnose *Proctoporus* s.l. (e.g. Peters and Donoso-Barros, 1970), which represents the model case of presumably monophyletic groups in the Cercosaurinae. In contrast, Kizirian and Coloma (1991) and Kizirian (1995, 1996) questioned the monophyly of *Proctoporus* s.l. Doan (2003a) resolved *Proctoporus* s.l. as a monophyletic group based on external morphology, but DNA analysis of Gymnophthalmidae by Castoe et al. (2004) supported Kizirian's view. Their molecular analyses resolved a

¹We follow Torres-Carvajal et al.'s (2016) delimitation of Cercosaurinae, which corresponds to Cercosaurini in the sense of Goicoechea et al. (2016).

polyphyletic *Proctoporus* s.l., and depicted scattered distributions of the absence and presence of prefrontals in the Cercosaurinae. Subsequently, Doan and Castoe (2005) split *Proctoporus* s.l. into three genera. First, *Proctoporus* s.s. held species from the Andes of southern Peru and Bolivia. It contained the type species, *Proctoporus pachyurus*, and its relatives (i.e. the *Proctoporus pachyurus* group sensu Uzzell, 1970). Second, *Petracola* Doan and Castoe, 2005 hosted species from the Andes of central and northern Peru. It included the *Proctoporus ventrimaculatus* group (sensu Uzzell, 1970) plus one species. Finally, *Riama* was resurrected for the remaining 24 species from the Andes of Peru, Ecuador, Colombia and Venezuela, the Cordillera de la Costa in Venezuela, and Trinidad. Subsequently, many new species were referred to *Proctoporus* s.s. (Doan et al., 2005; Goicoechea et al., 2013; Mamani et al., 2015), *Petracola* (Kizirian et al., 2008; Echevarría and Venegas, 2015) and *Riama* (Rivas et al., 2005; Arredondo and Sánchez-Pacheco, 2010; Sánchez-Pacheco, 2010a; Sánchez-Pacheco et al., 2011, 2012; Aguirre-Peñafiel et al., 2014). In their phylogenetic study of *Proctoporus* s.s., Goicoechea et al. (2012) transferred into *Proctoporus* two species of *Euspondylus* Tschudi, 1845, a genus whose monophyly had also been questioned (Köhler and Lehr, 2004), and the monotypic genus *Opipeuter* Uzzell, 1969, which have prefrontals. Similarly, in their recent phylogenetic analysis of Cercosaurinae, Torres-Carvajal et al. (2016) transferred three additional species of *Euspondylus*, as well as *R. laudahnae*, into *Proctoporus*.

Kizirian (1996) and Doan and Castoe (2005) provided a detailed systematic documentation of the diversity of *Riama*. Subsequently, most taxonomic activity on *Riama* has consisted of species descriptions (but see Torres-Carvajal et al., 2016).

Materials and methods

Taxon sampling

Taxa were selected based on availability of tissues (or DNA sequences in GenBank) and specimens for morphological study. The former criterion was considered for exclusion and in the absence of the latter, character states were retrieved from the literature. When multiple terminals for a given taxon were available, we chose those for which the greatest number of gene sequences were available, first, and the greatest length of gene sequences, second. Based on published and preliminary analyses, we selected divergent terminals in order to maximize intraspecific variation. When possible, we used two terminals per species.

The ingroup included 55 terminals representing 25 of the 30 (> 80%) currently recognized species of *Riama* plus five undescribed taxa from Colombia and Venezuela. Our sampling added 19 species to the 11 species (*R. anatoloros*, *R. balneator*, *R. cashcaensis*, *R. colomarmarani*, *R. labionis*, *R. meleagris*, *R. orcesi*, *R. simotera*, *R. stigmatoral*, *R. unicolor* and *R. yumborum*) included by Torres-Carvajal et al. (2016) as follows: *R. achlyens*, *R. afrania*, *R. aurea*, *R. columbiana*, *R. “Cordillera Central”*, *R. “Cordillera Occidental”*, *R. crypta*, *R. hyposticta*, *R. kizirianii*, *R. laevis*, *R. “Nariño”*, *R. oculata*, *R. raneyi*, *R. shrevei*, *R. “Sierra Nevada”*, *R. striata*, *R. “Venezuela”*, *R. vespertina* and *R. vieta*. Tissues for DNA extraction were not available for *R. inanis*, *R. luctuosa*, *R. petrurum*, *R. rhodogaster* and *R. stellae*.

In order to test the monophyly of *Riama*, and due to the uncertain phylogenetic affinities of most species of *Riama*, our outgroup sampling was largely drawn from the subfamily Cercosaurinae, as delimited by Torres-Carvajal et al. (2016). The outgroup included 38 species representing 11 of the remaining 13 nominal cercosaurine genera (*Anadia* Gray, 1845, *Cercosaura*, *Echinosaura* Boulenger, 1890, *Macropholidus* Noble, 1921, *Neusticurus* Duméril and Bibron, 1839, *Pantodactylus*, *Petracola*, *Pholidobolus* Peters, 1862; *Placosoma* Tschudi, 1847, *Potamites* Doan and Castoe, 2005; and *Proctoporus*). Our analyses did not include the recently erected *Gelanesaurus* Torres-Carvajal et al., 2016; and *Euspondylus*, for which no tissues were available. The secondary outgroup included representatives of the following taxa: Alopoglossidae Goicoechea et al., 2016 (*Ptychoglossus brevifrontalis*), which forms the sister taxon of Teiidae + Gymnophthalmidae (Goicoechea et al., 2016); Teiidae Gray, 1827 (*Ameivula ocellifera* and *Kentropyx calcarata*), the sister group of Gymnophthalmidae (Goicoechea et al., 2016). The outgroup also contained the following gymnophthalmid subfamilies: Bachiinae Colli et al., 2015 (*Bachia flavescens*), or Bachiini in the sense of Goicoechea et al. (2016); Ecpleopodinae Fitzinger, 1843 (*Ecpleopus gaudichaudii*), or Ecpleopodini in the sense of Goicoechea et al. (2016); Gymnophthalminae Fitzinger, 1826 (*Gymnophthalmus vanzoi*); Rachisaurinae Pellegrino et al., 2001 (*Rachisaurus brachylepis*); and Riolaminae Kok, 2015 (*Riolama leucosticta*). In total, the outgroup included 47 species. *Ptychoglossus brevifrontalis* was designated as the root for all analyses. Recent progress in understanding the diversification of cercosaurines led to correcting the identities of two terminals. KU 212687, *Proctoporus* cf. *ventrimaculatus* of Castoe et al. (2004) was included in the type series of *Petracola waka* (Kizirian et al., 2008). Similarly, ROM 22892, referred to as “*Neusticurus* sp. Guyana” by Fu (2000), was included as a paratype in the original description of *Echinosaura sulcarostrum*

(Donnelly et al., 2006). As suggested by Castoe et al. (2004: appendix 2), we swapped the 12S and 16S sequences of *Potamites juruazensis* (GenBank accession numbers AF420758, AF420704, respectively) with those of *Ptychoglossus brevifrontalis* (AF420757, AF420697).

Genotypic evidence

Most published molecular analyses of gymnophthalmid relationships used DNA sequences from four loci: nuclear DNA (nDNA) oocyte maturation factor gene (*C-mos*), mitochondrial DNA (mtDNA) NADH dehydrogenase subunit IV (ND4), and mitochondrial rRNA subunits 12S and 16S. Therefore, we sampled the same fragments obtaining up to 374, 860, 400 and 515 bp, respectively. Primers and their sources are provided in Table 1. We analysed a total of 2149 bp of sequences. Novel sequences were deposited in GenBank. Our own data were augmented with sequences in GenBank from Fu (2000), Pellegrino et al. (2001), Castoe et al. (2004), Goicoechea et al. (2012), Kok et al. (2012), Torres-Carvajal and Mafía-Endara (2013), Aguirre-Peñafiel et al. (2014), Kok (2015) and Torres-Carvajal et al. (2016). Voucher specimens and GenBank accession numbers are listed in Table 2.

DNA isolation, sequencing, and editing. Total genomic DNA was extracted from frozen and ethanol-preserved liver or muscle tissues using either

the DNeasy kit (Qiagen, Valencia, CA, USA), following the manufacturer's guidelines, or a guanidinium isothiocyanate protocol. Amplification of fragments of *C-mos*, ND4, 12S and 16S was performed with 25-μL final reactions. Negative controls were run on all amplifications to check for contamination. Primers and PCR conditions are detailed in Table 1. Double-stranded PCR-amplified segments were cleaned and then sequenced in both directions using standard protocols and conventional Sanger sequencers. Novel sequences constituted a consensus of both DNA strands. Sequences were visualized, assembled and edited using Geneious v.6.1.8 (<http://www.geneious.com>, Kearse et al., 2012).

Morphological evidence

Phenotypic character sampling targeted variation among cercosaurines. Thirty-five characters were scored, including 25 derived from external morphology (scutellation) and 10 from hemipenial anatomy (Appendix 1). Other sources of variation, such as osteology and myology, have been examined in too few cercosaurine taxa in general, and in too few *Riama* species in particular, to have allowed for their inclusion (e.g. see Montero et al., 2002). Twenty-seven characters were binary and the remaining eight multi-state characters were treated as nonadditive (Appendix 1). Characters 10, 13, 14, 20, 21, 28, 30, 31 and all hemipenial characters (0–9) have not been

Table 1
List of PCR and sequencing primers used in this study, and a summary of the PCR conditions

Gene region	Primer Name	Sequence (5'–3')	Source	PCR protocol
12S	12S1L	CAAACCTGGGATTAGATACCCCACTAT	Kocher et al. (1989)	1 cycle: 3 min 94 °C 33 cycles: 30 s 92 °C, 30 s 57 °C, 1:50 min 72 °C
	12S2H	AGGGTGACGGGCGGTGTGT		
16S	16SF.0	CTGTTTACCAAAAACATMRCCTYTAGC	Pellegrino et al. (2001) Whiting et al. (2003) Harris et al. (1998)	1 cycle: 10 min 72 °C 1 cycle: 3 min 96 °C 40 cycles: 30 s 95 °C, 1 min 51 °C, 1 min 72 °C 1 cycle: 10 min 72 °C
	16SR.0	TAGATAGAAACCGACCTGGATT		
	16SL	CGCCTGTTTAAACAAAACAT		
	16SH	CCGGTCTGAACTCAGATCACGT		
ND4	ND4L	CACCTATGACTACCAAAAGCTCATGTAGAAGC	Arévalo et al. (1994)	1 cycle: 3 min 94 °C 33 cycles: 30 s 92 °C, 30 s 57 °C, 1:50 min 72 °C 1 cycle: 10 min 72 °C
	Leu	CATTACTTTTACTTGGATTTCACCA		
<i>C-mos</i>	G73	GCGGTAAAGCAGGTGAAGAAA	Saint et al. (1998)	1 cycle: 10 min 72 °C 1 cycle: 3 min 96 °C 40 cycles: 30 s 95 °C, 1 min 52 °C, 1 min 72 °C 1 cycle: 10 min 72 °C
	G74	TGAGCATCCAAAGTCTCCAATC		
				1 cycle: 3 min 96 °C 35 cycles: 25 s 95 °C, 1 min 52 °C, 2 min 72 °C 1 cycle: 10 min 72 °C

Table 2

GenBank accession numbers for loci and terminals sampled in this study. Asterisks indicate new sequences obtained for this study. Species are listed following the new taxonomy proposed herein. Numbers and letters following species names are identifiers of conspecific terminals. See Materials and Methods for institutional abbreviations

Terminal ID	Voucher	C-mos	12S	16S	ND4
<i>Ameivula ocellifera</i>	MRT 946089	AF420862	AF420706	AF420759	AF420914
<i>Anadia rhombifera</i> 1	QCAZ 11061	KU902052	KU902133	KU902214	KU902289
<i>Anadia rhombifera</i> 2	QCAZ 11862	KU902053	KU902135	KU902216	KU902291
<i>Andinosaura afrania</i> 1	RH	–	KY670680*	KY681098*	–
<i>Andinosaura afrania</i> 2	RM	–	KY670681*	KY681099*	–
<i>Andinosaura aurea</i> 1	QCAZ 9649	KY670647*	KY670682*	KY681100*	KY710831*
<i>Andinosaura aurea</i> 2	QCAZ 9650	KY670648*	KY670683*	KY681101*	KY710832*
<i>Andinosaura crypta</i> 1	QCAZ 10455	KY670649*	KY670684*	KY681102*	KY710833*
<i>Andinosaura crypta</i> 2	QCAZ 6154	KY670650*	KY670685*	KY681103*	KY710834*
<i>Andinosaura hyposticta</i> 1	PSO-CZ 085	–	KY670686*	KY681104*	–
<i>Andinosaura hyposticta</i> 2	DHMECN 1360	KY670651*	KY670687*	KY681105*	–
<i>Andinosaura kiziriani</i> 1	QCAZ 9607	KY670652*	KY670688*	KY681106*	KY710835*
<i>Andinosaura kiziriani</i> 2	QCAZ 9667	KY670653*	KY670689*	KY681107*	KY710836*
<i>Andinosaura laevis</i>	WB 1330	KY670654*	KY670690*	KY681108*	KY799165*
<i>Andinosaura oculata</i> 1	QCAZ 10410	KY670655*	KY670691*	KY681109*	KY710837*
<i>Andinosaura oculata</i> 2	QCAZ 5474	KY670656*	KY670692*	KY681110*	KY710838*
<i>Andinosaura vespertina</i> 1	QCAZ 10286	KY670657*	KY670693*	KY681111*	KY710839*
<i>Andinosaura vespertina</i> 2	QCAZ 10306	KY670658*	KY670694*	KY681112*	KY710840*
<i>Andinosaura vieta</i> 1	QCAZ 10456	KY670659*	KY670695*	KY681113*	KY710841*
<i>Andinosaura vieta</i> 2	QCAZ 5287	KY670660*	KY670696*	KY681114*	KY710842*
<i>Bachia flavescens</i>	LSUMZ H12977	AF420859	AF420705	AF420753	AF420869
<i>Cercosaura argula</i>	LSUMZ H12591	AF420838	AF420698	AF420751	AF420896
<i>Cercosaura eigenmanni</i>	MRT 976979	AF420828	AF420690	AF420728	AF420895
<i>Cercosaura ocellata</i>	MRT 977406	AF420834	AF420677	AF420731	AF420883
<i>Cercosaura oshaughnessyi</i>	LSUMZ H13584	AF420852	AF420696	AF420750	AF420893
<i>Cercosaura quadrilineata</i>	LG 936	AF420830	AF420672	AF420717	–
<i>Cercosaura schreibersii</i> 1	LG 1168	AF420856	AF420650	AF420729	AF420882
<i>Cercosaura schreibersii</i> 2	LG 927	AF420817	AF420686	AF420749	AF420911
<i>Echinosaura sulcarostrum</i>	ROM 22892	–	AF206584	AF206584	–
<i>Ecpleopus gaudichaudii</i>	LG 1356	AF420855	AF420660	AF420738	AF420901
<i>Gymnophthalmus vanzoi</i>	MRT 946639	AF420827	AF420687	AF420743	AF420867
<i>Kentropyx calcarata</i>	MRT 978224	AF420864	AF420707	AF420760	AF420913
<i>Macropholidus annectens</i> 1	QCAZ 11120	–	KC894341	KC894355	KC894369
<i>Macropholidus annectens</i> 2	QCAZ 11121	–	KC894342	KC894356	KC894370
<i>Macropholidus huancabambae</i> 1	CORBIDI 10492	–	KC894343	KC894357	–
<i>Macropholidus huancabambae</i> 2	CORBIDI 10493	–	KC894344	KC894358	KC894372
<i>Macropholidus ruthveni</i>	CORBIDI 4281	–	KC894354	KC894368	KC894382
<i>Neusticurus bicarinatus</i>	MRT 968462	AF420816	AF420671	AF420708	–
<i>Neusticurus rudis</i>	MRT 926008	–	AF420689	AF420709	AF420905
<i>Oreosaurus achlyens</i>	ENS 11010	–	KY670697*	KY681115*	KY799160*
<i>Oreosaurus mediarmidi</i>	IRSNB 2674	KP283385	–	JQ742263	KP283392
<i>Oreosaurus</i> “Sierra Nevada”1	JJS 543	KY670661*	KY670698*	KY681116*	KY799163*
<i>Oreosaurus</i> “Sierra Nevada”2	JJS 548	KY670662*	KY670699*	KY681117*	KY799164*
<i>Oreosaurus shrevei</i>	UWIZM 2011.7	KY670663*	KY670700*	KY681118*	–
<i>Oreosaurus</i> “Venezuela”	GAR 5962	–	KY670701*	KY681119*	KY799161*
<i>Petracola ventrimaculata</i>	KU 219838	AY507910	AY507863	AY507883	AY507894
<i>Petracola waka</i>	KU 212687	AY507903	AY507864	AY507876	–
<i>Pholidobolus affinis</i> 1	QCAZ 9641	–	KC894348	KC894362	KC894376
<i>Pholidobolus affinis</i> 2	QCAZ 9900	–	KC894349	KC894363	KC894377
<i>Pholidobolus macbrydei</i> 1	KU 218406	AY507896	AY507848	AY507867	AY507886
<i>Pholidobolus macbrydei</i> 2	QCAZ 9914	–	KC894352	KC894366	KC894380
<i>Pholidobolus montium</i> 1	KU 196355	AF420820	AF420701	AF420756	AF420884
<i>Pholidobolus montium</i> 2	QCAZ 4051	–	KC894346	KC894360	KC894374
<i>Pholidobolus prefrontalis</i> 1	QCAZ 9908	–	KC894350	KC894364	KC894378
<i>Pholidobolus prefrontalis</i> 2	QCAZ 9951	–	KC894351	KC894365	KC894379
<i>Placosoma cordylinum</i>	LG 1006	AF420823	AF420673	AF420734	AF420879
<i>Placosoma glabellum</i>	LG 940	AF420833	AF420674	AF420742	AF420907
<i>Potamites ecpleopus</i>	MRT 0472	AF420829	AF420656	AF420748	AF420890
<i>Potamites juruazensis</i>	LSUMZ H13823	AF420857	AF420697	AF420757	AF420878
<i>Potamites strangulatus</i>	KU 212677	–	AY507847	AY507866	AY507885

Table 2
(Continued)

Terminal ID	Voucher	C-mos	12S	16S	ND4
<i>Proctoporus bolivianus</i> 1	MNCN 8989	JX436040	JX435940	JX435994	JX436071
<i>Proctoporus bolivianus</i> 2	MNCN 43679	JX436043	JX435943	JX435997	JX436069
<i>Proctoporus</i> cf. <i>bolivianus</i> Ca1a	UTA R-52945	–	AY968825	AY968832	AY968813
<i>Proctoporus</i> cf. <i>bolivianus</i> Ca1b	MHNC 5322	JX436045	JX435945	JX435988	–
<i>Proctoporus</i> cf. <i>bolivianus</i> Ca2	AMNH R-150695	–	AY968821	AY968828	AY968812
<i>Proctoporus carabaya</i> 1	MHNC 5428	JX436016	JX435912	JX435979	JX436083
<i>Proctoporus carabaya</i> 2	MHNC 5429	JX436019	JX435915	JX435982	JX436086
<i>Proctoporus chasqui</i> 1	MHNC 6771	JX436003	JX435887	JX435946	JX436051
<i>Proctoporus chasqui</i> 2	MNCN 44407	JX436004	JX435888	JX435947	JX436052
<i>Proctoporus guentheri</i> 1	UTA R-51515	AY507900	AY507849	AY507872	AY225185
<i>Proctoporus guentheri</i> 2	UTA R-51517	AY507901	AY507854	AY507873	AY225169
<i>Proctoporus iridescens</i> 1	MNCN 44224	JX436021	JX435920	JX435987	JX436078
<i>Proctoporus iridescens</i> 2	MHNC 6005	JX436049	JX435927	JX435966	JX436079
<i>Proctoporus kizirian</i> 1	MNCN 44216	JX436022	JX435900	JX435972	JX436096
<i>Proctoporus kizirian</i> 2	MHNC 5367	JX436011	JX435907	JX435978	JX436091
<i>Proctoporus lacertus</i> 1	UTA R-51487	AY507897	AY507850	AY507868	AY225180
<i>Proctoporus lacertus</i> 2	UTA R-51506	AY507898	AY507851	AY507869	AY225175
<i>Proctoporus pachyurus</i> 1	UTA R-52949	–	AY968824	AY968834	AY968816
<i>Proctoporus pachyurus</i> 2	MHNC 4599	JX436024	JX435891	JX435952	JX436055
<i>Proctoporus</i> sp. Ca	MNCN 23305	JX436006	JX435890	JX435949	JX436054
<i>Proctoporus succullucu</i> 1	UTA R-51478	AY507905	AY507857	AY507878	AY225171
<i>Proctoporus succullucu</i> 2	UTA R-51496	AY507906	AY507858	AY507879	AY225177
<i>Proctoporus unsaaca</i> 1	UTA R-51488	AY507908	AY507859	AY507881	AY225186
<i>Proctoporus unsaaca</i> 2	UTA R-51477	AY507909	AY507860	AY507882	AY225170
<i>Proctoporus xestus</i> 1	MNCN 6160	–	JX435898	JX436002	JX436101
<i>Proctoporus xestus</i> 2	MNCN 2425	JX436007	JX435899	JX436001	JX436100
<i>Ptychoglossus brevifrontalis</i>	MHNSM	AY507911	AY507865	AY507884	AY507895
<i>Rhachisaurus brachylepis</i>	MRT 887336	AF420853	AF420665	AF420737	AF420877
<i>Riama anatorlos</i> 1	QCAZ 9169	KY670664*	KY670702*	KY681120*	KY710843*
<i>Riama anatorlos</i> 2	QCAZ 9201	KY670665*	KY670703*	KY681121*	KY710844*
<i>Riama balneator</i> 1	QCAZ 11101	KY670666*	KY670704*	KY681122*	KY710845*
<i>Riama balneator</i> 2	QCAZ 11099	KU902115	KU902196	KU902271	KU902352
<i>Riama cashcaensis</i> 1	KU 217205	–	–	AY507870	AY507887
<i>Riama cashcaensis</i> 2	QCAZ 10686	KJ948210	KJ948180	KJ948122	KJ948162
<i>Riama colomaronani</i> 1	KU 217209	AY507899	AY507853	AY507871	AY507888
<i>Riama colomaronani</i> 2	QCAZ 8753	KY670667*	KY670705*	KY681123*	KY710846*
<i>Riama columbiana</i> 1	ICN 11298	KY670668*	KY670706*	KY681124*	KY710847*
<i>Riama columbiana</i> 2	ICN 11294	KY670669*	KY670707*	KY681125*	KY710848*
<i>Riama</i> “Cordillera Central”1	A1	KY670670*	KY670708*	KY681126*	–
<i>Riama</i> “Cordillera Central”2	A2	KY670671*	KY670709*	KY681127*	–
<i>Riama</i> “Cordillera Occidental”	JJM 2251	KY670672*	KY670710*	KY681128*	KY799162*
<i>Riama labionis</i> 1	QCAZ 10411	KJ948218	KJ948171	KJ948120	KJ948147
<i>Riama labionis</i> 2	QCAZ 10412	KJ948207	KJ948172	KJ948121	KJ948148
<i>Riama meleagris</i> 1	QCAZ 9840	KJ948214	KJ948182	KJ948129	KJ948164
<i>Riama meleagris</i> 2	QCAZ 9846	KJ948212	KJ948183	KJ948133	KJ948168
<i>Riama</i> “Nariño”1	SSP 058	KY670673*	KY670711*	KY681129*	KY710849*
<i>Riama</i> “Nariño”2	SSP 076	KY670674*	KY670712*	KY681130*	KY710850*
<i>Riama orcesi</i> 1	KU 2212772	–	AY507855	AY507874	AY507889
<i>Riama orcesi</i> 2	QCAZ 9035	KY670675*	KY670713*	KY681131*	KY710851*
<i>Riama raneyi</i> 1	QCAZ 10090	–	KY670714*	KY681132*	KY710852*
<i>Riama raneyi</i> 2	QCAZ 9034	–	KY670715*	KY681133*	KY710853*
<i>Riama simotera</i> 1	QCAZ 879	AY507904	AY507861	AY507877	AY507892
<i>Riama simotera</i> 2	QCAZ 4120	KY670676*	KY670716*	KY681134*	KY710854*
<i>Riama stigmatoral</i> 1	QCAZ 7374	KJ948217	KJ948187	KJ948128	KJ948161
<i>Riama stigmatoral</i> 2	QCAZ 11412	KJ948209	KJ948189	KJ948124	KJ948158
<i>Riama striata</i> 1	MAR 333	KY670677*	KY670717*	KY681135*	–
<i>Riama striata</i> 2	MAR 933	KY670678*	KY670718*	KY681136*	KY710855*
<i>Riama unicolor</i> 1	KU 217211	AY507907	AY507862	AY507880	AY507893
<i>Riama unicolor</i> 2	QCAZ 9662	KY670679*	KY670719*	KY681137*	KY710856*
<i>Riama yumborum</i> 1	QCAZ 10822	KJ948213	KJ948186	KJ948125	KJ948169
<i>Riama yumborum</i> 2	QCAZ 10827	KJ948216	KJ948195	KJ948142	KJ948170
<i>Riolama leucosticta</i> 1	VUB 3767	KP283389	–	JQ742254	KP283396
<i>Riolama leucosticta</i> 2	VUB 3263	–	–	JQ742256	–

included previously in phylogenetic analyses of gymnophthalmid lizards. In her morphology-based phylogenetic analyses of *Proctoporus* s.l. and *Cercosaura* s.l., Doan (2003a,b) used a set of 62 external morphological characters. Our characters 16 and 17 correspond to her characters 1 and 2, and our characters 11, 18, 15, 19, 29, 32, 33, 34 and (22–27) were modifications of her characters 3, 10, 13, (24–25), 36, 45, (40, 42), 41 and 46, respectively; parenthetical notation denotes multiple characters being treated as a single one. Character 12 was a modification of character 10 of Rodrigues et al. (2005). The remaining 50 mostly meristic, but also morphometric, characters of Doan were not included herein because Doan coded intraspecific polymorphism using the Generalized Frequency Coding method (Smith and Gutberlet, 2001), following argumentation by Wiens (1995, 1998), among others, which was shown to yield untenable results (Murphy and Doyle, 1998). Taxon phylogeny is to be inferred from hypothesized character-state transformations (Hennig, 1966). Only transformations from one character state to another ($a \rightarrow a'$) constitute evidence for relationships. In general, changes in the distribution of states among organisms, or in frequency of states in populations ($a \rightarrow aa' \rightarrow a'$), do not entail additional character-state transformations. Thus, methods that convert polymorphism into frequencies conflate population-level similarity with character transformation events (Grant and Kluge, 2003, 2004). Furthermore, because frequencies are not heritable (Murphy, 1993; Wiens, 2000) most of us consider them irrelevant in phylogenetic inference². In the case of meristic, continuous variation (i.e. counts), Doan kindly provided us with her raw data, which complemented our own observations. However, although we agree that continuous variation carries phylogenetic information (Goloboff et al., 2006), a defensible method of incorporating meristically continuous variables into phylogenetic inference awaits development (but see Goloboff et al., 2006)².

Character states for most species were coded directly from observations taken using a stereoscope and complemented with published data. For unavailable material, data were taken exclusively from the literature. Polymorphic species had multiple states that were scored for a character. When it was not possible to collect all phenotypic data for a particular species, unknown character states were treated as missing (“?”). Inapplicable characters were scored as “–”. Phenotypic characters and their states are described in detail in Appendix 1 (Analysis and description of phenotypic characters). The morphological matrix (Nexus

format) is deposited in Morphobank (O’Leary and Kaufman, 2011, 2012; permalink: <http://morphobank.org/permalink/?P2601>). The list of specimens examined is given in Appendix 2.

Hemipenial morphology. Hemipenes were prepared following the procedures described by Manzani and Abe (1988), as modified by Pesantes (1994) and Zaher (1999). The retractor muscle was severed manually and the everted organ was filled with stained petroleum jelly. Following Uzzell (1973) and Nunes et al. (2012), calcareous hemipenial structures were stained in an alcohol solution of alizarin red. Terminology follows Dowling and Savage (1960), Savage (1997) and Nunes et al. (2012). Hemipenes examined are listed in Appendix 3.

Institutional acronyms

Institutional abbreviations for specimen repositories generally follow Sabaj Pérez (2014). To this, we added the following collections: CORBIDI (Centro de Ornitología y Biodiversidad, Lima, Peru), DHMECN (División de Herpetología, Museo Ecuatoriano de Ciencias Naturales, Quito, Ecuador), EPNH (Escuela Politécnica Nacional, Colección Herpetología, Quito, Ecuador), FHGO (Fundación Herpetológica Gustavo Orcés, Quito, Ecuador), MHNCJS (Museo de Historia Natural, Colegio San José, Medellín, Colombia), MHNUC (Museo de Historia Natural, Universidad de Caldas, Manizales, Colombia), PSO-CZ (Museo de Historia Natural de la Universidad de Nariño, Pasto, Colombia) and UV-C (Museo de Vertebrados, Universidad del Valle, Cali, Colombia).

Phylogenetic analyses

We performed a TE analysis of the molecular and phenotypic data under the maximum parsimony optimality criterion. The rationale for this approach was advanced by Farris (1983) and discussed, among others, by Kluge (1989, 2004), Goloboff (2003), Goloboff and Pol (2005), and Kluge and Grant (2006). The cladogram that minimizes the transformations required to explain the observed character variation maximizes evidential congruence and provides the greatest explanatory power (Farris, 1983; Kluge and Grant, 2006). While maintaining that the TE analysis of all available evidence identifies the optimal explanation (Kluge, 1989, 2004), we also analysed the molecular data separately using the same parameters to evaluate the effect of a modest morphological matrix on an analysis dominated by a larger DNA sequence dataset (cf. de Sá et al., 2014). Following Padial et al. (2014), we employed POY 5.1.1 (Varón et al., 2010) for tree-alignment (i.e. direct optimization or dynamic

²This position does not reflect that of all coauthors (see Torres-Carvajal, 2007, for example), but did not interfere with our final phenotypic character sampling.

homology; e.g. Sankoff, 1975; Wheeler, 1996; Varón and Wheeler, 2012, 2013). The method tested hypotheses of nucleotide homology dynamically by optimizing unaligned DNA sequences directly onto alternative topologies (Kluge and Grant, 2006; Wheeler et al., 2006; Grant and Kluge, 2009) while simultaneously optimizing prealigned transformation series as standard static matrices.

We searched for optimal trees using the Museu de Zoologia da Universidade de São Paulo's high-performance computing cluster (Ace), as described in detail by Padial et al. (2014) and de Sá et al. (2014). We calculated tree costs using the standard direct optimization algorithm for unaligned data (Wheeler et al., 2006) with all transformations weighted equally. Following Grant et al. (2006: 56–57), we treated each sequenced individual as a separate terminal and duplicated the phenotypic data coded for the species as a whole for each conspecific terminal. We used the same search parameters to analyse both the TE and molecular-only datasets. Each analysis involved four 4-h searches on 704 CPUs (giving a total of 11 264 CPU-h). We used the command 'search,' which implemented a driven search that included random addition sequence Wagner builds, Subtree Pruning and Regrafting (SPR) and Tree Bisection and Reconnection (TBR) branch swapping (RAS + swapping; Goloboff, 1996), Parsimony Ratcheting (Nixon, 1999) and Tree Fusing (Goloboff, 1999). The shortest trees of each independent run were stored and used to perform a final round of Tree Fusing on the pooled trees. We then submitted the resulting trees to a final round of swapping using the iterative pass algorithm (Wheeler, 2003a). To verify the length reported during the tree-alignment analyses and search for additional optimal trees, we calculated the implied alignment (i.e. the matrix version of the tree-alignment; Wheeler, 2003b) and performed an additional 1280 random addition sequence Wagner builds plus TBR searches, saving five minimum-length trees per build.

We estimated clade support (Grant and Kluge, 2008a) using the Goodman–Bremer measure (GB; Goodman et al., 1982; Bremer, 1988; Grant and Kluge, 2008b), by determining the length difference between the optimal trees and all trees visited during a TBR swap of one of the optimal trees using the corresponding implied alignment. Although it is possible for shorter suboptimal trees to be found by calculating the optimal tree-alignment for each visited topology, the time requirements would be prohibitively costly unless each search was made extremely superficially. Furthermore, Padial et al. (2014) found that using the implied alignment to estimate support overestimates GB values considerably less than when GB is calculated using a MAFFT (Kato et al., 2005) similarity-alignment.

In order to evaluate the impact of the small morphological dataset on our results, we assessed differences between the TE and molecular-only analyses by examining clade-by-clade incongruences and by comparing the standardized support values obtained in the two analyses. For clades shared by both results, we calculated the ratio of explanatory power (REP) value (Grant and Kluge, 2007), which scales the observed support for a given clade relative to its maximum possible support (Grant and Kluge, 2010). We obtained the lengths of least-parsimonious trees by conducting 1280 random addition sequence Wagner builds plus TBR searches with all characters assigned a weight of -1 and taking the absolute value of the resulting lengths. To make REP values more manageable, we multiplied them by 10 000 and reported them to two significant figures.

Biogeography and character evolution

The novel knowledge that emerges from phylogenetic analysis has implications beyond the problems of systematics. By providing a causally relevant framework of reference, knowledge of phylogeny often leads to unanticipated insights and identifies novel problems for further investigation (Grant et al., 2006). In the section “*Biogeographical commentary*”, we analyse the implications of our phylogenetic results for patterns of distribution among major biogeographical units in the Neotropics. Thus, rather than performing a detailed biogeographical analysis, we explored the connection between the biogeographical units, as implied by phylogenetic evidence, within a hypothesis-testing framework. Similarly, in the section “*Character evolution*”, we analyse the implications of the TE phylogeny for the evolution of prefrontal scales in the Cercosaurinae.

Results

General total evidence results

Analysis of the TE dataset completed 35 533 replicates of random addition sequence Wagner builds plus TBR branch swapping, 189 895 rounds of Tree Fusing and 17 405 iterations of Ratcheting. The analyses identified two optimal trees of 9702 steps. A final round of swapping under the iterative pass algorithm and additional searches using the implied alignment resulted in two equally parsimonious trees of 9680 steps (not shown). Only one ingroup node collapsed in the strict consensus tree (Fig. 1), which involved terminals of *R. crypta* and resulted in the polytomy of a clade also composed of *R. hyposticta* and *R. oculata* (tree-alignment matrix and consensus tree deposited in MorphoBank; permalink: <http://morphobank.org/pe>

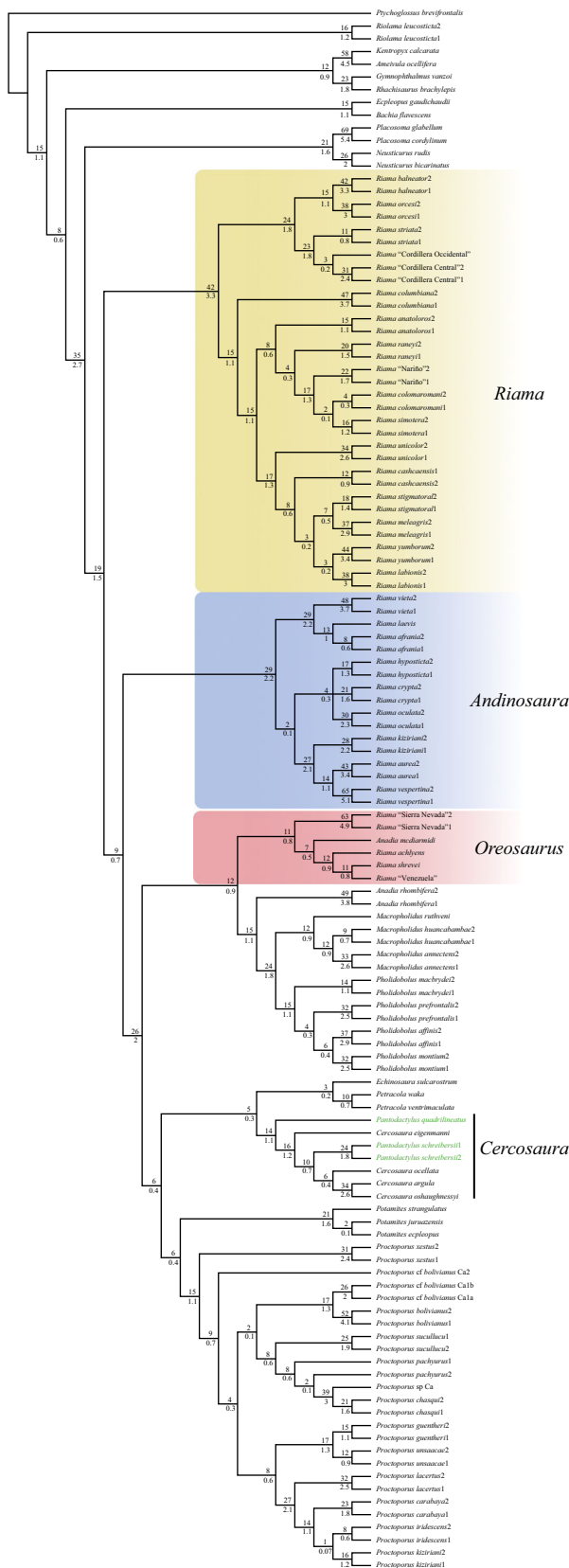


Fig. 1. Strict consensus of two most-parsimonious trees (9680 steps) from the total evidence analysis. Values above branches are Goodman–Bremer support and below branches are ratio of explanatory power (REP) support. Yellow = *Riama* s.s. (i.e. *R. unicolor*, type species of *Riama*, is included in this clade), including 14 nominal and three undescribed species; blue = a clade composed of nine nominal species currently referred to *Riama*; red = a clade comprising two nominal and two undescribed species referred to *Riama* plus *Anadia mediamidi*. The nonmonophyletic *Pantodactylus*, which is embedded within *Cercosaura*, is highlighted in green. The new taxonomy proposed herein (Appendix 4) is represented. [Colour figure can be viewed at wileyonlinelibrary.com]

rmalink/?P2601). Analyses resulted in a least-parsimonious tree of 22 325 steps, which we used for calculating REP values.

Riama polyphyly and general ingroup relationships

Analyses recovered a monophyletic Cercosaurinae (*sensu* Torres-Carvajal et al., 2016; Cercosaurini *sensu* Goicoechea et al., 2016) (Fig. 1). As defined currently, *Riama* was polyphyletic. Representatives fell into three clades, with no pair of clades as sister taxa (Fig. 1: yellow, blue and red). In sequence, (i) an Andean clade (yellow), *Riama* s.s., included the type species *R. unicolor* along with *R. balnearia*, *R. orcesi*, *R. striata*, *R. “Cordillera Occidental”*, *R. “Cordillera Central”*, *R. columbiana*, *R. anatorlos*, *R. raneyi*, *R. “Nariño”*, *R. colomarovani*, *R. simotera*, *R. cashcaensis*, *R. stigmatosa*, *R. meleagris*, *R. yumborum* and *R. labionis*. (ii) A second Andean clade (blue) was composed of *R. vieta*, *R. laevis*, *R. afrania*, *R. hyposticta*, *R. crypta*, *R. oculata*, *R. kiziriani*, *R. aurea* and *R. vespertina*. Finally, (iii) a third clade (red) comprised *R. “Sierra Nevada”* (from the Sierra Nevada de Santa Marta, Colombia), the Tepuian *Anadia mediamidi*, *R. achlyens* (from the Cordillera de la Costa, Venezuela, CC), the Trinidadian *R. shrevei*, and *R. “Venezuela”* (also from CC). The density of taxon sampling allowed the coherent delimitation of these three clades, whose monophyly was well supported (GB = 42, 29 and 11, respectively). This permitted development of a phylogenetic taxonomy (Appendix 4).

Following the new taxonomy, *Riama* s.s. contained two major clades (GB = 24 and 15) and was the sister group of (*Andinosaura* (*Oreosaurus* (*Anadia* (*Macropholidus*+*Pholidobolus*))) (*Echinosauro*+*Petracola* (*Cercosaura*) (*Potamites*+*Proctoporus*))). *Andinosaura* also had two major clades (GB = 29 and 2) (Fig. 1).

Relevant outgroup relationships

Outgroup sampling included representatives of *Proctoporus* s.s. and *Petracola*, both of which, plus *Riama*

s.l., formed the former *Proctoporus* s.l. Our analysis recovered both *Proctoporus* s.s. and *Petracola* as monophyletic (GB = 15 and 10, respectively), but they were not closely related to each other, nor to any of the three clades of *Riama* s.l. Further, the Tepuian *Anadia mediarmidi* nested within clade three of *Riama* s.l. (i.e. *Oreosaurus*), and the recently resurrected *Pantodactylus* (Goicoechea et al., 2016) nested within *Cercosaura* (Fig. 1).

Molecular-only results and comparison with the total evidence analysis

Analysis of the molecular-only dataset resulted in five most-parsimonious trees of 9464 steps (not shown). Three outgroup nodes collapsed in the strict consensus tree (Fig. 2), involving terminals of *Pholidobolus prefrontalis*, *Cercosaura schreibersii* and *Proctoporus pachyurus* (tree-alignment matrix and consensus tree deposited in MorphoBank; permalink: <http://morphobank.org/permalink/?P2601>). Analyses resulted in a least-parsimonious tree of 21 720 steps, which we used for calculating REP values.

Although the ingroup clades *Riama*, *Andinosaura* and *Oreosaurus* (following the new taxonomy) were monophyletic in both analyses, and the relationships within them identical, topologies from the TE and molecular-only analyses present important differences. Our molecular-only analysis placed *Andinosaura* as the sister group of *Riama* and *Oreosaurus* as sister to a clade composed of *Potamites*, *Petracola*, *Cercosaura* and *Proctoporus* (Fig. 2). In contrast, our TE analysis recovered *Riama* as the sister group of the remaining cercosaurines except for *Placosoma* + *Neusticurus*, followed by *Andinosaura* and *Oreosaurus* as sister to a clade composed of *Anadia*, *Macropholidus* and *Pholidobolus* (Fig. 1). Among outgroup taxa, incongruence between both analyses includes the placement of *Echinosaura sulcarostrum* and *Potamites* and relationships within *Proctoporus* (Figs 1 and 2).

In addition to topological differences, comparison of REP values for the ingroup clades between the two analyses shows that support for the three clades *Riama*, *Andinosaura* and *Oreosaurus* increased with the inclusion of morphological evidence. REP support for *Riama* was 3 in the molecular-only analysis and 3.3 in the TE analysis. Similarly, REP supports for *Andinosaura* and *Oreosaurus* were 1.7 and 0.3 in the



Fig. 2. Strict consensus of five most-parsimonious trees (9464 steps) from the molecular-only analysis. Values above branches are Goodman-Bremer support and below branches are ratio of explanatory power (REP) support. Taxonomic changes proposed herein are adopted (Fig. 1 and Appendix 4). [Colour figure can be viewed at wileyonlinelibrary.com]

molecular-only analysis, and increased to 2.2 and 0.8, respectively, in the TE analysis (Figs 1 and 2). Among outgroup taxa, REP values increased for four clades (*Neusticurus*, *Pholidobolus*, *Potamites* and *Cercosaura*), remained the same for one clade (*Macropholidus*), and decreased for four clades (*Placosoma*, *Anadia*, *Petracola* and *Proctoporus*; Figs 1 and 2).

Discussion

Ingroup relationships

When Doan and Castoe (2005: 408) resurrected *Riama*, they cautioned that “[w]e much prefer to take the chance of creating a paraphyletic *Riama* [than to create a paraphyletic *Proctoporus*], because there is much greater likelihood that the northern *Proctoporus* s.l. species belong there”. However, the present analysis, which is the first to combine both the molecular and phenotypic evidence of cercosaurine lizards, resolves *Riama sensu* Doan and Castoe (2005) as a polyphyletic genus (Fig. 1). Torres-Carvajal et al. (2016) recently reported nonmonophyly for *Riama sensu* Doan and Castoe (2005) because “*R. laudahnae* nested deeply within (and was transferred to) *Proctoporus*. Previous molecular-only phylogenetic analyses dealing with Cercosaurinae diversification only included representatives (usually five species) of *Riama* s.s. Our analyses resolve *Riama* s.s. as the sister group of the remaining cercosaurines except for *Placosoma* + *Neusticurus*. This finding agrees with the results of Castoe et al. (2004)³ (following the current taxonomy), Goicoechea et al. (2012, 2016) and Colli et al. (2015), but disagrees with those of Pyron et al. (2013), Kok (2015) and Torres-Carvajal et al. (2015). The latter three studies resolved *Riama* s.s. as the sister group of all other cercosaurines. Using denser taxon sampling of cercosaurines, Torres-Carvajal et al. (2016) recently found *Riama* s.s. to be the sister of the remainder cercosaurines except for *Placosoma* + *Neusticurus* and *Echinosaura* (excluding *E. sulcarostrum*).

Based on morphological similarity, Uzzell (1958) recognized the *Proctoporus luctuosus* group, as currently consisting of *Riama achlyens*, *R. laevis*, *R. luctuosa* (not included herein), *R. oculata* and *R. shrevei*. Our results differ because *R. laevis* and *R. oculata* nest within the second clade of *Riama* (i.e. *Andinosaura*), but *R. achlyens* and *R. shrevei* nest within the third clade (i.e.

Oreosaurus). The nonmonophyly of the *luctuosus* group is congruent with Doan (2003a) in her morphological analysis of *Proctoporus* s.l. Uzzell (1958: 12) also suggested that *R. achlyens* and *R. shrevei* were sister species, and Doan recovered them as sister taxa. When describing *R. rhodogaster* (not included herein), Rivas et al. (2005) mapped seven morphological traits onto Doan’s phylogeny. They hypothesized the clade (*R. achlyens* (*R. rhodogaster* + *R. shrevei*)). Our analyses resolve *R. achlyens*, *R. shrevei* and *R. “Venezuela”* as being closely related, and they nest together along with *R. “Sierra Nevada”* and *Anadia mdiarmidi*. This placement of *A. mdiarmidi* is surprising for two reasons: first, Kok and Rivas (2011) and Montero et al. (2002), among others, associated *Anadia* with other cercosaurine genera, such as *Euspondylus*, based on morphology; and second, Kok et al. (2012) and Kok (2015) included for the first time a species of *Anadia* (*A. mdiarmidi*) in analyses of DNA sequence data (16S and ND1; and 16S, ND4 and *C-mos*, respectively). Kok et al. (2012: Suppl. info., fig. 2) recovered *A. mdiarmidi* as part of a cercosaurine clade that contained two species of *Potamites*, *Cercosaura ocellata*, and *Echinosaura sulcarostrum*. Because the position of the latter species was unresolved, a sister-species relationship for *A. mdiarmidi* also was unresolved. Later, Kok (2015: fig. 8) recovered a cercosaurine clade of similar content; it included *Proctoporus* and *Petracola*, which were not sampled in Kok et al.’s (2012) study. His analyses resolved *Anadia* (*mdiarmidi*) as the sister taxon of *Echinosaura* (*sulcarostrum*). This relationship was also found by Goicoechea et al. (2016: fig. 12), although they also recovered *A. mdiarmidi* as the sister taxon of *Potamites* (their figs 4 and 8). Because these studies lacked rigorous taxon sampling of cercosaurines, the phylogenetic relationships of *A. mdiarmidi* were inconclusive. The denser taxon sampling of Torres-Carvajal et al. (2016), which included for the first time additional members of *Anadia* (the Andean *A. petersi* and *A. rhombifera*), resulted in a nonmonophyletic *Anadia*. *Anadia mdiarmidi* formed the sister taxon of a clade composed of *A. petersi* + *A. rhombifera*, their unnamed clade 1, and *Macropholidus* + *Pholidobolus*. Our results corroborate the nonmonophyly of *Anadia*. *Anadia mdiarmidi* does not form a monophyletic group with *A. rhombifera* (Fig. 1). Thus, although the placement of *A. mdiarmidi* within our third clade of *Riama* (i.e. *Oreosaurus*) is surprising, no data challenge this result.

The dearth of taxon sampling of *Riama* s.s. in most previous molecular-based analyses precludes meaningful comparisons with our results. Aguirre-Peñafiel et al. (2014) and Torres-Carvajal et al. (2016) added four and six species (seven including “*R. laudahanae*”, now in *Proctoporus*), respectively, to the five taxa of Castoe et al. (2004). The study by Aguirre-Peñafiel et al. lacked rigorous outgroup sampling, but their main objective

³Castoe et al.’s (2004) Bayesian analysis of the concatenated nuclear and mitochondrial data recovered *Riama* s.s. as the sister group of all cercosaurines except *Placosoma* + *Neusticurus* s.s. (Doan and Castoe, 2005), whereas their strict consensus of two most parsimonious trees embedded *Riama* s.s. within Cercosaurinae (*sensu* Torres-Carvajal et al., 2016) in an unresolved position.

was to infer the phylogenetic position of *R. yumborum* rather than to resolve the phylogeny of *Riama*. Nevertheless, they resolved *R. unicolor* as the sister taxon of (*R. cashcaensis* (*R. meleagris*+*R. stigmator* (*R. yumborum*+*R. labionis*))). Our results (Fig. 1), and those of Torres-Carvajal et al. (2016), corroborate this clade. Previously, Kizirian and Coloma (1991) suggested that *R. cashcaensis* was probably most closely related to *R. unicolor*, and Doan (2003a) found *R. stigmator*, *R. labionis*, *R. meleagris* and *R. unicolor* to be closely related. Torres-Carvajal et al.'s (2016) analysis placed *R. orcesi* and *R. balneator* as sister species. Our results corroborate this hypothesis.

Doan's (2003a) densely sampled phylogenetic analysis of *Proctoporus* s.l. yielded a poorly resolved strict consensus tree of two reconstructions that used different weighting schemes. However, her tree included several hypotheses of sister-species relationships supported by evidence. Furthermore, several authors have proposed additional sister-species relationships on the basis of morphological similarity and/or geographical proximity. Doan (2003a) found *Riama colomaroni* and *R. simotera* to be sister species. However, she used specimens of an undescribed species to score morphological characters for *R. simotera* (Sánchez-Pacheco et al., 2010; herein referred to as *R. "Nariño"*). Therefore, Doan actually found *R. colomaroni* and *R. "Nariño"* to be sister species. Our analysis recovers *R. "Nariño"* as the sister taxon of *R. colomaroni* + *R. simotera* (Fig. 1). Although Doan found *R. striata* and *R. vieta* to be sister species, our results assign *R. striata* to *Riama* s.s., and *R. vieta* within the second clade of *Riama* (i.e. *Andinosaura*). Our results place *R. vieta* as the sister taxon of *R. laevis* + *R. afrania*. Arredondo and Sánchez-Pacheco (2010) previously hypothesized that *R. laevis* and *R. afrania* were sister species based on morphological similarity and relative geographical proximity. Similarly, Sánchez-Pacheco et al. (2011) interpreted the shared occurrence of single, distal filiform appendages on the hemipenial lobes of *R. crypta* and *R. hyposticta* as a putative synapomorphy uniting these two species. Our analysis nests *R. crypta* within a clade also composed of *R. hyposticta* and *R. oculata*, but forming a polytomy (Fig. 1). The placement of *R. oculata* in this clade provides a prediction that filiform appendages may also occur on the hemipenial lobes of *R. oculata*. Finally, Sánchez-Pacheco et al. (2012), based on morphological similarity, suggested that *R. vespertina*, *R. aurea* and *R. kiziriani* (and *R. petrorum*, not included in this study) were closely related, which our results also support (Fig. 1).

Outgroup relationships

Our study is designed to test, as severely as possible—in terms of taxon and character sampling—

monophyly of *Riama* s.l., and to explore the relationships among its species. Because our outgroup sampling is largely drawn from Cercosaurinae, our topology (Fig. 1) deserves some discussion. We comment on *Cercosaura* (including *Pantodactylus*) and *Proctoporus*.

Cercosaura and *Pantodactylus*. Pellegrino et al.'s (2001) molecular phylogenetic analyses of Gymnophthalmidae, based on mtDNA 16S, 12S and *ND4*, and nuDNA *C-mos* and 18S, included representatives of *Cercosaura* (one species), *Pantodactylus* (two species), and *Prionodactylus* O'Shaughnessy, 1881 (three species). Pellegrino et al. sampled the type species of *Cercosaura* (*C. ocellata* Wagler, 1830) and *Pantodactylus* (*P. d'orbignyi* Dumeril and Bibron, 1939 = *P. schreibersii*). The species of *Pantodactylus* and *Prionodactylus* formed a clade with *C. ocellata*. Based on 61 morphological characters for all 11 species of *Cercosaura*, *Pantodactylus* and *Prionodactylus*, Doan (2003b) found *Prionodactylus* to be paraphyletic with respect to *C. ocellata* and species of *Pantodactylus*. Consequently, she relegated *Pantodactylus* and *Prionodactylus* junior synonyms of *Cercosaura*.

Castoe et al. (2004) included five species of *Cercosaura* in their molecular phylogenetic analysis of Gymnophthalmidae. *Cercosaura* was monophyletic in their preferred Bayesian inference tree (Castoe et al., 2004; fig. 6), but it was polyphyletic in the strict consensus of their two most-parsimonious solutions (their fig. 1) because *C. quadrilineata* was sister to a clade composed of *Potamites*, *Pholidobolus*, *Petracola*, *Cercosaura* s.s. and *Proctoporus* (following the current taxonomy). Pyron et al. (2013) included six species of *Cercosaura*. They recovered a monophyletic *Cercosaura*. Torres-Carvajal et al. (2015; see also Torres-Carvajal et al., 2016) performed the largest molecular phylogenetic analysis of *Cercosaura* to date. They sampled 11 species, including the type species of *Prionodactylus* (*P. manicatus* O'Shaughnessy, 1881 = *C. manicata*). Their analysis found *Cercosaura*, as defined by Doan (2003b), to be nonmonophyletic because *C. dicra* and *C. vertebralis* nested deeply within *Pholidobolus*. They transferred both of these species to *Pholidobolus* and in doing so redefined *Cercosaura*.

Goicoechea et al. (2016) included six species of *Cercosaura*. They resolved a monophyletic *Cercosaura* (Goicoechea et al., 2016: SA + PA and SA + ML analyses) and a nonmonophyletic *Cercosaura* (their TA + PA analysis), because *C. quadrilineata* was sister to a clade composed of *Anadia mediarmidi*, *Potamites*, *Cercosaura* s.s. and *Proctoporus*. Ultimately, Goicoechea et al. (2016) resurrected *Pantodactylus* from the synonymy of *Cercosaura* for *C. quadrilineata* and *C. schreibersii*, arguing that (p. 34):

It is possible that the name *Prionodactylus* O'Shaughnessy (1881) is available but the type species of that genus, *Cercosaura manicata* O'Shaughnessy, 1881, was not included in our analysis. We suspect that “*Cercosaura*” *quadrilineata* will ultimately be placed in its own genus, but at present we cannot exclude the possibility that *Prionodactylus* is the appropriate assignment for this species and *Cercosaura manicata*. Until more data are available, we tentatively resurrect *Pantodactylus* to allocate *C. quadrilineata* and *C. schreibersii* [sic].

However, Goicoechea et al. (2016) found that the type species of *Pantodactylus* (*C. schreibersii*) nested consistently within a monophyletic group containing the type species of *Cercosaura* (*C. ocellata*) in all of their analyses. Multiple phylogenetic studies, including the present one (Fig. 1), have also imbedded *C. schreibersii* within *Cercosaura* s.s. (e.g. Pellegrino et al., 2001; Castoe et al., 2004; Torres-Carvajal et al., 2015, 2016). Furthermore, in none of their trees did Goicoechea et al. (2016) recover a sister-species relationship between *C. schreibersii* and *C. quadrilineata* (which they proposed as members of *Pantodactylus*). Our study corroborates the nonmonophyly of *Pantodactylus sensu* Goicoechea et al. (2016) (Fig. 1). Therefore, the placement of *C. schreibersii* within *Cercosaura* and the nonmonophyly of *Pantodactylus* render the resurrection of *Pantodactylus* by Goicoechea et al. (2016) an arbitrary change because they overlooked existing evidence regarding the phylogenetic relationships of *C. schreibersii*. In addition, the denser taxon sampling of Torres-Carvajal et al. (2016), in terms of *Cercosaura* (including *C. manicata*) and Cercosaurinae species diversity, resulted in a monophyletic *Cercosaura*, as defined by Torres-Carvajal et al. (2015).

Our TE parsimony analysis includes a denser sampling of cercosaurines than the molecular analyses of Goicoechea et al. (2016), as well as the same terminals of *Cercosaura*. Our results (Fig. 1) resemble those of Pellegrino et al. (2001), Castoe et al. (2004: Bayesian analysis), Pyron et al. (2013), and Torres-Carvajal et al. (2015, 2016—excluding *Pholidobolus dicrus* and *P. vertebralis*) regarding the monophyly of *Cercosaura*. This contrasts with the TA + PA analysis of Goicoechea et al. (2016) and the parsimony analysis of Castoe et al. (2004). Similar to these analyses, our near-optimal trees (not shown) resolve a nonmonophyletic *Cercosaura* due to the placement of *C. quadrilineata*. Therefore, we return *Pantodactylus* to the synonymy of *Cercosaura* (Appendix 4).

Proctoporus. Our analysis resolves monophyly for *Proctoporus* (Fig. 1), as delimited by Goicoechea et al. (2012). This finding agrees with the results of Torres-Carvajal et al. (2015) and Goicoechea et al. (2016: TA + PA and SA + PA analyses). Using denser sampling of cercosaurines, analysis by Torres-Carvajal et al. (2016) nested *Euspondylus rahmi*, *E. spinalis*,

E. oreades and *Riama laudahnae* within *Proctoporus* s.s. Therefore, Torres-Carvajal et al. (2016) transferred them to this genus. Further, *Proctoporus sensu* Goicoechea et al. (2012) was polyphyletic. The polyphyly of *Proctoporus* remains to be tested, and, insofar as Torres-Carvajal et al. (2016) did not propose taxonomic changes, we recognize the content of *Proctoporus* as defined by Goicoechea et al. (2012, 2013), and as complemented by Torres-Carvajal et al. (2016).

The relationships within *Proctoporus* are uncertain owing to conflicting topologies (Goicoechea et al., 2012, 2016; Torres-Carvajal et al., 2016; our work). These include two critical considerations. First, our analysis (Fig. 1) corroborates the hypothesis of Torres-Carvajal et al. (2016) that *P. pachyurus*, as delimited by Goicoechea et al. (2012, 2013), is a composite of at least two species from Junin and Cusco, Peru. Torres-Carvajal et al. (2016) included one sample of *P. pachyurus* from Cusco used by Goicoechea et al. (2012); it clustered with *P. rahmi*. Although the phylogeny of Goicoechea et al. (2012) was consistent with the recognition of a single species, levels of genetic divergences, the findings of Torres-Carvajal et al. (2016), and our results suggest the occurrence of two species. Second, different hypotheses of relationships within *Proctoporus* (Goicoechea et al., 2016; Torres-Carvajal et al., 2016; this work) challenge the biogeographical scenario of Goicoechea et al. (2012).

Impact of phenotypic evidence on molecular datasets

Epistemologically, the increased explanatory power that results from including additional evidence validates TE analysis (Grant and Kluge, 2003; Kluge, 2004). However, to evaluate the effect of phenotypic evidence on an analysis dominated by a larger DNA sequence dataset, we repeated the analyses using only the molecular evidence. Assuming that truly optimal trees were obtained in both heuristic searches (i.e. TE and molecular-only analyses), differences between the results of the two analyses must be due to the inclusion of the morphological evidence.

Topologies from the two analyses present important differences (Results and Figs 1 and 2). Topological incongruence between the two analyses is surprising given that the TE analysis is dominated by molecular evidence. Morphological evidence comprises only 1.2% of the TE matrix (2719 aligned nucleotides, 35 morphological characters). This finding is similar to those of de Sá et al. (2014), who found that the inclusion of phenotypic data resulted in 15 topological differences. In addition to topological incongruence, comparison of REP values for clades that do not differ between the two analyses demonstrates that support

varies with the inclusion of morphological evidence. More importantly, support for the ingroup clades increases. de Sá et al. (2014) also found differences in REP values between both analyses.

In conclusion, relative to the size of the entire dataset phenotypic evidence had a disproportionately large impact on our TE results, showing that the inclusion of a comparatively small amount of morphology can alter both the topology and support values in analyses dominated by DNA sequence data.

Character evolution

Our results identify the optimal phylogenetic explanation of the species diversity of *Riama* s.l. and have implications for the evolutionary origins, losses and reversals of a number of morphological characters, particularly those related to scutellation and hemipenial anatomy. Below we focus on the evolution of prefrontal scales in the Cercosaurinae. However, the future inclusion of key taxa (e.g. *Euspondylus* and *Gelanesaurus*) might overturn our hypotheses and favour alternative evolutionary explanations.

Prefrontal scales. The occurrence of prefrontals (Character 11; Appendix 1) has played a pivotal role in cercosaurine systematics, having been used both to diagnose genera and species in Cercosaurinae, and to infer phylogenetic relationships. For example, the absence of prefrontal scales was used to diagnose the former, polyphyletic *Proctoporus* s.l. (e.g. Peters and Donosos-Barros, 1970) and as a synapomorphy of this group (Doan, 2003a). The ancestral state for Cercosaurinae optimizes unambiguously as plesiomorphically present in our analysis. Prefrontals were then lost in the most recent common ancestor of the immediately less inclusive clade (i.e. Cercosaurinae excluding *Placosoma* + *Neusticurus*), with no fewer than five independent reversals to present (*Oreosaurus mcdiarmidi*, *Anadia*, *Pholidobolus prefrontalis* and *P. affinis*, and the most recent common ancestor of the clade composed of *Echinosaura sulcarostrum*, *Petracola*, *Cercosaura*, *Potamites* and *Proctoporus*). Furthermore, two subsequent returns to absent occur in *Petracola* and *Proctoporus* (excluding *Proctoporus xestus*), with one gain in *Proctoporus chasqui* + *Proctoporus* sp.

Biogeographical commentary

Our results also have implications for patterns of distribution among major biogeographical units, and especially the connection between the Sierra Nevada de Santa Marta in Colombia (SNSM), the Cordillera de la Costa in Venezuela (CC), the island of Trinidad, and the tepuis (Venezuelan Guyana and Guyana Shield) (Fig. 3). Our inclusion of the undescribed SNSM

endemic *Oreosaurus* “Sierra Nevada”, two endemic species from the CC (*O. achlyens* and *O. “Venezuela”*), the Trinidadian endemic *O. shrevei* (Aripo Northern Range), and the tepui endemic *O. mcdiarmidi* allows us to test previous biogeographical hypotheses. Although each of these highland complexes has a unique geological history, cumulative phylogenetic evidence suggests an ancient connection between them. Species form monophyletic groups despite the considerable geographical distances that separate them. For example, our analysis recovers *O. “Sierra Nevada”* as the sister of the remaining species of *Oreosaurus*, followed by *O. mcdiarmidi*. *Oreosaurus achlyens* is the sister of *O. shrevei* + *O. “Venezuela”* (Figs 1 and 3). The distribution of *Oreosaurus* (SNSM, CC, Trinidadian highlands and tepuis) constitutes a biogeographical pattern (as a whole) not repeated in other vertebrates. This distribution strongly implies an ancient biogeographical connection between the SNSM and the CC as part of the explanation for the origin of the montane SNSM endemic vertebrate fauna.

Cordillera de la Costa (CC)—island of Trinidad. The Venezuelan CC extends eastwards along the Caribbean coast from the Andean Cordillera de Mérida and it has two main sections. First, the Barquisimeto Depression separates the CC Central (locality of *Oreosaurus achlyens* and *O. luctuosus*) from the Cordillera de Mérida. Second, the CC Oriental extends farther east along the coast toward the island of Trinidad, which lies 12 km off the northeastern coast of Venezuela (Doan and Schargel, 2003; Rivas et al., 2005) (Fig. 3). In turn, the CC Oriental consists of two separate mountain chains situated in extreme northeastern Venezuela: the Península de Paria, the type locality of *O. rhodogaster*, and the massif of Turimiquire, locality of *O. “Venezuela”* (Rivas et al., 2005). The CC originally extended from the Mérida Andes onto the island of Trinidad (Liddle, 1946). Thus, the northern range of Trinidad, the type locality of *O. shrevei*, was stratigraphically contiguous with the coastal range of Venezuela during the Pliocene and Pleistocene. This connection facilitated the exchange of species through land connections. A Miocene downwarping event severed the land connection (Liddle, 1946; Doan, 2003a; Rivas and de Freitas, 2015). Accordingly, the CC Oriental shares many species with Trinidad (Rivas and de Freitas, 2015). Steyermark (1979, 1982) and Kaiser et al. (2015) suggested that some species endemic to the massif of Turimiquire and the Península de Paria (CC Oriental) may be closely related to those of the CC Central and the island of Trinidad. Brown and Lomolino (1998) suggested that the ancestor of *O. shrevei* may have arrived in Trinidad using an ephemeral Pleistocene landbridge.

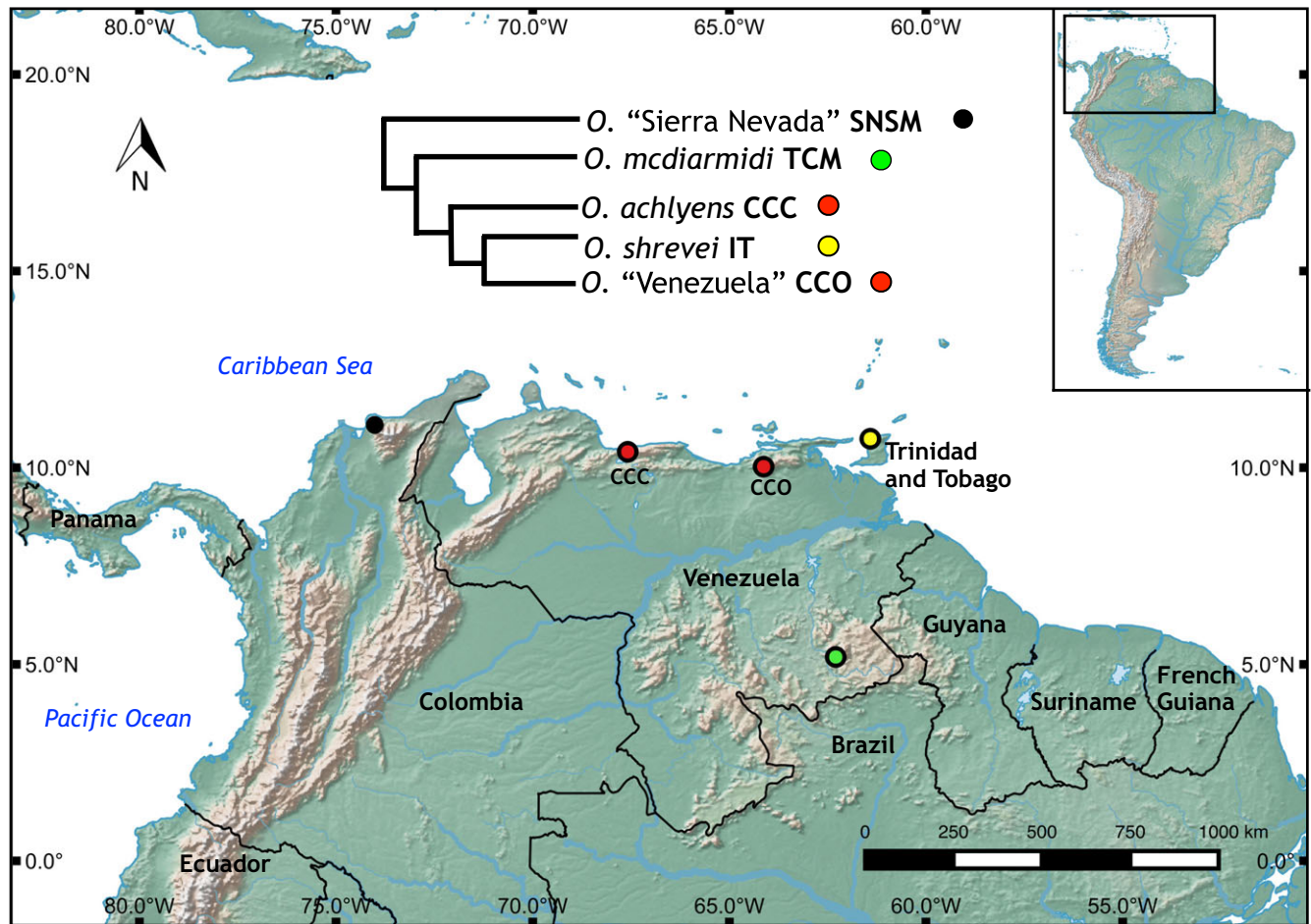


Fig. 3. Map of northern South America and summary of the phylogeny and geographical distribution of *Oreosaurus*. SNSM, Sierra Nevada de Santa Marta, Colombia; TCM, tepuis from the Chimantá massif, Venezuela; CCC, Cordillera de la Costa Central, Venezuela; IT, island of Trinidad; CCO, Cordillera de la Costa Oriental, Venezuela. [Colour figure can be viewed at wileyonlinelibrary.com]

The relationship between Trinidadian and CC taxa is, therefore, not surprising. For example, Manzanilla et al.'s (2009) analysis of *Mannophryne* (Anura: Aromobatidae) placed the Trinidadian endemic *M. trinitatis* and the CC endemic *M. venezuelensis* as sister species. As for *Oreosaurus*, Doan (2003a) reported a sister relationship for *O. shrevei* and *O. achlyens*. Rivas et al. (2005) hypothesized *O. achlyens* as sister of *O. shrevei* + *O. rhodogaster* (not included herein). Our analyses resolve *O. achlyens* as sister of *O. shrevei* + *O. 'Venezuela'*.

Cordillera de la Costa (CC) + island of Trinidad–tepuis. The Venezuelan Guayana contains remnants of the ancient Guyana Shield, which supports an endemic biota, especially in the tepuis (Doan and Schargel, 2003; and citations therein). Tepuis are geographically isolated mountains derived from the Precambrian sandstone of the Roraima Group (southern Venezuela, western Guyana, and northern Brazil), and surrounded by savannas and tropical

forests (Bonaccorso and Guayasamin, 2013; and citations therein). The origin of the tepuis' biodiversity remains uncertain (Rull, 2009; Kok and Rivas, 2011; Bonaccorso and Guayasamin, 2013). The closest relatives of some taxa, including endemic fauna, (may) occur in the surrounding lowlands, the Península de Paria and the massif of Turimiquire (CC Oriental), and the Andes (Chapman, 1931; Steyermark, 1974, 1979, 1982; Gorzula, 1987; Pérez-Emán, 2005; Rivas et al., 2005; Schargel et al., 2005; Mauck and Burns, 2009; Bonaccorso et al., 2011; Salerno et al., 2012; Bonaccorso and Guayasamin, 2013; Kok et al., 2013; Rivas and de Freitas, 2015). Our results support the hypothesis of a biogeographical association between the CC and the tepuis. *Oreosaurus mcdiarmidi*, which is endemic to the summit of Abakapá-tepui, and *O. 'Venezuela'*, which occurs endemically on the Turimiquire massif (CC Oriental), are placed as sister species (Figs 1 and 3). Similarly, Pérez-Emán (2005) found *Myioborus pariae* (Aves: Parulidae), which is endemic to the Península de Paria (CC Oriental), to be

the sister taxon of a clade composed of three species of *Myioborus* that are endemic to the tepuis. Three hypotheses exist for the origin of the tepuis' biota that have close affinities to other montane regions. First, tepuis taxa come from widely distributed species in the Neotropical montane regions and vicariance drove their speciation. Second, multiple dispersal events from the Andes and other montane regions account for these taxa. Third, an 'ancient tepui' biota has contributed elements to younger montane regions, including the Andes (Bonaccorso and Guayasamin, 2013; and citations therein).

Sierra Nevada de Santa Marta (SNSM): origin of its montane, endemic vertebrate fauna. Lower elevation dry forests, xeric shrublands and wide alluvial plains isolate the SNSM (c. 5800 m maximum elevation) from other Andean wet forests. It does not have a physical association with the other Andean ranges, and seems to be older than the Andes (Tschanz et al., 1974; Simpson, 1975; Lynch and Ruíz-Carranza, 1985; Guayasamin et al., 2009). Consequently, the SNSM is a centre of endemism for multiple plant and animal groups, especially in the highland cloud forests and páramos (Ruthven, 1922; Cadena et al., 2016 and citations therein). Several hypotheses have been proposed to explain the origin and associations of the endemic vertebrates of the SNSM. Ruthven (1922) and Carriker (in Ruthven, 1922) attributed the fauna to the lowland forest of the Magdalena basin. Carriker⁴, Walker and Test (1955), Rivero (1961), and Lynch (in Duellman, 1979) tied it to the Cordillera de la Costa (CC). Lynch (1976) suggested affinities with the West Indies (Antilles). Lynch and Ruíz-Carranza (1985) pointed to the (northern) Andes and/or other Santa Martan species. The inclusion of montane, endemic terrestrial vertebrates from the SNSM in modern phylogenetic studies using DNA sequences (including the present analysis) allow testing of these historical biogeographic scenarios.

In their phylogenetic analysis of the (current) genus *Arremon* (Aves: Emberizidae), Cadena et al. (2007; see also Cadena and Cuervo, 2010) included the SNSM endemic *A. basilicus* (300–1200 m a.s.l.). Their combined analysis of mitochondrial and nuclear genes recovered *A. basilicus* and *A. phygas*, which is endemic to the CC Oriental (Serranía de Turimiquire and Peninsula de Paria), as sister species. The phylogeographic analysis of *Henicorhina leucophrys* (Aves:

Troglodytidae) by Caro et al. (2013; see also Cadena et al., 2016) found *H. anachoreta* (1800–3600 m a.s.l.) and *H. l. bangsi* (600–2100 m a.s.l.), two congeneric (and until recently conspecific) taxa that are endemic to the SNSM, to be more closely related to different populations of *H. leucophrys* on the northern Andes than to each other. Notwithstanding, the high capacity of birds to disperse might have played an important role in initially colonizing the SNSM from geographically proximate areas (e.g. Serranía de Perijá). This scenario leaves uncertain the phylogenetic relationships of SNSM endemic non-avian terrestrial vertebrates. Guayasamin et al. (2009) included the SNSM endemic *Ikakogi tayrona* (980–1790 m a.s.l.) in their molecular-based phylogenetic analyses of glassfrogs (Amphibia: Centrolenidae). Their combined analysis of mitochondrial and nuclear genes found *I. tayrona* to be the sister taxon of all other Centrolenidae (150 species distributed throughout Tropical Central America, Tropical Andes, CC, Tobago, Guiana Shield, Amazon Basin and Atlantic Forest of Brazil). Thus, this study does not shed light on specific biogeographical patterns. In contrast, Castroviejo-Fisher et al. (2015) included the SNSM endemic *Cryptobatrachus boulengeri* (360–1790 m a.s.l.) in their molecular phylogenetic analysis of egg-brooding frogs (Anura: Hemiphractidae). This species nested within a monophyletic *Cryptobatrachus*, a genus also composed of five montane species from the northern Andes of Colombia and Venezuela (e.g. Serranía de Perijá).

Our study is the first to include a SNSM endemic non-avian reptile in a phylogenetic analysis using DNA sequences. Again, *Oreosaurus* “Sierra Nevada” (2156 m a.s.l.) is the sister of its congeners, which occur in the CC, on the island of Trinidad, and the tepuis (Figs 1 and 3). Thus, *O.* “Sierra Nevada” does not have a close relationship with Andean radiations of cercosaurines (e.g. *Riama*). This leads to two scenarios for relationships of montane SNSM endemic vertebrates. First, Caro et al. (2013) suggested allopatric speciation for two SNSM endemic birds (*Henicorhina anachoreta* and *H. l. bangsi*) after independent colonization events from geographically proximate Andean ranges (e.g. Serranía de Perijá). The phylogenetic relationships of one SNSM endemic frog (*Cryptobatrachus boulengeri*; Castroviejo-Fisher et al., 2015) support the hypothesis of a biogeographical association between the SNSM and the northern Andes (Lynch and Ruíz-Carranza, 1985). Geologically, the SNSM and the Serranía de San Lucas (northern Cordillera Central of Colombia) are both “composed of Palaeozoic and Precambrian continental rocks intruded by Mesozoic and Cenozoic plutons”, with the SNSM being displaced by the Santa Marta–Bucaramanga fault (Taboada et al., 2000: 797). Second, for the case of one bird (*Arremon basilicus*) and one lizard (*O.* “Sierra Nevada”), we

⁴Carriker (in Ruthven, 1922) stated that “we have in the mountain mass an absolutely isolated area containing its own distinctive habitats and faunal characteristics, into which enter but two outside influences, that of the Magdalena basin on the southwest and that of the central plateau of Venezuela through the Goajira Peninsula on the east” [sic]. We interpret the latter as the CC Central.

hypothesize that an ancient biogeographical connection facilitated the exchange of species between the SNSM and the CC, but geological events subsequently severed the connection. Isolation drove genetic differentiation and speciation. The phylogenetic evidence provided by Cadena et al. (2007) and our analyses cannot reject this hypothesis. Previously, Carriker (in Ruthven, 1922), Walker and Test (1955), Rivero (1961) and Lynch (in Duellman, 1979) suggested affinities between the biota of the SNSM and CC. The Seranía de Macuira may be a remnant of this connection. This mountain range (maximum height of c. 864 m a.s.l.) stands in the middle of the La Guajira desert (Guajira Peninsula, Colombia). It is isolated from the SNSM and the Andean Cordillera Oriental of Colombia, and located approximately halfway (northward) between the SNSM and the westernmost portion of the CC. Its vegetation is composed mainly of wet dwarf and cloud forests. Geological data from the Sevilla Complex of the SNSM include the occurrence of rocks such as Palaeozoic orthogneisses and schists, which were intruded by Permian–Late Triassic syntectonic granitoids. These rocks are similar to those observed in the Macuira Formation (Cardona Molina et al., 2006). Future phylogenetic analysis can test our hypothesis by using Macuira endemic species, such as the aromobatid frog *Allobates wayuu*.

Relevant to the proposed biogeographical scenario, *Oreosaurus rhodogaster* and *O. luctuosus* from the CC were not included herein. Both species were hypothesized to be closely related to *O. achlyens*, also from CC, and *O. shrevei* from Trinidad, which were included. Further, *Riama inanis* from the Venezuelan Mérida Andes was not included in our analyses but was referred herein to Andean *Riama* (Appendix 4). Although ultimately these actions may be found to be false, only the embedding of *R. inanis* within *Oreosaurus* might overturn our hypothesis and favor alternative biogeographical explanations.

Lynch (1978) and Duellman (1979) said the SNSM fauna was Andean, but later Lynch and Ruíz-Carranza (1985) pointed out that these conclusions were based on shared, widely distributed species. Based on morphology, Lynch and Ruíz-Carranza (1985) suggested that SNSM frogs of the (current) genus *Pristimantis* (including eight endemic species) were not closely related to taxa in the Antilles (Lynch, 1976) and the CC, but instead to either species found in the northern Andes of Colombia or to other SNSM species. These hypotheses remain to be tested. Similarly, the influence of the surrounding lowlands (e.g. Magdalena basin; Ruthven, 1922) on the origin of the montane SNSM endemic vertebrates awaits clarification. Finally, future phylogenetic analyses should try to include multiple SNSM endemic congeneric species (e.g. frogs of the genus *Pristimantis* and lizards of the genus *Anolis*).

Acknowledgements

Funding for S.J.S-P. was provided by a COLCIENCIAS doctoral fellowship (Becas Francisco José de Caldas), an Ontario Graduate Scholarship (OGS) at the University of Toronto, a Coordenadoria de Aperfeiçoamento de Pessoal de Ensino Superior (CAPES) master's fellowship, and an American Museum of Natural History Collection Study Grant. NSERC Discovery Grant 3148 supported the research. T.G. was supported by Conselho Nacional de Desenvolvimento Científico e Tecnológico Proc. 307001/2011-3 and Fundação de Amparo à Pesquisa do Estado de São Paulo (FAPESP) Proc. 2012/10000-5. Field, specimen curation, and laboratory work by O.T-C. and V.A-P were funded by grants from Secretaría de Educación Superior, Ciencia, Tecnología e Innovación (SENES-CYT, Arca de Noé Initiative; S.R. Ron and O.T-C. Principal Investigators). M.T.R. was supported by Conselho Nacional de Desenvolvimento Científico e Tecnológico and FAPESP Proc. 2003/10335-8 and 2011/50146-6. P.M.S.N. was supported by Fundação de Amparo à Ciência e Tecnologia do Estado de Pernambuco (FACEPE) and FAPESP Proc. 2012/00492-8. We thank M. O'Leary, J.M. Padial and an anonymous reviewer for constructive criticism of the manuscript. S.J.S-P. thanks D. Frost and D.A. Kizirian for workspace and other facilities provided during his stay at the AMNH. For access to collections and specimen and tissue loans we are grateful to D.A. Kizirian (AMNH), K. de Queiroz and T.D. Hartsell (USNM), J. Rosado (MCZ), R.A. Nussbaum and G. Schneider (UMMZ), A. Resetar (FMNH), L. Trueb and A. Campbell (KU), S. Kullander and E. Ahlander (NRM), F. Castro and W. Bolívar (UV-C), J.J. Calderón (PSO-CZ), V. Páez (MHUA), A. Zamudio and A. Ortiz (MHNCSJ), J. Salazar and H.F. Arias (MHNUC), J.A. Maldonado (IAvH), M.L. Calderón Espinosa (ICN), C.L. Spencer and S. Werning (MVZ), J.V. Vindum (CAS-SUR), A. Almendáriz (EPNH), M. Yáñez-Muñoz (DHMECN), J. Valencia (FHGO), P.J. Venegas and L.Y. Echevarría (CORBIDI), M. Borges Martins (UFRGS), J.M. Hoyos (MUJ), M.G. Rutherford (UWI), M. Rada, A. Mejía Tobón, and J.J. Mueses Cisneros. S.J.S-P. thanks P. Pulido-Santacruz, S.B. Arroyo, J.J. Ospina-Sarria, M. Anganoy-Criollo, S. Marques Sousa, L. Saboyá-Acosta and M. Targino Rocha for arranging logistics and collaborating on fieldwork in Colombia.

References

- Aguirre-Peñafiel, V., Torres-Carvajal, O., Nunes, P.M.S., Peck, M.R., Maddock, S.T., 2014. A new species of *Riama* Gray, 1858 (Squamata: Gymnophthalmidae) from the tropical Andes. *Zootaxa* 3866, 246–260.

- Andersson, L.G., 1914. A new *Telmatobius* and new teiidoid lizards from South America. *Arkiv Zool.* 9, 1–12.
- Arévalo, E.S., Davis, S.K., Sites, J.W. Jr, 1994. Mitochondrial DNA sequence divergence and phylogenetic relationships among eight chromosome races of the *Sceloporus grammicus* complex (Phrynosomatidae) in central Mexico. *Syst. Biol.* 43, 387–418.
- Arredondo, J.C., Sánchez-Pacheco, S.J., 2010. New endemic species of *Riama* (Squamata: Gymnophthalmidae) from northern Colombia. *J. Herpetol.* 44, 610–617.
- Bonaccorso, E., Guayasamin, J.M., 2013. On the origin of Pantepui montane biotas: a perspective based on the phylogeny of *Aulacorhynchus* toucanets. *PLoS ONE*, 6732, 1.
- Bonaccorso, E., Guayasamin, J.M., Peterson, A.T., Navarro-Siguenza, A.G., 2011. Molecular phylogeny and systematics of Neotropical toucanets in the genus *Aulacorhynchus* (Aves, Ramphastidae). *Zool. Scripta* 40, 336–349.
- Boulenger, G.A., 1885. *Catalogue of the Lizards in the British Museum (Natural History)*, 2nd edn, Vol. 2. Taylor and Francis, London.
- Bremer, K., 1988. The limits of amino acid sequence data in angiosperm phylogenetic reconstruction. *Evolution* 42, 795–803.
- Brown, J.H., Lomolino, M.V., 1998. *Biogeography*. Sinauer Associates, Sunderland, MA.
- Burt, C.E., Burt, M.D., 1931. South American lizards in the collection of the American Museum of Natural History. *Bull. Am. Mus. Nat. Hist.* 61, 227–395.
- Cadena, C.D., Cuervo, A.M., 2010. Molecules, ecology, morphology, and songs in concert: how many species is *Arremon torquatus* (Aves: Emberizidae)? *Biol. J. Linn. Soc.* 99, 152–176.
- Cadena, C.D., Klicka, J., Ricklefs, R.E., 2007. Evolutionary differentiation in the Neotropical montane region: molecular phylogenetics and phylogeography of *Buarremon* brush-finches (Aves, Emberizidae). *Mol. Phylogenet. Evol.* 44, 993–1016.
- Cadena, C.D., Caro, L.M., Caycedo, P.C., Cuervo, A.M., Bowie, R.C.K., Slabbekoorn, H., 2016. *Henicorhina anachoreta* (Troglodytidae), another endemic bird species for the Sierra Nevada de Santa Marta, Colombia. *Ornitología Colombiana* 15, 82–89.
- Cardona Molina, A., Cordani, U.G., MacDonald, W.D., 2006. Tectonic correlations of pre-Mesozoic crust from the northern termination of the Colombian Andes, Caribbean region. *J. South Am. Earth Sci.* 21, 337–354.
- Caro, L.M., Caycedo-Rosales, P.C., Bowie, R.C.K., Slabbekoorn, H., Cadena, C.D., 2013. Ecological speciation along an elevational gradient in a tropical passerine bird? *J. Evol. Biol.* 26, 357–374.
- Castoe, T.A., Doan, T.M., Parkinson, C.L., 2004. Data partitions and complex models in Bayesian analysis: the phylogeny of gymnophthalmid lizards. *Syst. Biol.* 53, 448–469.
- Castroviejo-Fisher, S., Padial, J.M., De la Riva, I., Pombal, J.P. Jr, Da Silva, H.R., Rojas-Runjaic, F.J.M., Medina-Méndez, E., Frost, D.R., 2015. Phylogenetic systematics of egg-brooding frogs (Anura: Hemiphractidae) and the evolution of direct development. *Zootaxa* 4004, 1–75.
- Chapman, F.M., 1931. The upper zonal bird-life of Mts. Roraima and Duida. *Bull. Am. Mus. Nat. Hist.* 63, 1–135.
- Colli, G.R., Hoogmoed, M.S., Canatella, D.C., Cassimiro, J., Oliveira Gomes, J., Ghellere, J.M., Nunes, P.M.S., Pellegrino, K.C.M., Salerno, P., Marques de Souza, S.M., Rodrigues, M.T., 2015. Description and phylogenetic relationships of a new genus and two new species of lizards from Brazilian Amazonia, with nomenclatural comments on the taxonomy of Gymnophthalmidae (Reptilia: Squamata). *Zootaxa* 4000, 401–427.
- Doan, T.M., 2003a. A south-to-north biogeographic hypothesis for Andean speciation: evidence from the lizard genus *Proctoporus* (Reptilia, Gymnophthalmidae). *J. Biogeogr.* 30, 361–374.
- Doan, T.M., 2003b. A new phylogenetic classification for the gymnophthalmid genera *Cercosaura*, *Pantodactylus* and *Prionodactylus* (Reptilia: Squamata). *Zool. J. Linn. Soc.* 137, 101–115.
- Doan, T.M., Castoe, T.A., 2003. Using morphological and molecular evidence to infer species boundaries within *Proctoporus bolivianus* Werner (Squamata: Gymnophthalmidae). *Herpetologica* 59, 432–449.
- Doan, T.M., Castoe, T.A., 2005. Phylogenetic taxonomy of the Cercosaurini (Squamata: Gymnophthalmidae), with new genera for species of *Neusticurus* and *Proctoporus*. *Zool. J. Linn. Soc.* 143, 405–416.
- Doan, T.M., Schargel, W.E., 2003. Bridging the gap in *Proctoporus* distribution: a new species (Squamata: Gymnophthalmidae) from the Andes of Venezuela. *Herpetologica* 59, 68–75.
- Doan, T.M., Castoe, T.A., Arizabal Arriaga, W., 2005. Phylogenetic relationships of the genus *Proctoporus* sensu stricto (Squamata: Gymnophthalmidae), with a new species from Puno, southeastern Peru. *Herpetologica* 61, 325–336.
- Donnelly, M.A., MacCulloch, R.D., Ugarte, C.A., Kizirian, D., 2006. A new riparian gymnophthalmid (Squamata) from Guyana. *Copeia* 3, 396–403.
- Dowling, H.G., Savage, J.M., 1960. A guide to the snake hemipenis: a survey of basic structure and systematic characteristics. *Zoologica* 45, 17–28.
- Duellman, W.E., 1979. The herpetofauna of the Andes: patterns of distribution, origin, differentiation, and present communities. In: Duellman, W.E. (Ed.), *The South American Herpetofauna: Its Origin, Evolution, and Dispersal*. Monogr. Mus. Nat. Hist., Univ. Kans. 7. MNHUK, Lawrence, KA, pp. 371–459.
- Echevarría, L.Y., Venegas, P.J., 2015. A new elusive species of *Petracola* (Squamata: Gymnophthalmidae) from the Utcubamba basin in the Andes of northern Peru. *Amphib. Reptile Conserv.* 9, 26–33.
- Estes, R., Queiroz, K., Gauthier, J. 1988. Phylogenetic relationships within the Squamata. In: Estes, R., Pregill, G. (Eds.), *Phylogenetic Relationships of the Lizard Families - Essays Commemorating Charles L. Camp*. Stanford University Press, Stanford, CA, pp. 119–281.
- Farris, J.S., 1983. The logical basis of phylogenetic analysis. In: Platnick, N.I., Funk, V.A. (Eds.), *Advances in Cladistics: Proceedings of the Third Meeting of the Willi Hennig Society II*. Columbia University Press, New York, NY, Vol. 2, pp. 7–36.
- Frost, D.R., Grant, T., Faivovich, J., Bain, R.H., Haas, A., Haddad, C.F.B., de Sá, R.O., Channing, A., Wilkinson, M., Donnellan, S.C., Raxworthy, C.J., Campbell, J.A., Blotto, B.L., Moler, P., Drewes, R.C., Nussbaum, R.A., Lynch, J.D., Green, D.M., Wheeler, W.C., 2008. Is *The Amphibian Tree of Life* really fatally flawed? *Cladistics* 24, 385–395.
- Fu, J., 2000. Toward the phylogeny of the family Lacertidae—Why 4708 base pairs of mtDNA sequences cannot draw the picture. *Biol. J. Linn. Soc.* 71, 203–217.
- García-Pérez, J.L., Yustiz, E.E., 1995. Una nueva especie de *Proctoporus* (Sauria: Gymnophthalmidae) de los Andes de Venezuela. *Rev. Ecol. Latinoam.* 4, 1–5.
- Goicoechea, N., Padial, J.M., Chaparro, J.C., Castroviejo-Fisher, S., De la Riva, I., 2012. Molecular phylogenetics, species diversity, and biogeography of the Andean lizards of the genus *Proctoporus* (Squamata: Gymnophthalmidae). *Mol. Phylogenet. Evol.* 65, 953–964.
- Goicoechea, N., Padial, J.M., Chaparro, J.C., Castroviejo-Fisher, S., De la Riva, I., 2013. A taxonomic revision of *Proctoporus bolivianus* Werner (Squamata: Gymnophthalmidae) with the description of three new species and resurrection of *Proctoporus lacertus* Stejneger. *Am. Mus. Novit.* 3786, 1–32.
- Goicoechea, N., Frost, D.R., De la Riva, I., Pellegrino, K.C.M., Sites, J. Jr, Rodrigues, M.T., Padial, J.M., 2016. Molecular systematics of teioid lizards (Teioidea/Gymnophthalmoidea: Squamata) based on the analysis of 48 loci under tree-alignment and similarity-alignment. *Cladistics* 32, 624–671.
- Goloboff, P.A., 1996. Methods for faster parsimony analysis. *Cladistics* 12, 199–220.
- Goloboff, P.A., 1999. Analyzing large data sets in reasonable times: solutions for composite optima. *Cladistics* 15, 415–428.

- Goloboff, P.A., 2003. Parsimony, likelihood, and simplicity. *Cladistics* 19, 91–103.
- Goloboff, P.A., Pol, D., 2005. Parsimony and Bayesian phylogenetics. In: Albert, V.A. (Ed.), *Parsimony, Phylogeny, and Genomics*. Oxford University Press, Oxford, pp. 148–159.
- Goloboff, P.A., Mattoni, C.I., Quinteros, A.S., 2006. Continuous characters analyzed as such. *Cladistics* 22, 589–601.
- Goodman, M., Olson, C.B., Beeber, J.E., Czelusniak, J., 1982. New perspectives in the molecular biological analysis of mammalian phylogeny. *Acta Zool. Fenn.* 169, 19–35.
- Gorzula, S., 1987. Una revisión de los orígenes de la fauna de vertebrados del Pantepui. *Pantepui* 3, 4–10.
- Grant, T., Kluge, A.G., 2003. Data exploration in phylogenetic inference: scientific, heuristic, or neither. *Cladistics* 19, 379–418.
- Grant, T., Kluge, A.G., 2004. Transformation series as an ideographic character concept. *Cladistics* 20, 23–31.
- Grant, T., Kluge, A.G., 2007. Ratio of explanatory power (REP): a new measure of group support. *Mol. Phylog. Evol.* 44, 483–487.
- Grant, T., Kluge, A.G., 2008a. Clade support measures and their adequacy. *Cladistics* 24, 1051–1064.
- Grant, T., Kluge, A.G., 2008b. Credit where credit is due: the Goodman-Bremer support metric. *Mol. Phylog. Evol.* 49, 405–406.
- Grant, T., Kluge, A.G., 2009. Parsimony, explanatory power, and dynamic homology testing. *Syst. Biodivers.* 7, 357–363.
- Grant, T., Kluge, A.G., 2010. REP provides meaningful measurement of support across datasets. *Mol. Phylog. Evol.* 55, 340–342.
- Grant, T., Frost, D.R., Caldwell, J.P., Gagliardo, R., Haddad, C.F.B., Kok, P.J.R., Means, D.B., Noonan, B.P., Schargel, W.E., Wheeler, W.C., 2006. Phylogenetic systematics of dart-poison frogs and their relatives (Amphibia: Athesphatanura: Dendrobatidae). *Bull. Am. Mus. Nat. Hist.* 299, 1–262.
- Guayasamin, J.M., Castroviejo-Fisher, S., Trueb, L., Ayarzagüena, J., Rada, M., Vilà, C., 2009. Phylogenetic systematics of Glassfrogs (Amphibia: Centrolenidae) and their sister taxon *Allophryne ruthveni*. *Zootaxa* 2100, 1–97.
- Harris, D.J., Arnold, E.N., Thomas, R.H., 1998. Relationships of lacertid lizards (Reptilia: Lacertidae) estimated from mitochondrial DNA sequences and morphology. *Proc. R. Soc. Lond. B* 265, 1939–1948.
- Hennig, W., 1966. *Phylogenetic Systematics*. University of Illinois Press, Chicago, IL.
- Kaiser, H., Barrio-Amorós, C.L., Rivas, G.A., Steinlein, C., Schmid, M., 2015. Five new species of *Pristimantis* (Anura: Strabomantidae) from the coastal cloud forest of the Península de Paria, Venezuela. *J. Threat. Taxa* 7, 7047–7088.
- Katoh, K., Kuma, K., Toh, H., Miyata, T., 2005. MAFFT, a novel method for rapid multiple sequence alignment based on fast Fourier transform. *Nucleic Acids Res.* 30, 3059–3066.
- Kearse, M., Moir, R., Wilson, A., Stones-Havas, S., Cheung, M., Sturrock, S., Buxton, S., Cooper, A., Markowitz, S., Duran, C., Thierer, T., Ashton, B., Menjites, P., Drummond, A., 2012. Geneious Basic: an integrated and extendable desktop software platform for the organization and analysis of sequence data. *Bioinformatics* 28, 1647–1649.
- Kizirian, D.A., 1995. A new species of *Proctoporus* (Squamata: Gymnophthalmidae) from the Andean Cordillera Oriental of northeastern Ecuador. *J. Herpetol.* 29, 66–72.
- Kizirian, D.A., 1996. A review of Ecuadorian *Proctoporus* (Squamata: Gymnophthalmidae) with descriptions of nine new species. *Herpetol. Monogr.* 10, 85–155.
- Kizirian, D.A., Coloma, L.A., 1991. A new species of *Proctoporus* (Squamata: Gymnophthalmidae) from Ecuador. *Herpetologica* 47, 420–429.
- Kizirian, D., Bayefsky-Anand, S., Eriksson, A., Le, M., Donnelly, M.A., 2008. A new *Petracola* and re-description of *P. ventrimaculatus* (Squamata: Gymnophthalmidae). *Zootaxa* 1700, 53–62.
- Kluge, A.G., 1983. Cladistics and the classification of the great apes. In: Cicochon, R.I., Corruccini, R.S. (Eds.), *New Interpretations of Ape and Human Ancestry*. Plenum Press, New York, NY, pp. 151–177.
- Kluge, A.G., 1989. A concern for evidence and a phylogenetic hypothesis of relationships among *Epicrates* (Boidae, Serpentes). *Syst. Zool.* 38, 7–25.
- Kluge, A.G., 2004. On total evidence: for the record. *Cladistics* 20, 205–207.
- Kluge, A.G., Grant, T., 2006. From conviction to anti-superfluity: old and new justifications of parsimony in phylogenetic inference. *Cladistics* 22, 276–288.
- Kocher, T.D., Thomas, W.K., Meyer, A., Edwards, S.V., Pääbo, S., Villablanca, F.X., Wilson, A.C., 1989. Dynamics of mitochondrial DNA evolution in animals: amplification and sequencing with conserved primers. *Proc. Natl Acad. Sci. USA* 86, 6196–6200.
- Köhler, G., Lehr, E., 2004. Comments on *Euspondylus* and *Proctoporus* (Squamata: Gymnophthalmidae) from Peru, with the description of three new species and a key to the Peruvian species. *Herpetologica* 60, 501–518.
- Kok, P.J.R., 2015. A new species of the Pantepui endemic genus *Riolama* (Squamata: Gymnophthalmidae) from the summit of Murispán-tepui, with the erection of a new gymnophthalmid subfamily. *Zool. J. Linn. Soc.* 174, 500–518.
- Kok, P.J.R., Rivas, G.A., 2011. A new species of *Anadia* (Reptilia, Squamata) from the Venezuelan ‘Lost World’, northern South America. *Eur. J. Taxon.* 3, 1–18.
- Kok, P.J.R., MacCulloch, R.D., Means, D.B., Roelants, K., Bocxlaer, I.V., Bossuyt, F., 2012. Low genetic diversity in tepui summit vertebrates. *Curr. Biol.* 22, 589–590.
- Kok, P.J.R., Means, D.B., Rivas, G.A., 2013. First record of the genus *Anadia* (Reptilia: Squamata: Gymnophthalmidae) from Guyana based on an enigmatic specimen from mount Kopinang, Wokomung massif. *Bol. Mus. Para. Emílio Goeldi Cienc. Nat.* 8, 27–39.
- Liddle, R.A., 1946. *The Geology of Venezuela and Trinidad*. Paleontological Research Institution, Ithaca, NY.
- Lynch, J.D., 1976. The species groups of the South American frogs of the genus *Eleutherodactylus* (Leptodactylidae). *Occ. Pap. Mus. Nat. Hist. Univ. Kansas* 61, 1–24.
- Lynch, J.D., 1978. A new eleutherodactyline frog from the Andes of northern Colombia (Leptodactylidae). *Copeia* 1978, 17–21.
- Lynch, J.D., Ruiz-Carranza, P.M., 1985. A synopsis of the frogs of the genus *Eleutherodactylus* from the Sierra Nevada de Santa Marta, Colombia. *Occ. Pap. Mus. Zool. Univ. Mich.* 711, 1–59.
- Mamani, L., Goicoechea, N., Chaparro, J.C., 2015. A new species of Andean lizard *Proctoporus* (Squamata: Gymnophthalmidae) from montane forest of the Historic Sanctuary of Machu Picchu, Peru. *Amphib. Reptile Conserv.* 9, 1–11.
- Manzani, P.R., Abe, A.S., 1988. Sobre dois novos métodos de preparo do hemipenis de serpentes. *Mem. Inst. Butantan* 50, 15–20.
- Manzanilla, J., La Marca, E., García-París, M., 2009. Phylogenetic patterns of diversification in a clade of Neotropical frogs (Anura: Aromobatidae: *Mannophryne*). *Biol. J. Linn. Soc.* 97, 185–199.
- Mauck, W.M., Burns, K.J., 2009. Phylogeny, biogeography, and recurrent evolution of divergent bill types in the nectar-stealing flowerpiercers (Thraupini: *Diglossa* and *Diglossopsis*). *Biol. J. Linn. Soc.* 98, 14–28.
- Mirande, J.M., 2016. Combined phylogeny of ray-finned fishes (Actinopterygii) and the use of morphological characters in large-scale analyses. *Cladistics*. doi: 10.1111/cla.12171
- Molina, C., Señaris, J.C., 2003. Una nueva especie del género *Riolama* (Reptilia: Gymnophthalmidae) de las tierras altas del estado Amazonas, Venezuela. *Mem. Fund. La Salle Cienc. Nat.* 155, 5–19.
- Montero, R., Moro, S.A., Abdala, V., 2002. Cranial anatomy of *Euspondylus acutirostris* (Squamata: Gymnophthalmidae) and its placement in a modern phylogenetic hypothesis. *Russ. J. Herpetol.* 9, 215–228.

- Murphy, R.W., 1993. The phylogenetic analysis of allozyme data: invalidity of coding alleles by presence/absence and recommended procedures. *Biochem. Syst. Ecol.* 21, 25–38.
- Murphy, R.W., Doyle, K.D., 1998. Phylogenetics: frequencies and polymorphic characters in genealogical estimation. *Syst. Biol.* 47, 737–761.
- Myers, C.W., Donnelly, M.A., 2001. Herpetofauna of the Yutajé–Corocoro massif, Venezuela: second report from the Robert G. Goelt American Museum–Terrarum expedition to the Northwestern tepuis. *Bull. Am. Mus. Nat. Hist.* 261, 1–85.
- Myers, C.W., Rivas Fuenmayor, G., Jadin, R.C., 2009. New species of lizards from Auyantepui and La Escalera in the Venezuelan Guayana, with notes on “microteiid” hemipenes (Squamata: Gymnophthalmidae). *Am. Mus. Novit.* 3660, 1–31.
- Nixon, K.C., 1999. The parsimony ratchet, a new method for rapid parsimony analysis. *Cladistics* 15, 407–414.
- Nunes, P.M.S. 2011. Morfologia hemipeniana dos lagartos microteídeos e suas implicações nas relações filogenéticas da família Gymnophthalmidae (Teioidea: Squamata). Ph.D. Dissertation, Universidade de São Paulo, São Paulo, Brazil.
- Nunes, P.M.S., Fouquet, A., Curcio, F.F., Kok, P.J.R., Rodrigues, M.T., 2012. Cryptic species in *Iphisa elegans* Gray, 1851 (Squamata: Gymnophthalmidae) revealed by hemipenial morphology and molecular data. *Zool. J. Linn. Soc.* 166, 361–376.
- Nunes, P.M.S., Curcio, F.F., Roscito, J.G., Rodrigues, M., 2014. Are hemipenial spines related to limb reduction? A spiny discussion focused on gymnophthalmid lizards (Squamata: Gymnophthalmidae). *Anat. Rec.* 297, 482–495.
- Oftedal, O.T., 1974. A revision of the genus *Anadia* (Sauria, Teiidae). *Arqu. Zool.* 25, 203–265.
- O’Leary, M.A., Kaufman, S.G., 2011. MorphoBank: phylogenomics in the ‘cloud’. *Cladistics* 27, 1–9.
- O’Leary, M.A., Kaufman, S.G., 2012. MorphoBank 3.0: Web application for morphological phylogenetics and taxonomy. Available at: <http://www.morphobank.org>. (accessed 24 January 2017)
- Padial, J.M., Grant, T., Frost, D.R., 2014. Molecular systematics of terraranas (Anura: Brachycephaloidea) with an assessment of the effects of alignment and optimality criteria. *Zootaxa* 3825, 1–132.
- Pellegrino, K.C.M., Rodrigues, M.T., Yonenaga-Yassuda, Y., Sites, J.W. Jr, 2001. A molecular perspective on the evolution of microteiid lizards (Squamata, Gymnophthalmidae), and a new classification for the family. *Biol. J. Linn. Soc.* 74, 315–338.
- Pérez-Emán, J., 2005. Molecular phylogenetics and biogeography of the Neotropical redstars (Myioborus: Aves, Parulidae). *Mol. Phylog. Evol.* 37, 511–528.
- Pesantes, O.S., 1994. A method for preparing the hemipenis of preserved snakes. *J. Herpetol.* 28, 93–95.
- Peters, W., 1862. Über *Cercosaura* und die mit dieser Gattung verwandten Eidechsen aus Südamerika. *Aus Den Abhandlungen der Königl. Akad. Wiss. Berlin* 1862, 165–225.
- Peters, J.A., Donoso-Barros, R., 1970. Catalogue of the Neotropical Squamata, Part II, lizards and amphisbaenians. *Bull. U.S. Nat. Mus.* 297, 1–293.
- Pyron, R.A., Burbrink, F.T., Wiens, J.J., 2013. A phylogeny and revised classification of Squamata, including 4161 species of lizards and snakes. *BMC Evol. Biol.*, 13, 93.
- Reeder, T.W., 1996. A new species of *Pholidobolus* (Squamata: Gymnophthalmidae) from the Huancabamba depression of northern Peru. *Herpetologica* 52, 282–289.
- Rivas, G.A., de Freitas, S.M., 2015. Discovery of the critically endangered Golden Tree Frog, *Phytotriades auratus* (Boulenger, 1917), in eastern Venezuela, with comments on its distribution, conservation, and biogeography. *Herpetol. Rev.* 46, 153–157.
- Rivas, G., Schargel, W.E., Meik, J.M., 2005. A new species of *Riama* (Squamata: Gymnophthalmidae), endemic to the Península de Paria, Venezuela. *Herpetologica* 61, 461–468.
- Rivas, G.A., Molina, C.R., Ugueto, G.N., Barros, T.R., Barrio-Amorós, C.L., Kok, P.J.R., 2012. Reptiles of Venezuela: an updated and commented checklist. *Zootaxa* 3211, 1–64.
- Rivero, J.A., 1961. Salientia of Venezuela. *Bull. Mus. Comp. Zool.* 126, 1–207.
- Rodrigues, M.T., Freire, E.M.X., Pellegrino, K.C.M., Sites, J.W. Jr, 2005. Phylogenetic relationships of a new genus and species of microteiid lizard from the Atlantic forest of north-eastern Brazil (Squamata, Gymnophthalmidae). *Zool. J. Linn. Soc.* 144, 543–557.
- Rodrigues, M.T., Pellegrino, K.C.M., Dixo, M., Verdade, V.K., Pavan, D., Argolo, A.J.S., Sites, J.W. Jr, 2007. A new genus of microteiid lizard from the Atlantic forests of state of Bahia, Brazil, with a new generic name for *Colobosaura mentalis*, and a discussion of relationships among the Heterodactylini (Squamata, Gymnophthalmidae). *Am. Mus. Novit.* 3565:1–27.
- Rull, V., 2009. Pantepui. In: Gillespie, R.G., Clague, D.A. (Eds.), *Encyclopedia of Islands*. University of California Press, Berkeley, CA, pp. 717–720.
- Ruthven, A.G., 1922. The amphibians and reptiles of the Sierra Nevada de Santa Marta, Colombia. *Misc. Publ. Mus. Zool. Univ. Mich.* 8, 1–69.
- de Sá, R.O., Grant, T., Camargo, A., Heyer, W.R., Ponsa, M.L., Stanley, E., 2014. Systematics of the Neotropical genus *Leptodactylus* Fitzinger, 1826 (Anura: Leptodactylidae): Phylogeny, the relevance of non-molecular evidence, and species accounts. *South Am. J. Herpetol.* 9, S1–S128.
- Sabaj Pérez, M.H. 2014. Standard symbolic codes for institutional resource collections in herpetology and ichthyology: an Online Reference. Version 5.0 (22 September 2014). Electronically Available at: <http://www.asih.org/>, American Society of Ichthyologists and Herpetologists, Washington, DC.
- Saint, K.M., Austin, C.C., Donnellan, S.C., Hutchinson, M.N., 1998. C-mos, a nuclear marker useful for squamate phylogenetic analysis. *Mol. Phylogenet. Evol.* 10, 259–263.
- Salerno, P.E., Ron, S.R., Señaris, J.C., Rojas-Runjaic, F.J.M., Noonan, B.P., Cannatella, D.C., 2012. Ancient tepui summits harbor young rather than old lineages of endemic frogs. *Evolution* 66, 3000–3013.
- Sánchez-Pacheco, S.J., 2010a. A new “microteiid” lizard (Squamata: Gymnophthalmidae: *Riama*) from southwestern Colombia. *Herpetologica* 66, 349–356.
- Sánchez-Pacheco, S.J., 2010b. Lectotype designation and redescription of the gymnophthalmid lizard *Riama columbiana* (Andersson, 1914) with notes on the type locality. *Pap. Avulsos Zool.* 50, 31–41.
- Sánchez-Pacheco, S.J., Rueda-Almonacid, J.V., Rada, M., 2010. Notes on the occurrence of *Riama simotera* (Squamata, Gymnophthalmidae) in Colombia. *Herpetol. Bull.* 113, 11–13.
- Sánchez-Pacheco, S.J., Kizirian, D.A., Nunes, P.M.S., 2011. A new species of *Riama* from Ecuador previously referred to as *Riama hyposticta* (Boulenger, 1902) (Squamata: Gymnophthalmidae). *Am. Mus. Novit.* 3719, 1–15.
- Sánchez-Pacheco, S.J., Aguirre-Peñafiel, V., Torres-Carvajal, O., 2012. Lizards of the genus *Riama* (Squamata: Gymnophthalmidae): the diversity in southern Ecuador revisited. *South Am. J. Herpetol.* 7, 259–275.
- Sankoff, D., 1975. Minimal mutation trees of sequences. *SIAM J. Appl. Math.* 28, 35–42.
- Savage, J.M., 1997. On terminology for the description of the hemipenes of squamate reptiles. *Herpetol. J.* 7, 23–25.
- Schargel, W.E., Rivas F., G., Myers, C.W., 2005. An enigmatic new snake from cloud forest of the Península de Paría, Venezuela (Colubridae: genus *Taeniophallus*?). *Am. Mus. Novit.* 3484, 1–22.
- Simpson, B., 1975. Pleistocene changes in the flora of the tropical Andes. *Paleobiology* 1, 273–294.
- Smith, E.N., Gutberlet, R.L. Jr, 2001. Generalized frequency coding: a method of preparing polymorphic multistate characters for phylogenetic analysis. *Syst. Biol.* 50, 156–169.
- Steyermark, J.A., 1974. Relación florística entre la Cordillera de la Costa y la zona de Guayana y Amazonas. *Acta Bot. Venez.* 9, 245–252.

- Steyermark, J.A., 1979. Plant refuge and dispersal centres in Venezuela: their relict and endemic element. In: Larsen, K., Holm-Nielsen, L.B. (Eds.), *Tropical Botany*. Academic Press, London, pp. 185–221.
- Steyermark, J.A., 1982. Relationship of some Venezuelan forest refuges with lowland tropical floras. In: Prance, G.T. (Ed.), *Biological Diversification in the Tropics*. Columbia University Press, New York, NY, pp. 182–220.
- Taboada, A., Rivera, L.A., Fuenzalida, A., Cisternas, A., Philip, H., Bijwaard, H., Olaya, J., Rivera, C., 2000. Geodynamics of the northern Andes: Subductions and intracontinental deformation (Colombia). *Tectonics* 19, 787–813.
- Torres-Carvajal, O., 2007. Phylogeny and biogeography of a large radiation of Andean lizards (Iguania, *Stenocercus*). *Zool. Scr.* 36, 311–326.
- Torres-Carvajal, O., Mafla-Endara, P., 2013. Evolutionary history of Andean *Pholidobolus* and *Macropholidus* (Squamata: Gymnophthalmidae) lizards. *Mol. Phylog. Evol.* 68, 212–217.
- Torres-Carvajal, O., Lobos, S.E., Venegas, P.J., 2015. Phylogeny of Neotropical *Cercosaura* (Squamata: Gymnophthalmidae) lizards. *Mol. Phylog. Evol.* 93, 281–288.
- Torres-Carvajal, O., Lobos, S.E., Venegas, P.J., Chávez, G., Aguirre-Peñafiel, V., Zurita, D., Echevarría, L.Y., 2016. Phylogeny and biogeography of the most diverse clade of South American gymnophthalmid lizards (Squamata, Gymnophthalmidae, Cercosaurinae). *Mol. Phylog. Evol.* 99, 63–75.
- Tschanz, C.M., Marvin, R.F., Cruzb, J., Mehnert, H.H., Cebula, G.T., 1974. Geologic evolution of Sierra-Nevada-de-Santa-Marta, northeastern Colombia. *Bull. Geol. Soc. Am.* 85, 273–284.
- Uetz, P., Hošek, J., 2017. The Reptile Database. Available at <http://www.reptile-database.org>. (accessed 30 January 2017)
- Uzzell, T.M., 1958. Teiid lizards related to *Proctoporus luctuosus*, with the description of a new species from Venezuela. *Occ. Pap. Mus. Zool. Univ. Mich.* 597, 1–15.
- Uzzell, T., 1970. Teiid lizards of the genus *Proctoporus* from Bolivia and Peru. *Postilla* 142, 1–39.
- Uzzell, T., 1973. A revision of lizards of the genus *Prionodactylus*, with a new genus for *P. leucostictus* and notes on the genus *Euspondylus* (Sauria, Teiidae). *Postilla* 159, 1–67.
- Varón, A., Wheeler, W.C., 2012. The tree alignment problem. *BMC Bioinformatics* 13, 293.
- Varón, A., Wheeler, W.C., 2013. Local search for the generalized tree alignment. *BMC Bioinformatics* 14, 66.
- Varón, A., Vinh, L.S., Wheeler, W.C., 2010. POY version 4, phylogenetic analysis using dynamic homologies. *Cladistics* 26, 72–85.
- Walker, C.F., Test, F.H., 1955. New Venezuelan frogs of the genus *Eleutherodactylus*. *Occ. Pap. Mus. Zool. Univ. Mich.* 561, 1–10.
- Wheeler, W.C., 1996. Optimization alignment: the end of multiple sequence alignment in phylogenetics? *Cladistics* 12, 1–9.
- Wheeler, W.C., 2003a. Iterative pass optimization of sequence data. *Cladistics* 19, 254–260.
- Wheeler, W.C., 2003b. Implied alignment: a synapomorphy-based multiple-sequence alignment method and its use in cladogram search. *Cladistics* 19, 261–268.
- Wheeler, W.C., Aagesen, L., Arango, C.P., Faivovich, J., Grant, T., D'Haese, C., Janies, D., Smith, W.L., Varón, A., Giribet, G., 2006. Dynamic Homology and Phylogenetic Systematics: A Unified Approach Using POY. American Museum of Natural History, New York, NY.
- Whiting, A.S., Bauer, A.M., Sites, J.W. Jr, 2003. Phylogenetic relationships and limb loss in sub-Saharan African scincine lizards (Squamata: Scincidae). *Mol. Phylog. Evol.* 29, 582–598.
- Wiens, J.J., 1995. Polymorphic characters in phylogenetic systematics. *Syst. Biol.* 44, 482–500.
- Wiens, J.J., 1998. Testing phylogenetic methods with tree congruence: phylogenetic analysis of polymorphic morphological characters in phrynosomatid lizards. *Syst. Biol.* 47, 427–444.
- Wiens, J.J. 2000. Coding morphological variation within species and higher taxa for phylogenetic analysis. In: Wiens, J.J. (Ed.), *Phylogenetic Analysis of Morphological Data*. Smithsonian Institution Press, Washington, DC, pp. 115–145.
- Zaher, H., 1999. Hemipenial morphology of the South American xenodontine snakes, with a proposal for a monophyletic Xenodontinae and a reappraisal of colubroid hemipenes. *Bull. Am. Mus. Nat. Hist.* 240, 1–168.

Appendix 1

Analysis and description of phenotypic characters

The following analysis of character variation and transformation series individuation follows the current taxonomy of cercosaurines.

Hemipenial anatomy (characters 0–9)

The hemipenial anatomy of cercosaurines has been documented traditionally in the context of alpha taxonomy (e.g. Uzzell, 1970; Kizirian, 1996; Sánchez-Pacheco et al., 2011) and interpreted phylogenetically by several authors (e.g. Myers et al., 2009; Nunes et al., 2014). Although hemipenial morphology of cercosaurines is unquestionably a useful source of evidence of phylogenetic relationships, variation has not been coded as transformation series and incorporated into phylogenetic analyses. Consequently, we delimited a number of novel hemipenial characters and character states based mainly

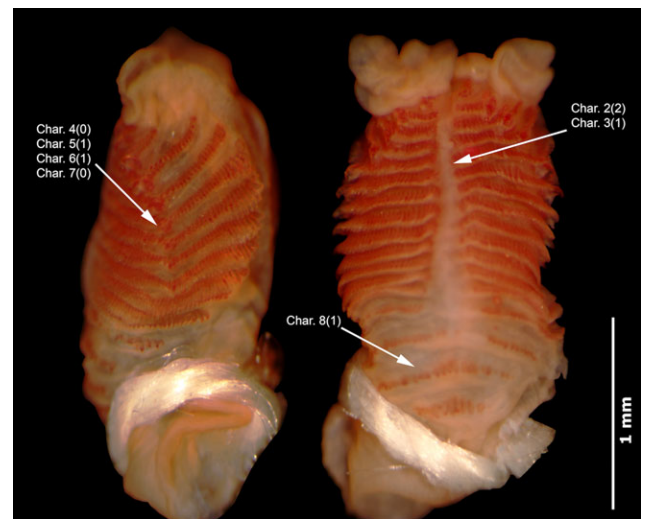


Fig. 4. Lateral view and asulcate face of the hemipenis of *Riama orcesi* (KU 142919). Character 0, shape of hemipenial body; state 0, cylindrical. Char. 2(2): Character 2, flounce orientation on asulcate face of hemipenial body; state 2, horizontal (with no vertex). Char. 3 (1): Character 3, asulcate central nude area; state 1, narrow, restricted to a sagittal stripe. Char. 4(0): Character 4, orientation of lateral body flounces; state 0, chevron-shaped. Char. 5(1): Character 5, lateral body flounce ornamentation; state 1, present. Char. 6(1): Character 6, position of lateral body flounce ornamentation; state 1, distributed over entire flounce. Char. 7(0): Character 7, shape of lateral body flounce ornamentation; state 0, comb-like series of spicules. Char. 8(1): Character 8, isolated transversal flounces on proximal-central region of asulcate face; state 1, present. [Colour figure can be viewed at wileyonlinelibrary.com]

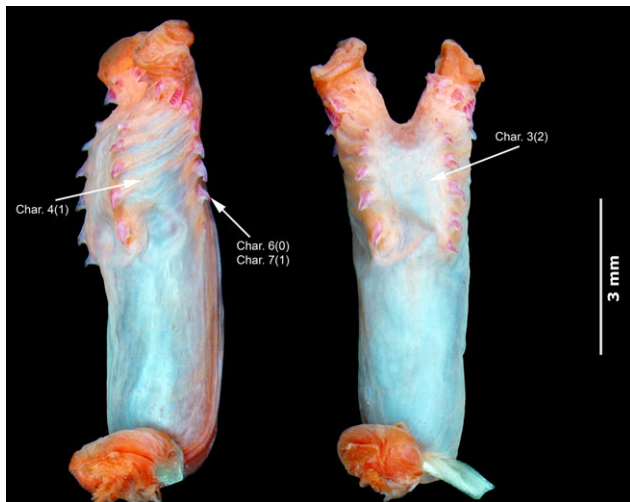


Fig. 5. Lateral view and asulcate face of the hemipenis of *Riama balneator* (DHMECN 4111). Character 0, shape of hemipenial body; state 1, elongated. Char. 3(2): Character 3, asulcate central nude area; state 2, broad, occupying approximately 50% of the asulcate face. Char. 4(1): Character 4, orientation of lateral body flounces; state 1, extended diagonally from anterior (asulcate) to posterior (sulcate) face. Char. 6(0): Character 6, position of lateral body flounce ornamentation; state 0, distal, restricted to flounce extremities. Char. 7(1): Character 7, shape of lateral body flounce ornamentation; state 1, isolated hook-shaped spines. [Colour figure can be viewed at wileyonlinelibrary.com]

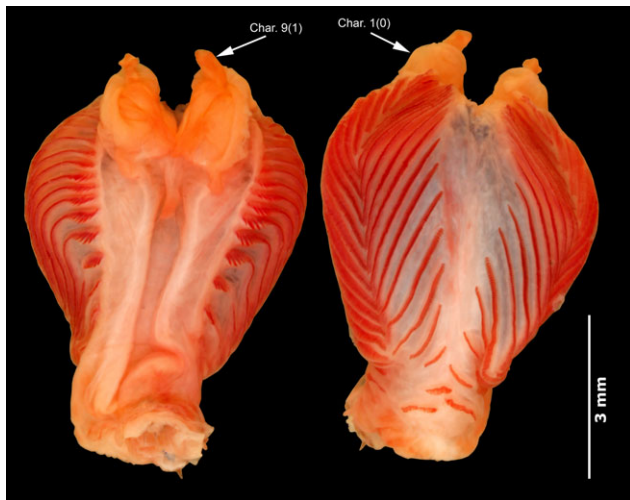


Fig. 6. Sulcate and asulcate faces of the hemipenis of *Riama crypta* (KU 135104). Character 0, shape of hemipenial body; state 2, conical, with proximal region distinctly thinner than distal and lobes. Char. 1(0): Character 1, lobes; state 0, large, distinct from hemipenial body. Char. 9(1): Character 9, distal filiform appendages on the hemipenial lobes, state 1, present. [Colour figure can be viewed at wileyonlinelibrary.com]

on the study of gymnophthalmid hemipenial morphology by Nunes (2011). Some characters required attention because they were highly prone to artifacts of preparation and/or preservation of the organs (e.g. characters 0 and 9). Thus, we coded the following characters on

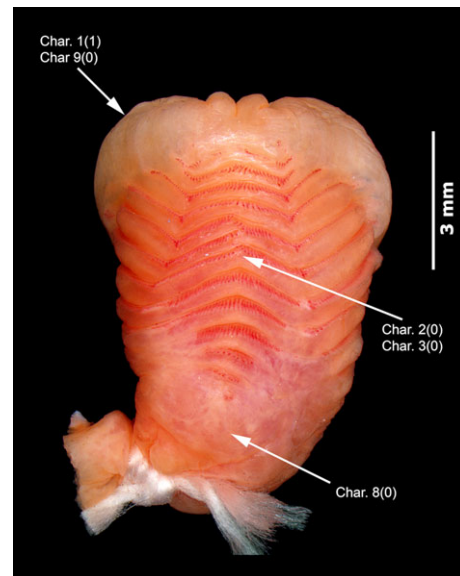


Fig. 7. Asulcate face of the hemipenis of *Riama simotera* (ICN-R 9836). Character 0, shape of hemipenial body; state 3, globose. Char. 1(1): Character 1, lobes; state 1, narrow, uniform with the hemipenial body. Char. 2(0): Character 2, flounce orientation on asulcate face of hemipenial body; state 0, lateral (with a central vertex directed distally). Char. 3(0): Character 3, asulcate central nude area; state 0, absent, flounces extended across entire asulcate face. Char. 8(0): Character 8, isolated transversal flounces on proximal-central region of asulcate face; state 0, absent. Char. 9(0): Character 9, distal filiform appendages on the hemipenial lobes; state 0, absent. [Colour figure can be viewed at wileyonlinelibrary.com]

the basis of distinct character-states as observed only in fully everted and sufficiently filled hemipenes.

Character 0. Shape of hemipenial body (SHB; Figs 4–7): cylindrical = 0; elongated = 1; conical, with proximal region distinctly thinner than distal and lobes = 2; globose = 3. Nonadditive.

SHB was coded as cylindrical when its lateral borders approximately paralleled each other in sulcate and asulcate views, and without evidence of curvatures or expansions (Fig. 4; e.g. *Riama orcesi*; state 0). It was coded as elongated when its lateral borders paralleled each other and its length (height) was more than twice the largest width (Fig. 5; e.g. *R. balneator*; state 1). Likewise, we considered SHB to be conical when its proximal region was distinctly thinner than its distal region and lobes (Fig. 6; e.g. *R. crypta*; state 2). Globose hemipenes had lateral borders that were curved uniformly, thus providing the body with a roughly rounded condition (Fig. 7; e.g. *R. simotera*; state 3). The absence of intermediacy among states suggested nonadditivity, and, therefore, we scored this transformation series as being nonadditive.

Character 1. Lobes (Figs 6 and 7): large, distinct from hemipenial body = 0; narrow, indistinct from hemipenial body = 1.

Hemipenial lobes were prominent and distinct from the rest of the organ by projecting considerably from the distal limits of the hemipenial body (Fig. 6; e.g. *Riama crypta*; state 0). Alternatively, hemipenial lobes were small and indistinct from the rest of the organ by projecting only slightly from the hemipenial body, often making it difficult to delimit lobes from body (Fig. 7; e.g. *R. simotera*; state 1).

Character 2. Flounce orientation on asulcate face (Figs 4, 7, 8): lateral (central vertex directed distally, in contact on the center of asulcate face) = 0; medial (central vertex directed proximally, in contact on the center of asulcate face) = 1; horizontal (with no vertex) = 2. Nonadditive.



Fig. 8. Asulcate face of the hemipenis of *Riama cashcaensis* (KU 217206). Char. 2(1): Character 2, flounce orientation on asulcate face of hemipenial body; state 1, medial (with a central vertex directed proximally). [Colour figure can be viewed at wileyonlinelibrary.com]

All ingroup taxa had flounces on both lateral regions of the hemipenial body, which expand from opposite lateral regions and invade the asulcate face, either reaching the center of it, or not. Species in which the flounces reach the center of the asulcate area were assigned to one of three patterns: flounces continuous forming chevron-shaped lines with the vertex directed either distally (“Λ”; Fig. 7; e.g. *Riama anatorlos*, *R. colomaromani*, *R. columbiana*, *R. laevis*, *R. “Nariño”*, *R. simotera* and *R. stigmatoral*; state 0) or proximally (“V”; Fig. 8; e.g. *R. cashcaensis* and *R. yumborum*; state 1); and flounces forming discontinuous (but nearly complete) horizontal lines, with no vertex (“–”; Fig. 4; e.g. *R. orcesi*, *R. raneyi* and *R. striata*; state 2). Species in which the flounces did not reach the center of the asulcate face were coded as inapplicable. No intermediate state(s) in flounce orientation on asulcate face of the hemipenial body existed. Thus, we evaluated this transformation series as being nonadditive.

Character 3. Asulcate central nude area (Figs 4, 5, 7): absent, flounces extended across entire asulcate face = 0; narrow, restricted to a sagittal stripe = 1; broad, occupying approximately 50% of the asulcate face = 2. Nonadditive.

Flounces expanding from opposite lateral regions of the hemipenial body and occupying the asulcate face formed continuous or discontinuous lines on this face. A vertical “nude” area of the asulcate face was formed where the flounces were discontinuous, (nearly) horizontal and equal-length lines (e.g. Fig. 4). Depending on the proximity between flounces from opposite lateral regions, nude areas varied in width. Nude areas were coded narrow when they were restricted to a sagittal stripe (Fig. 4; e.g. *Riama orcesi*, *R. raneyi*, *R. stigmatoral* and *R. striata*; state 1) and broad if they occupied at least 50% of the asulcate face (Fig. 5; e.g. *R. balneator*; state 2). When the flounces formed continuous lines that extended across the entire asulcate face, we considered the nude area to be absent (Fig. 7; e.g. *R. anatorlos*, *R. cashcaensis*, *R. colomaromani*, *R. columbiana*, *R. laevis*, *R. maxima*, *R. meleagris*, *R. simotera*, *R. unicolor* and *R. yumborum*; state 0). The increasing (or

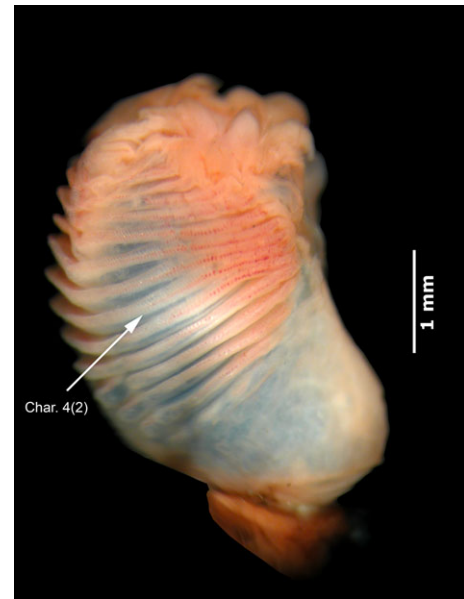


Fig. 9. Lateral view of the hemipenis of *Riama striata* (KU 217206). Char. 4(2): Character 4, orientation of lateral body flounces; state 2, horizontal. [Colour figure can be viewed at wileyonlinelibrary.com]

decreasing) degree of proximity between flounces from opposite lateral regions was indicative of additivity. However, we did not treat this character as additive because no ontogenetic evidence suggested that transformations between states 0 and 2 passed through state 1.

Characters 2 and 3 were transformationally independent and, as such, were coded separately. No evidence indicated a relationship between flounce (dis)continuity and orientation on the center of the asulcate face. Therefore, we did not consider horizontal flounce orientation (character 2, state 2; “–”) and a narrow, vertical nude area (character 3, state 1; “≡”), as well as continuous, chevron-shaped flounces (character 2, e.g. state 1; “V”) and the absence of vertical nude areas (character 3, state 0; “≈”), as identical character states.

Character 4. Orientation of lateral body flounces (Figs 4, 5, 9): chevron-shaped = 0; extended diagonally from anterior (asulcate) to posterior (sulcate) face = 1; horizontal = 2. Nonadditive.

All ingroup taxa had flounces on both lateral regions of the hemipenial body. In most species, these lateral flounces formed chevron-shaped lines with the vertex directed proximally (“V”; Fig. 4; e.g. *Riama orcesi*; state 0). In other species, the lateral flounces either extended diagonally from the asulcate (anterior) to the sulcate (posterior) face (“/”; Fig. 5; e.g. *R. balneator*; state 1) or were directed horizontally (“–”; Fig. 9; e.g. *R. striata*; state 2). The absence of intermediacy among states suggested nonadditivity.

Character 5. Lateral body flounce ornamentation (Figs 4 and 10): absent = 0; present = 1.

Most gymnophthalmids have calcified structures ornamenting the lateral body flounces. Estes et al. (1988) suggested that this character state was a putative synapomorphy of Gymnophthalmidae. In contrast, based on the topology presented by Pellegrino et al. (2001), Nunes et al. (2014) interpreted the presence of such structures as either a synapomorphy of a less inclusive group within the family (Gymnophthalmidae except Alopoglossinae—now Alopoglossidae according to Goicoechea et al., 2016) with subsequent independent reversals, or as independently evolved at least twice within Gymnophthalmidae. Alternatively, based on the topology presented by Castoe et al. (2004), Nunes et al. (2014) interpreted this condition as the result of three independent origins within the family.

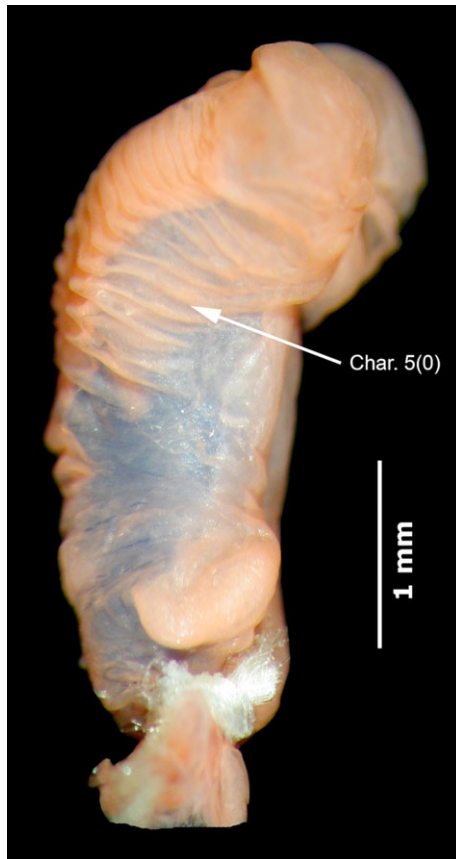


Fig. 10. Lateral view of the hemipenis of *Bachia flavescens* (AMNH 140925). Char. 5(0): Character 5, lateral body flounce ornamentation; state 0, absent. [Colour figure can be viewed at wileyonlinelibrary.com]

Our assessment of the hemipenes revealed the presence of calcified ornamentation on the lateral body flounces (Fig. 4; state 1) in all species of *Riama* and most cercosaurines. These structures are absent (Fig. 10; state 0) in two cercosaurines (*Neusticurus bicarinatus* and *N. rudis*), *Bachia flavescens*, *Ecleopus gaudichaudii*, *Rachisaurus brachylepis*, and the non-gymnophthalmid taxa (*Kentropyx calcarata*, *Ameivula ocellifera* and *Ptychoglossus brevifrontalis*).

Character 6. Position of lateral body flounce ornamentation (Figs 4 and 5): distal, restricted to flounce extremities = 0; distributed over entire flounce = 1.

Among the sampled species with ornamented lateral flounces, the calcified structures may be distributed over the entire flounce without interruption (Fig. 4; e.g. *Riama orcesi*; state 1), or restricted to the extremities of the flounce, with the rest of the flounce being “nude” (Fig. 5; *Echinosaura sulcarostrum*, *R. anatoloros*, *R. balneator* and *Riolama leucosticta*; state 0).

Character 7. Shape of lateral body flounce ornamentation (Figs 4 and 5): comb-like series of spicules = 0; isolated hook-shaped spines = 1; calcified lamina = 2. Nonadditive.

The calcified ornamentation on the lateral body flounces varied in shape and disposition. Most cercosaurines and a few gymnophthalmines possess small calcified spicules organized in series along each flounce (Fig. 4; e.g. *Riama orcesi*; state 0), which have been generally referred to as “comb-like” series of spicules (e.g. Myers and Donnelly, 2001; Rodrigues et al., 2005, 2007; Nunes et al., 2014). Sometimes calcified spines on less conspicuous lateral flounces

were enlarged and elongated, isolated and hook-shaped (Fig. 5; *Echinosaura sulcarostrum*, *R. balneator* and *Riolama leucosticta*; state 1). Some species of *Gymnophthalmus* Merrem, 1820 had expanded calcified lamina, as represented by *G. vanzoi* (state 2). We analysed this transformation series as nonadditive because of the absence of intermediate states.

Character 8. Isolated horizontal flounces on proximal-central region of asulcate face (Figs 4 and 7): absent = 0; present = 1.

Many cercosaurines, including approximately half of the species of *Riama* included herein, possess isolated, nearly horizontal flounces on the proximal-central region of the asulcate face (Fig. 4; e.g. *R. orcesi*; state 1). The other species did not have it (Fig. 7; e.g. *R. simotera*; state 0). Ornamentation occurs on these flounces, but interspecific variation in shape and disposition was much more complicated than that observed in lateral body flounces. Because we were unable to delimit transformation series objectively, we did not code ornamentation of proximal flounces of the asulcate face.

Character 9. Distal filiform appendages on the hemipenial lobes (Figs 6 and 7): absent = 0; present = 1.

Sánchez-Pacheco et al. (2011) documented the occurrence of single, distal filiform appendages on the hemipenial lobes of *Riama crypta* and *R. hyposticta* (Fig. 6), which they interpreted as a putative synapomorphy uniting these two species. They cautioned that the detection of such structures required the hemipenial lobes to be fully everted, which may not have been the case for the described hemipenes of other putatively related species (e.g. *R. afrania*; Arredondo and Sánchez-Pacheco, 2010). These appendages were distinctly thinner than the rest of the lobe (Fig. 6). Among other gymnophthalmids, similar appendages have been documented for *Cercosaura manicata* and an unnamed species of *Iphisa* Gray, 1851 (Nunes, 2011; Nunes et al., 2012). However, these differed in length, especially those of *Iphisa* sp. Köhler and Lehr (2004: 510, Fig. 7) described and illustrated the hemipenis of *Proctoporus laudahnae*, and reported the “apex [of the organ] with two large protrusions separated by the distal end of the sulcus spermaticus”. These protuberances seemed to be more integrated with other lobular folds (i.e. less distinct from the rest of the lobe) than those of *R. crypta* and *R. hyposticta*, and the hemipenes of four more cercosaurines (*R. “Cordillera Occidental”*, *Proctoporus bolivianus*, *P. guentheri* and *P. pachyurus*) examined herein had similar structures. Apical soft-tissue papillae also occurred atop each lobe in the cercosaurines *Anadia ocellata* and *A. blakei* (Myers et al., 2009). However, these structures were paired and distinctly robust. *Cercosaura manicata*, *Iphisa* sp., *P. laudahnae*, *A. ocellata* and *A. blakei* were not included in the current study.

Variation in length and degree of integration with the rest of the lobe suggested that the single distal filiform appendages on the hemipenial lobes of *Riama crypta* and *R. hyposticta* may not be homologous with those of *R. “Cordillera Occidental”*, *Proctoporus bolivianus*, *P. guentheri* and *P. pachyurus*. It was also possible that two transformation series have been conflated under “present”; thus, one involving occurrence of the appendages, the other variation in their length. For the purpose of the present phylogenetic analysis, we recognized only two character-states: single, distal filiform appendages on the hemipenial lobes absent (Fig. 7; e.g. *R. simotera*; state 0) and single, distal filiform appendages on the hemipenial lobes present (Fig. 6; e.g. *R. crypta*; state 1).

External morphology (scutellation, characters 10–34)

Traditionally, variation in scutellation has been used descriptively and comparatively in taxonomic studies of cercosaurines. Because of this, we reviewed its usage in the context of cercosaurine phylogenetic systematics. We defined a number of novel characters and states (characters 10, 13, 14, 20, 21, 28, 30, 31), modified a series of characters that have been used in previous phylogenetic analyses (11,

12, 15, 18, 19, 22–27, 29, 32–34), and perpetuated the use of two characters (16 and 17).

Character 10. Minute tubercles on dorsal head scales: absent = 0; present = 1.

In state 0, all dorsal head scales were smooth and glossy because they lacked minute tubercles or granules (e.g. *Petracola* spp., *Proctoporus* spp., *Riama* spp.). State 1 consisted of dense rounded, minute tubercles or granules on the dorsal head scales and was confined to some species in the outgroup (*Neusticurus* spp., *Potamites* spp., *Ameivula ocellifera* and *Kentropyx calcarata*).

Character 11. Prefrontal scales occurrence: absent = 0; present = 1.

Because the occurrence of prefrontals has been used to diagnose genera and species, and to hypothesize phylogenetic relationships, it has played a pivotal role in cercosaurine systematics. The absence of prefrontals has been used to diagnose the former *Proctoporus* s.l. (e.g. Peters and Donoso-Barros, 1970), and interpreted as a synapomorphy of this group (Doan, 2003a). Although prefrontals vary in size and degree of medial contact, which was the basis of Doan's (2003b; character 3) coding of this character, prefrontal scales were absent in all ingroup species and some relevant outgroup taxa (e.g. *Petracola* spp., most of *Proctoporus* spp.) (but see below). Therefore, we scored only the absence (state 0) and presence (state 1) of prefrontals, despite the occurrence of conflated transformation series under "present".

Intraspecific variation in the occurrence of prefrontal scales was found to occur rarely in cercosaurines. An undescribed species referred to herein as *Riama* "Cordillera Occidental", as well as *Macropholidus huancabambae*, *Pholidobolus macbrydei* and *Proctoporus sucullucu* exhibited polymorphism, though the presence of prefrontal scales is rare in *R.* "Cordillera Occidental" and *P. sucullucu*. Therefore, we coded these species as polymorphic (absent/present).

Characters 12–14. Nuchal scale relief

Dorsal scale relief has been used descriptively and comparatively in alpha taxonomic studies of cercosaurines, and of *Riama* in particular (e.g. Kizirian, 1996). Studies have rarely distinguished posterior and nuchal scales probably because of the usually uniform relief of dorsal scales, such as when both nuchal and posterior scales were keeled. However, the texture of posterior dorsal scales and nuchal scales sometimes differed. For example, Sánchez-Pacheco (2010a) noted that the nuchals of *R. striata* and two undescribed species were rugose but the posterior scales were striated. Species of *Riama* had smooth nuchals but keeled or striated posterior dorsals (Sánchez-Pacheco et al., 2011, 2012; Aguirre-Peñafiel et al., 2014). Thus, the textures of nuchal and posterior dorsal scales have independent transformations, which further examination of additional ingroup and outgroup taxa reinforced. Therefore, we coded nuchal (characters 12–14) and posterior dorsal scale relief (characters 22–28) separately.

The texture of nuchal scales has been noted sporadically in diagnoses and descriptions. Uzzell (1958) first reported that the nuchal scales of *R. achlyens* and *R. luctuosa* (not included herein) were keeled. Sánchez-Pacheco (2010a) reported the nuchals of *R.* "Cordillera Occidental" (*R.* "sp. 2" in that study), *R.* "Cordillera Central" (*R.* "sp. 1"), *R. striata*, *R. vieta* and *R. stellae* as being rugose. Sánchez-Pacheco (2010b), Sánchez-Pacheco et al. (2011, 2012) and Aguirre-Peñafiel et al. (2014) described the nuchal scales of *R. aurea*, *R. columbiana*, *R. crypta*, *R. hyposticta*, *R. kiziriani* and *R. yumborum* as smooth. In general, character states related to scale relief, including the smooth condition, have been combined into a single character under the assumption that they represented a unique transformation series (e.g. Doan, 2003a; character 46; Rodrigues et al., 2005; characters 10 and 11). However, this oversimplification of coding involved independent transformations. For example, the absence of keels or rugosities (or striations in the case of posterior dorsal scales), does not necessarily imply smoothness. In contrast, the absence of all these different conditions determines smoothness. In addition, minute tubercles and keels may occur together on

nuchal scales (e.g. *Neusticurus* spp., *Placosoma cordylinum*), or may not (e.g. *Potamites* spp., only tubercles; *R. achlyens* and *R. shrevei*, only keels). Therefore, we coded the different conditions as independent characters. Kizirian (1996), Sánchez-Pacheco (2010a) and Sánchez-Pacheco et al. (2012) discussed variation in dorsal scale relief among species of *Riama*. They proposed explicit character-states, which we employed in delimitating characters related to nuchal scale relief, specifically characters 12 and 13.

Character 12. Keels on nuchal scales: absent = 0; present = 1.

Following Sánchez-Pacheco et al. (2012), state 1 involved a (generally weak) keel in the middle of the nuchal scale, not flanked by striations (e.g. *Riama achlyens*). Species lacking such keels were scored as state 0. No intraspecific variation in this character was detected.

Character 13. Rugosities on nuchal scales: absent = 0; present = 1.

Kizirian (1996) and Sánchez-Pacheco (2010a) referred the rugose condition to scales with multiple, minute, nearly longitudinally positioned ridges (state 1; e.g. *Riama striata*). Species without rugosities were scored as state 0. Intraspecific variation occurred in *Pholidobolus macbrydei*, which was coded as absent/present.

Character 14. Minute tubercles on nuchal scales: absent = 0; present = 1.

Species with rounded, minute tubercles or granules distributed densely over the nuchal scales were scored as state 1. Scale texture appeared granular under high magnification. This character-state only occurred in the outgroup species *Neusticurus* spp., *Potamites* spp., *Placosoma* spp., and *Kentropyx calcarata*. Species lacking these tubercles were scored as 0. No intraspecific variation was detected.

Character 15. Palpebral disc of lower eyelid: undivided = 0; divided = 1.

The palpebral disc of the lower eyelid has long been used in gymnophthalmid systematics (e.g. Boulenger, 1885). Uzzell (1958, 1970) used this structure to diagnose species groups in the former *Proctoporus* s.l. Most gymnophthalmids possess fully movable eyelids. The palpebral disc of their lower eyelid is either undivided (e.g. most *Proctoporus* s.s. spp., *Macropholidus* spp.; state 0) or divided into several scales (e.g. *Riama* spp., *Petracola* spp.; state 1). *Potamites juruazensis* exhibited intraspecific variation and we coded this species as polymorphic (single/divided). Doan (2003a; character 13) noted interspecific variation in the number of scales in the palpebral disc of the lower eyelid. We scored only the condition of the palpebral disc—undivided or divided—because, when divided, variation was continuous (i.e. meristic), which must be accounted for when individuating characters (see Materials and Methods: Phenotypic evidence). Some gymnophthalmids lack eyelids (tribe Gymnophthalmini Fitzinger, 1826, except *Tretioscincus* Cope, 1862), including *Gymnophthalmus vanzoi*, the only eyelidless gymnophthalmid included herein. This species was coded as missing ("–").

Character 16. Frontonasal scale: undivided = 0; divided = 1.

All species of *Riama* possess an undivided frontonasal scale (state 0), and it is both undivided and divided (state 1) in our outgroup species. Differences occur in frontonasal division. Vertical divisions into two scales occurs in some taxa (e.g. *Cercosaura argula* and *C. oshaughnessyi*), and into three scales in others (e.g. *Echinosaura sulcarostrum*). Only several outgroup taxa exhibit variation. Therefore, we treated the division of frontonasal scale as a single character state. This character corresponded to character 1 of Doan (2003b).

Character 17. Relative frontonasal length: shorter than frontal = 0; same length as frontal = 1; longer than frontal = 2. Nonadditive.

Given the consistency of frontal length, this reference point was used to compare interspecific variation in the size of frontonasals. Following Kizirian (1996) and character 2 of Doan (2003a,b), coding of the frontonasal length was based on it being shorter (state 0), equal to (state 1), or longer than the frontal (state 2). The considerable intraspecific variation that occurred within *Riama* was

accounted for by polymorphic coding (e.g. 0/1/2). Although state 1 was intermediate in the degree of frontonasal “expansion”, no ontogenetic evidence suggested that transformations between states 0 and 2 passed through state 1. Furthermore, the frontonasal was either shorter or longer than the frontal in some species (e.g. *R. laevis*). Therefore, we evaluated this character as being nonadditive.

Character 18. Nasoloreal suture: absent = 0; incomplete = 1; complete (i.e. loreal scale present) = 2. Nonadditive.

Occurrence of the loreal scale usually has been reported as absent or present. However, Kizirian (1996: 89) pointed out that in *Riama* “[t]he nasoloreal suture can be absent (= loreal absent), complete (= loreal present), or incomplete. In some cases, where the suture is incomplete, the scale is referred to as a nasoloreal scale [= loreal absent]”. Doan (2003a: 373) modified the terminology by coding this character as “nasal condition: undivided 0 (i.e. nasal and loreal fused), incompletely divided 1, divided into separate nasal and loreal scales 2”. Although Doan’s intention was the same as Kizirian’s, her character delimitation described the observed variation somewhat less precisely. For this reason, our coding followed Kizirian.

In state 0, specimens lacked a nasoloreal suture. When present, the nasoloreal suture extended from the supralabial or frenocular scales part-way to the frontonasal scale (state 1), or all the way to the frontonasal (state 2), forming the loreal scale. For illustrations of these three states, see Kizirian (1996). State 1 was intermediate in the degree of suture development, yet no ontogenetic evidence suggested it was the transformational state between states 0 and 2. In some species the nasoloreal suture is either absent or complete (e.g. *Riama meleagris*). Therefore, the character was evaluated as nonadditive.

Unlike most cercosaurine and gymnophthalmid genera, the degree of development of the nasoloreal suture varied considerably among conspecifics of *Riama*. For example, whereas intraspecific variation has been reported for only three of the outgroup taxa included herein, it has been detected in 16 of the sampled ingroup species. Thus, we coded these terminals as polymorphic (0/1, 0/2, 1/2, 0/1/2). Interspecific variation was common in *Riama*, but less so in the outgroup genera. Incomplete nasoloreal sutures occurred in some *Riama* spp., several specimens of *Proctoporus bolivianus* (Uzzell, 1970; Goicoechea et al., 2013) and the holotype of *Riolama leucosticta* (Uzzell, 1973).

Character 19. Scale organs on labials: absent = 0; present = 1.

Sensory scale organs occurred on the labial scales in all species of *Riama*. Among the sampled outgroup taxa, scale organs on labials were both present (e.g. *Proctoporus* spp., *Petracola* spp.; state 1) and absent (e.g. *Neusticurus* spp., *Placosoma* spp., *Rhachisaurus brachylepis*; state 0). No intraspecific variation was detected. Doan (2003a,b) treated the variation in number of scale organs on the first supralabial and the first infralabial as characters 24 and 25, respectively. We did not follow Doan’s coding for several reasons. First, if present, minute scale organs occur in most, if not all labials, and we do not consider exclusion of the remaining labials to be precise. Likewise, delimitation of the number of scale organs between the first infralabial and the first supralabial is arbitrary, and we do not consider a distinction between both scales to constitute different transformations series. Second, variation is continuous (i.e. meristic), which must be accounted for when individuating transformations series (see Materials and Methods: *Phenotypic evidence*). Third, as coded by Doan, the character excludes absence of scale organs on labials, which was precise in that study given the taxon sampling (only species with scale organs), but it does not consider our observed variation.

Character 20. Association of supralabial and subocular: separated = 0; fused = 1.

Kizirian (1996) diagnosed *Riama labionis* based on the “supralabial–subocular fusion”, and summarized observed variation (both intra- and interspecific) in Ecuadorian species as absent or present. Subsequent alpha taxonomic studies of some cercosaurine genera (e.g. *Petracola*, *Riama*) have reported the supralabial–subocular

association. Although Kizirian described the holotype of *R. labionis* as having the “subocular fused to fourth supralabial”, he did not explicitly mention which subocular was fused, making it difficult to recognize homologous fusions in other species. However, figure 12 of Kizirian (1996) showed the third subocular and fourth supralabial fused. Kizirian noted that some specimens of *R. cashcaensis*, *R. raneyi* and *R. simotera* exhibited the supralabial–subocular fusion. Close examination of specimens of these species (Appendix 3) revealed that, when fusion occurs, variation encompasses only the supralabial being fused with the subocular (fourth supralabial in *R. simotera* and *R. cashcaensis*, fifth supralabial in *R. raneyi*). In all cases, the third subocular fused with the fourth or fifth supralabial.

Among the included outgroup taxa, this unusual fusion has been detected in *Anadia mediarmidi* (Kok and Rivas, 2011), and *Riolama leucosticta* (Molina and Señaris, 2003: 16; fig. 3). In both cases, the fifth supralabial fused with the third subocular, as in specimens of *Riama raneyi*. Terminology has varied in the literature. Molina and Señaris (2003: 15, translated freely from the Spanish) termed the fusion as “the supralabial series interrupted by a subocular scale”. Kok and Rivas (2011: 5) stated “one [subocular] scale slightly protruding downward between 4th and 5th supralabial [sic]”.

Variation involving the supralabials being fused with the third subocular suggested nonhomology. However, we treated the variants as homologous and considered all fusions as a single character-state. When present, the second and third supralabials fused in an elongated “second” supralabial in *Riama labionis* (Kizirian, 1996: 115; fig. 12), *R. cashcaensis* and *R. simotera*. Hence, the supralabial scale that fused with the third subocular was the same as in the other species. Herein, we delimited this character as an association of the third subocular and the fourth or fifth supralabials as follows: separated (state 0), and fused (state 1). Intraspecific variation has been detected in seven species of *Riama* (Kizirian, 1996; Sánchez-Pacheco et al., 2012; this study); these were scored as polymorphic (separated/fused).

Character 21. Association of anterior supraocular and anterior superciliary: separated = 0; fused = 1.

In most cercosaurines, a suture separates the anterior supraocular and anterior superciliary medially (state 0). When an enlarged scale occupied the area shared by both scales (e.g. *Petracola* spp., some *Proctoporus* spp.), we, like some other authors (Uzzell, 1973; Kizirian, 1996; Köhler and Lehr, 2004; Kizirian et al., 2008), interpreted this as evidence of fusion (state 1). This state has also been referred to as the first superciliary expanding onto the dorsal surface of the head (e.g. Uzzell, 1970; Goicoechea et al., 2013). Intraspecific variation (0/1) has been observed in *Proctoporus lacertus* (Goicoechea et al., 2013), *Riolama leucosticta* (Uzzell, 1973), and *Riama* “Cordillera Central” (this study), the only species of *Riama* in which supraocular–superciliary fusion was detected.

Characters 22–28. Dorsal scale relief.

In addition to the keels, rugosities and minute tubercles described in characters of nuchal scale relief (12–14), there is interspecific variation in posterior dorsal scale relief involving striations and longitudinal rows of tubercles, as well as the morphology of keels and striations. Therefore, we individuated additional transformation series encompassing the observed variation. Kizirian (1996), Sánchez-Pacheco (2010a) and Sánchez-Pacheco et al. (2012) discussed variation in dorsal scale relief among species of *Riama*. They proposed explicit character states that we employed in the delimitation of the following characters (specifically characters 23–27).

Character 22. Minute tubercles on posterior dorsal scales: absent = 0; present = 1.

Species with rounded, minute tubercles or granules distributed densely over the posterior dorsal scales, making scale texture appear granular under high magnification, were scored as state 1. This character state only occurred in the outgroup (*Neusticurus* spp., *Potamites* spp., *Placosoma* spp. and *Kentropyx calcarata*). Species that

lacked minute tubercles on posterior dorsals were scored as 0. No intraspecific variation in this character was detected.

Character 23. Keels on posterior dorsal scales: absent = 0; present = 1.

Following Sánchez-Pacheco et al. (2012), presence of a keel in the middle of the dorsal scale, not flanked by striations, was scored as state 1. Species that lacked these keels were scored as state 0. Intraspecific variation was detected in some species of *Pholidobolus*, *Proctoporus* and *Riama*. We coded these occurrences as polymorphisms (absent/present).

Character 24. Morphology of keels on posterior dorsal scales: weak (low, rounded keel) = 0; strong (prominent keel) = 1.

When present, keels on posterior dorsals were weak (i.e. low and rounded; state 0) or strong (i.e. prominent). When present, keels in species of *Riama* were usually weak but several species had strong keels (e.g. *R. achlyens*, *R. shrevei* and *R. “Venezuela”*). Intraspecific variation was not detected. Species without keels on posterior dorsal scales were coded as inapplicable.

Character 25. Striations on posterior dorsal scales: absent = 0; present = 1.

Following Kizirian (1996) and Sánchez-Pacheco et al. (2012), the striated condition referred to two centrally positioned, longitudinal and parallel furrows (state 1). Species without these striations were scored as state 0. Intraspecific variation occurred in some species of *Pholidobolus*, *Proctoporus* and *Riama*. These species were coded as polymorphic (absent/present).

Character 26. Morphology of striations on posterior dorsal scales: weak (shallow furrows) = 0; strong (deep furrows) = 1.

When present, striations on posterior dorsals were either weak (shallow furrows; state 0) or strong (deep furrows; state 1). When present, the striations were usually weak in species of *Riama*. However, several species exhibited strong striations (e.g. *R. striata* and undescribed *R. “Cordillera Occidental”* and *R. “Cordillera Central”*). Intraspecific variation was not detected. Species without the striations were coded as inapplicable.

Character 27. Rugosities on posterior dorsal scales: absent = 0; present = 1.

Kizirian (1996) and Sánchez-Pacheco (2010a) considered the rugose condition to indicate scales with multiple, minute, nearly longitudinally positioned ridges (state 1). This condition occurred in the posterior dorsals of *Riama vieta* and *R. stellae* only (one of the five species of *Riama* not included in this study). The remaining ingroup and outgroup species were scored as state 0 (absent). Intraspecific variation was not observed.

Character 28. Longitudinal rows of tubercles on dorsum: absent = 0; present = 1.

Longitudinal rows of tubercles on the dorsum (state 1) were confined to the outgroup species *Neusticurus* spp. and *Potamites* spp. The remaining outgroup and ingroup species were scored as state 0 (absent). Intraspecific variation was not detected.

Characters 29–30. Anterior row of cloacal plate.

Kizirian (1996) reviewed the occurrence of, and variation in, the anterior cloacal plate row of Ecuadorian *Riama*. The different conditions have been reported consistently for both ingroup taxa (e.g. Sánchez-Pacheco, 2010b; Aguirre-Peñafiel et al., 2014) and outgroup species (e.g. Goicoechea et al., 2013; *Proctoporus* spp.). Doan (2003a,b): character 36) coded variation in cloacal plate rows as “number of cloacal plate rows (1 or 2)”, where “1” referred to the absence of the anterior row. We did not follow this coding because it lacked explicit delimitation of character-states, and two transformations series were combined under her character state “2” (i.e. anterior row present; see below).

Character 29. Anterior cloacal plate row: absent = 0; present = 1.

The anterior cloacal plate row was either absent (e.g. *Bachia flavescens* and *Ecpleopus gaudichaudii*; state 0) or present (e.g. *Riama*

columbiana; state 1). Rivas et al. (2005: 463, fig. 2; absence (top), presence (bottom)) and Aguirre-Peñafiel et al. (2014: 252, fig. 3; absence (left), presence (right)) illustrated examples. Some species of *Riama* exhibited intraspecific variation, which was coded as a polymorphism (0/1).

Character 30. Condition of anterior cloacal plate row: one scale = 0; paired scales = 1.

When present, the anterior cloacal plate row was composed of either a small scale (e.g. *Riama meleagris* and *R. shrevei*; state 0) or two large scales (e.g. *R. crypta*; state 1). Species without the anterior plate row were coded as inapplicable. Kizirian (1996: 102, fig. 5; a single small scale (bottom), two large scales (top)) illustrated examples. Intraspecific variation in *Ptychoglossus brevifrontalis* and several species of *Riama* was coded as a polymorphism (0/1).

Character 31. Rugosities on ventral scales: absent = 0; present = 1.

Rugose ventral scales are extremely rare in Gymnophthalmidae. Herein, only *Riama vieta* and undescribed *R. “Cordillera Occidental”* possessed rugosities (as defined in characters 13 and 27; state 1) on their ventrals. Not included herein, *R. stellae* had rugose ventrals. All remaining ingroup and outgroup taxa were scored as state 0. Intraspecific variation was not detected.

Character 32. Dorsal scale shape: approximately quadrangular = 0; rectangular = 1; hexagonal or sub-hexagonal = 2; irregular = 3. Nonadditive.

The shape of the dorsal scales has been used in gymnophthalmid systematics for decades (e.g. Boulenger, 1885). Considerable variation occurred within Cercosaurinae. Our species possessed roughly quadrangular (e.g. *Placosoma* spp.; state 0), rectangular (e.g. *Proctoporus* spp.; state 1), hexagonal or sub-hexagonal (e.g. *Pholidobolus* spp.; state 2), or irregular (e.g. *Potamites* spp.; state 3) dorsals. Most species of *Riama* exhibited state 1, whereas a few taxa from Venezuela and Trinidad had state 2. Intraspecific variation was detected only in *Kentropyx calcarata*, which was coded accordingly (2/3). This character corresponded to character 45 of Doan (2003a,b), except for the inclusion of irregularly shaped scales and the exclusion of the states “rhomboid” and “pyramidal”, presumably due to differences in taxon sampling and observed variation. The absence of intermediate states suggested nonadditive analyses.

Characters 33–34. Occurrence of femoral pores.

The occurrence and number of femoral pores are two of the most useful characters for discriminating species of *Riama*. These two characters are sexually dimorphic, with males usually possessing more femoral pores than females. In some species, females lacked them (Kizirian, 1996). Therefore, we coded males and females as separate semaphoronts. Distinction between preanal and femoral pores has been commonly used in cercosaurine systematics. As such, Doan (2003a,b): characters 40–42) coded preanal and femoral pores separately. However, explicit discrimination of preanal and femoral pores has been generally lacking. Kizirian (1996: 92) stated “[p]reanal pores are femoral pores that occur medially, inside a line congruent with the outside edge of the tail. The presence of femoral pores that are preanal in position is actually difficult to determine”. Consequently, the distinction between preanal and femoral pores has been arbitrary. As pointed out by Grant et al. (2006: 66) “[a]lthough such arbitrariness is relatively harmless in descriptive taxonomic studies, the cumulative effect of arbitrary delimitations can be disastrous in phylogenetic analyses.” Therefore, we considered the complete pore series to be femoral pores. In addition, femoral pores varied in number, and Doan (2003a,b) coded this variation accordingly. However, frequencies do not entail additional character-state transformations and mistakenly equate population-level similarity with transformation events (see Materials and Methods: *Phenotypic evidence*). Therefore, we scored only the absence and presence of femoral pores, despite the fact

that we have conflated additional transformation series under “present”.

Character 33. Femoral pores in males: absent = 0; present = 1.

Males usually had femoral pores (e.g. *Riama* spp.; state 1). Nevertheless, several male cercosaurines lacked femoral pores (e.g. *Macropholidus huancabambae*, *Pholidobolus montium* and *P. prefrontalis*; state 0). Intraspecific variation in *M. annectens*, *P. affinis* and *P. macbrydei* was coded as a polymorphism (absent/present).

Character 34. Femoral pores in females: absent = 0; present = 1.

Females lacked femoral pores (e.g. *Riama cashcaensis* and *R. orcesi*; state 0) or had them (e.g. *R. achlyens* and *R. oculata*; state 1). Intraspecific variation was more common than in males (e.g. eight species of *Riama*). Therefore, we coded these cases as polymorphisms (absent/present).

Appendix 2

Specimens examined

The following list of specimens examined includes material used to individuate the transformation series and score the character states, as well as for species identification and generic allocation. Ingroup species are listed following the new taxonomy proposed below. See Materials and Methods for institutional abbreviations.

Ingroup taxa

Andinosaura

A. afrania: COLOMBIA: Antioquia: municipio de Urrao, 13 km NE on Urrao–Caicedo road, Valle Real, 2350 m (a.s.l.) (MHNCSJ 1048 (holotype), MHNCSJ 801–03, 1044, 1051–52, IAvH-R 3957, 3959–60 (paratypes)), vereda El Chuscal, quebrada Las Juntas, 2430–2490 m (ICN 9513 (paratype)). *A. aurea*: ECUADOR: El Oro: Guanazán, 2789 m (QCAZ 07886 (holotype)); El Panecillo, 2775 m (QCAZ 09649–50 (paratypes)); Guishaguiña, Zaruma (EPNH 06196 (paratype)); El Chiral (AMNH 18310). *A. crypta*: ECUADOR: Cotopaxi: Pilaló, 2700 m (KU 121153–54 (paratypes)); 2500 m (KU 135100–02 (paratypes)), 135103 (holotype), 135104–15 (paratypes)); 2400 m (KU 179455–65 (paratypes)); 2320 m (KU 196386–89 (paratypes)); 3 km W Pilaló on Quevedo–Latacunga road (USNM 229638–39 (paratypes)). *A. hyposticta*: COLOMBIA: Nariño: municipio de Barbacoas, corregimiento Altaquer, vereda El Barro, Reserva Natural Río Nambí (PSO-CZ 085). *A. kiziriani*: ECUADOR: Azuay: San Antonio, 1900 m (QCAZ 9667 (holotype)); El Chorro de Girón, Girón, 2546 m (QCAZ 9607 (paratype)). *A. laevis*: COLOMBIA: Valle del Cauca: municipio Cumbre, 2000 m (IAvH 4916), vereda Chicoral (UV-C 11266); 15 km al oeste del Cairo, base cerro del Ingles, c. 2000 m (UV-C 10103). Risaralda: río San Rafael, Municipio de Tatamá, 2250 m (IAvH 5197–98); quebrada Risaralda, vereda Planos de San Rafael, Parque Municipal San Rafael, municipio de Santuario (IAvH 5199, 5200); quebrada San Rafael, municipio de Santuario, 2820 m (IAvH [formerly IND-R] 3967). *A. oculata*: ECUADOR: Pichincha: Nanegal (USNM 229640), 3 km E of Nanegal Chico (USNM 229642). Cotopaxi: San Francisco de las Pampas (UMMZ 188630). *A. petrorum*: ECUADOR: Morona-Santiago: trail between Sevilla de Oro and Mendez on E slopes of the mountains between Cerro Negro and Pailas (tambos) (USNM 196266 (paratype)); San Vicente, slightly S of W of Limon and 35 km E Gualaceo by road (USNM 196268). *A. stellae*: COLOMBIA: Nariño: municipio de Barbacoas, corregimiento de Ricaurte, reserva La Planada (PSO-CZ 102 (holotype), PSO-CZ 103 and 109, ICN 12068 [formerly

PSO-CZ 108] (paratypes)). *A. vespertina*: ECUADOR: Loja: [Pampa] Chitoque, between San Bartolo and Piñas (AMNH 22130 (holotype)); reserva biológica Utuana, 48.3 km SE to the type locality, 2600 m (DHMECN 4113–14); Guachaurco, 2824–2958 m (QCAZ 10283, 10286, 10288, 10306–13). *A. vieta*: ECUADOR: Guayas: km 85 on Durán–Tambo road (USNM 142601).

Oreosaurus

O. achlyens: VENEZUELA: Aragua: Rancho Grande (AMNH 137260, 137267–69, 137271–76, 137278–82, 137297). *O. “Venezuela”*: VENEZUELA: Anzoátegui: Cerro El Guamal, Macizo del Turimiquire, municipio Freites, 2150 m (a.s.l.) (GAR 5962). *O. luctuosus*: VENEZUELA: Aragua: Rancho Grande (AMNH 137270, 137277, MCZ 100410, USNM 196336), Parque Nacional Henri Pittier, Rancho Grande (USNM 259170). *O. “Sierra Nevada”*: COLOMBIA: Magdalena: Santa Marta, corregimiento Minca, finca Vista Hermosa, cabecera río Guachacos, 2156 m (seven specimens awaiting assignment of permanent collection number). *O. rhodogaster*: VENEZUELA: Sucre: between Las Melenas and Cerro Humo, Península de Paria, c. 650 m (MHNLS 16645 (holotype), 15730–31 (paratypes)). *O. shrevei*: TRINIDAD & TOBAGO: Horne Tucuche (MCZ 62506–07); El Teluche [in error, probably Tucuche] (MCZ 100466–68); Mt. Tucuche (MCZ 160065–66).

Riama

R. anatoloros: ECUADOR: Napo: La Bonita (USNM 229706–45); Napo-Pastaza [= Napo]: Abitagua (AMNH 38821–22). Zamora-Chinchipe: cuenca del río Jamboe, Romerillos, Parque Nacional Podocarpus, 1700 m (a.s.l.) (FHGO 2405). *R. balneario*: ECUADOR: Tungurahua: San Antonio mountains, eastern slope of the Tungurahua volcano, 10.5 km N of the type locality (DHMECN 04111–12). *R. cashcaensis*: ECUADOR: Bolívar: Guaranda, 2640 m (KU 135019–21 (paratypes)); 4.0 km E Guanujo, 2870 m (QCAZ 877 (paratype)). *R. colomaramani*: ECUADOR: Pichincha: 19.8 km W Chillogallo, c. Quito–Chiriboga rd (KU 221737 (paratype)). Carchi: 26.9–27.3 km from Maldonado on road to Tulcán (KU 217209); 58 km E tulcán, 2900 m (QCAZ 4250, 4252). *R. columbiana*: COLOMBIA: probably Antioquia: Municipio de Sonsón (NRM 1631 (lectotype), NRM 1633, 1634, 6168 (paralectotypes)). Caldas: municipio de Villa María, vereda Montaña, 2450 m (MHNLC 0088), predio La Mesa, bosques de la CHEC, 2640 m (ICN 11295–98), 2600 m (ICN 11299–301); municipio de Neira, vereda La Cristalina, finca La Cristalina, 2300 m (ICN 11302). Quindío: between the haciendas El Brillante and San Julian, vereda San Julian, municipio de Calarcá, 2100 m (ICN 6479). Risaralda: Santuario de Fauna y Flora Otún Quimbaya (IAvH-R 4941); parque municipal Campo Alegre, municipio de Santa Rosa de Cabal (IAvH-R 5194). *R. “Cordillera Central”*: COLOMBIA: Antioquia: 7 km N (by road) Santa Rosa de Osos on road to Yarumal (MVZ 190563); municipio de Yarumal, 3.5 km N por La carretera a Llanos de Cuivá, 2700 m (ICN 6471–78); municipio de Yarumal, 5 km N por La carretera a Llanos de Cuivá, 2650 m (ICN 6480–89); municipio de Yarumal, Llanos de Cuivá, 1–2 km hacia San José de las Montañas (ICN 11262); San Antonio de Prado, Medellín, 2000 m (MLS 1223); municipio de Santa Rosa de Osos, vereda Vallecitos, El Ventadero (MHUA 10573); municipio de Caldas, Alto de San Miguel, vereda La Clara (MHUA 10009); Medellín (AMNH 32706–07, 89833); Santa Rosa (AMNH 19960–68, 32708–13). Tolima: 15 km W Cajamarca, 2350 m (KU 169940–42); Quindío mts [Quindío–Tolima border?] (MCZ 15942–47, 15949–52); No other data (UMMZ 56443 [five specimens]). Not located (AMNH 32764–65). *R. “Cordillera Occidental”*: COLOMBIA: Caquetá: municipio de Florencia, vereda Gabinete, 0.7–1.1 km abajo del Alto Gabinete, 2300–2310 m (ICN 9780–81). Cauca: Puracé, 2700 m (ICN 2171–

73); km 41 carretera Belalcázar–Tacuello, 2600–2800 m (ICN 1992), km 34.5 carretera Belalcázar–Tacuello, 2400 m (ICN 1993); entre Paletara y quebrada Bujios, 2960 m (ICN 4463–69 and 4540); 27 km por carretera E de Coconuco, quebrada Ullucos, 2930 m (ICN 4471–74); municipio de Inza, vereda Río Sucio, km 66–67 carretera Popayan–Inza (ICN 6029–32). Huila: 39 km NW arriba de San José de Isnos, 2880 m (ICN 4470); No other data (UMMZ 121034). Valle del Cauca: Cali, Parque Nacional Natural Los Farallones, campamento Corea, 2600 m (ICN 2930–31), 2700 m (UV-C 7821). *R. inanis*: VENEZUELA: Portuguesa: Carretera Chabasquén–Córdova, Sierra de Portuguesa, 1450 m (MCNG 827 (holotype), 825–26 and 828 (paratypes)). Barinas: Los Alcaravanes, Calderas, 1100 m (MBLUZ 952). *R. labionis*: ECUADOR: Cotopaxi: Naranjito, Reserva de Bosque Integral Otonga, 1985 m (QCAZ 10411–12). *R. meleagris*: ECUADOR: [Tungurahua]: Baños (FMNH 28037–42, 28049 [six specimens]). In error: El Oro: Machala (USNM 196264–65). *R. “Nariño”*: COLOMBIA: Nariño: municipio de San Juan de Pasto, corregimiento de Genoy (PSO-CZ 28, 29, 242–46); corregimiento de Obonuco, predios Corpoica (UV-C 14982–83); municipio de Buesaco, km 17 carretera Pasto–Buesaco, Páramo de Daza, 2850 m (ICN 9816); Municipio de Tangua, Quebrada Chavez (UMMZ 171659–61, formerly UV-C 2778–79 and 2781 respectively); 3 km al norte de Tangua, quebrada Chavez (UMMZ 171662); 8 km NE Pasto, 3020 m (KU 169943, 169945). *R. orcesi*: ECUADOR: Napo: 12 km W (via road) Baeza (AMNH 124044 (paratype)); 31 km N Jondachi, 2190 m (QCAZ 2829, 2835); vertiente del volcán Sumaco, 2200 m (QCAZ 931–40). *R. ranyei*: ECUADOR: Napo: 3.3 km ESE Cuyuja, 2350 m (KU 142903 (paratype)). Sucumbios: near Santa Barbara (MCZ 175160–62); Napo [= sucumbios]: immediate environs of Santa Barbara (USNM 229750); 2 km E of Santa Barbara (USNM 229749); 3 km SW Santa Barbara at bridge (covered) over river (USNM 229748). Sucumbios: 32 km E Julio Andrade on road to Santa Barbara, 2610 m (QCAZ 2827). Carchi: Santa Bárbara, Santa Bárbara–Guanderal, 2980 m (QCAZ 1379). *R. simotera*: ECUADOR: Carchi: 14.6 km NW El Carmelo, 3130 m (KU 179478); km 13 carretera a El Carmelo, 3300 m (ICN 9823–34); km 16 Tulcán–Tufino, 3130–3160 m (ICN 9835–36); 15.3 km W Tulcán on road to Tufino, 3080 m (QCAZ 915, 918); km 13 desvío carretera Panamericana, el Ángel (ICN 9837). COLOMBIA: Nariño: municipio de Pupiales (IAvH [formerly IND-R] 1553); municipio de Túquerres, km 10 carretera Túquerres–Guachucal, hacienda Alsacia, 3140 m (ICN 9817); municipio de Cumbal, km 4 Cumbal–volcán Cumbal, 3260 m (ICN 9818–22). *R. stigmatoral*: ECUADOR: Azuay: Sevilla de Oro (USNM 229644 (paratype)); San Vicente, camino a las antenas (QCAZ 11414). Morona-Santiago: Pailas, a tambo on trail between Sevilla de Oro and Mendez, on E- or NE-facing slope (USNM 229647–48 (paratypes)); between tambos called Cerro Negro and Pailas on trail Sevilla de Oro and Mendez (USNM 229643 (paratype)); between Pailas and Mirador, on trail between Sevilla de Oro and Mendez (USNM 229645 (paratype)); San Juan Bosco, a posada on trail between Limon (General Plaza) and Gualeceo, slightly S of W of Limon (USNM 229649); El Cruzado, a posada on trail between Limon (General Plaza) and Gualeceo, slightly S of W of Limon (c. 0.5 h up trail from San Juan Bosco) (USNM 229650). No other data (AMNH 32778); San Jose (AMNH 38820). Cañar: Mazar, reserva Mazar (QCAZ 7374, 7884, 6657); Biblian, iglesia de Biblian (QCAZ 9946). *R. striata*: COLOMBIA: Boyacá: municipio de Villa de Leyva, sector rural vereda El Roble (IAvH 4895); Pesca (IAvH [formerly IND-R] 0665–66); municipio de Turmequé, vereda Joyagua (MUJ 816); Toquilla, Vadohondo, km 71 carretera Sogamoso–Pajarito (ICN 2800). Cundinamarca: Bogotá (CAS-SUR 8280, MCZ 14166–67, 16979–80, 16982–83, 17129, 110415–16, USNM 75969, 153974–82, 194744, ICN 2181); Bogotá, salón de clases de la Pontificia Universidad Javeriana (MUJ 229); Bogotá, instalaciones del laboratorio de fauna “Venado de Oro”, vivero Inderena (IAvH [formerly IND-R] 1100–01, 1499, 1602, 3006); Bogotá, laboratorio de fauna Unifem Inderena (IAvH

[formerly IND-R] 3130–31, 3934, 4163, 4262); Bogotá, ladera del cerro Guadalupe (IAvH [formerly IND-R] 3503, ICN 2436, 2535, 2537, 2541, 2543–44, 2546); mt. Guadalupe (FMNH 177075–81, 177243–47); Salto del Tequendama (IAvH [formerly IND-R] 3985); municipio de San Francisco, vereda Sabaneta (ICN 5991), cerro Cueva Grande, 2590 m (ICN 5737), finca La Quebrada, quebrada El Vino, 2540–2560 m (ICN 9759–65); páramo Cruz Verde, 3100 m (ICN 675–76); municipio de Fómique (ICN 2232); between Alban and Sasaima, 50 km NW Bogotá, D.C. (MVZ 191880); 6 km S Alban on road to Bogotá D.C. (MVZ 191878); represa del Hato, S of Usme, c. 2800 m (FMNH 165800–03, ICN 2371, 2373, 2375); municipio de Suesca, vereda el Hatillo, microcuenca Santa Helena, 2950 m (MUJ 644–48), 3 km al sur de la laguna Suesca, 2860 m (ICN 7276); no other data (UMMZ 56448, 56760 [11 specimens], 89417 [seven specimens], 123315, 203767–70, ICN 2362); PNN Chingaza, 3300 m (IAvH [formerly IND-R] 4241–42), sitio Montere-dondo, 3030 m (MUJ 906–09), sector de Chuza (IAvH [formerly IND-R] 3891–94), embalse cerca del casino (MUJ 228). Santander: SFF Guanentá, alto río Fonce, 2650 m (MUJ 910); municipio de Virolín, Cañaverales km 72 carretera a Charalá, río Cañaverales, 1830 m (ICN 9783). Not located: tanques de Vitelma (IAvH [formerly IND-R] 0649). *R. unicolor*: ECUADOR: Carchi: Montufar Atal-Vínculo, 2700 m (UMMZ 105895–97). Imbabura: lago de Cuicocha (MCZ 154515–16, 154628). Pichincha: Quito (MCZ 22154, 164616, 164662, 164665–68, 164670); Pasochoa Volcano Forest, 40 km SE Quito, 2800–2880 m (MCZ 175052–53); Machachi (QCAZ 758). Not located: Chillo (MCZ 21070). Not located (QCAZ 6122). *R. yumborum*: ECUADOR: Pichincha: Nanegal, Santa Lucía Cloud Forest Reserve, 1580–1591 m (QCAZ 10827 (holotype), 10822, 11077, 11079–81 (paratypes)).

Outgroup taxa

Bachia flavescens: GUYANA: Essequibo: Tukeit beach (ROM 20515). *Cercosaura argula*: PERU: Cuzco: La Convención, Bajo Puyantimari, 1176 m (a.s.l.) (CORBIDI 9795). Loreto: Datem, Sector 4, 210 m (CORBIDI 8754). Madre de Dios: Tambopata, Baltimore, 204 m (CORBIDI 5458). *Cercosaura ocellata*: GUYANA: District 8: Paramakatoi vicinity, 750 m (ROM 28352). PERU: Cuzco: La Convención, CC NN Poyentimari, 725 m (CORBIDI 8330). San Martin: Picota, Area de Conservación Municipal Chambira, 679 m (CORBIDI 6374). *Cercosaura schreibersii*: BRAZIL: Rio Grande do Sul: Santana do Livramento, Cerros Verdes (UFRGS 5114). Mato Grosso: Itiquira, fazenda Espigão (UFRGS 6205). *Echinosaura sulcatrostrum*: GUYANA: District 8: mount Wokomung, vicinity of camp 1 to camp 2, 698 m (ROM 43805). Northwest: Baramita, vicinity of camp, 100 m (ROM 22893 (holotype), 22892, 22894 (paratypes)). *Macropholidus huancabambae*: PERU: Piura: Huancabamba, Las Pozas, camino El Tambo–La Mina, 2732 m (CORBIDI 10492–93, 10501–02). *Macropholidus ruthveni*: PERU: Lambayeque: Lambayeque, El Totoral, quebrada Palacios, distrito de Salas, 837 m (CORBIDI 4281). *Neusticurus rudis*: GUYANA: District 7: Mount Ayanganna, NE plateau, 1490 m (ROM 39497–500). District 8: mount Wokomung, vicinity of camp 1, 698 m (ROM 42642); 1234 m (ROM 42643–44). Essequibo: Tukeit, banks of Tukei creek, 500 m from mouth, 100 m (ROM 42228, 20517). *Petracola waka*: PERU: Cajamarca: Cajamarca, cataratas de Llacanora, 2705 m (CORBIDI 8639). *Petracola ventrimaculata*: PERU: Cajamarca: Cajamarca, Tantauay, 3593 m (CORBIDI 3628, 3633); Michiquillay–Quinuayoc, 3817 m (CORBIDI 9247). *Potamites ecpleopus*: PERU: Cuzco: La Convención, Pongo de Mainique, 670 m (CORBIDI 5519); CC NN Poyentimari, 725 m (CORBIDI 8331); Shokoriari, 602 m (CORBIDI 9753). Loreto: Datem, sector 4, 210 m (CORBIDI 8690); Loreto, Andoas, 187 m (CORBIDI 4746). San Martin: Picota, Chambirillo, puesto de control 16,

Parque Nacional Cordillera Azul (CORBIDI 8834). *Potamites juruazensis*: PERU: Cuzco: La Convención, Pagoreni Norte, Malvinas, 428 m (CORBIDI 10004). *Potamites strangulatus*: PERU: San Martín: Picota, puesto de control 16 Chambirillo, Cordillera Azul, 1122 m (CORBIDI 9209); Tarapoto, carretera Tarapoto–Yurimaguas, cerro Escalera, 771 m (CORBIDI 6368). *Proctoporus bolivianus*: PERU: Ayacucho: Yucay, 3126 m (CORBIDI 10757–58). *Proctoporus chasqui*: PERU: Ayacucho: Chiquintirka, 2635 m (CORBIDI 8413, 8420). *Proctoporus pachyurus*: PERU: Junín: Tarma, distrito de Palca, anexo Huandunga, 2429 m (CORBIDI 11808–09). *Ptychoglossus brevifrontalis*: BRAZIL: Acre: Serra do Divisor (MTR 28305, 28462).

Appendix 3

Hemipenes examined

Ingroup species are listed following the new taxonomy proposed below. See Materials and Methods for institutional abbreviations. See Appendix 2 for locality data, if not included below.

Ingroup taxa

Andinosaura crypta: KU 135104 (paratype). *Riama orcesi*: ECUADOR: Napo: 3.3 km ESE Cuyujua, 2350 m (KU 142919 (paratype)). *Riama balnearior*: DHMECN 4111. *Riama simotera*: ICN 9836. *Riama cashcaensis*: ECUADOR: Chimborazo: 35.0 km SW Cajabamba on road to Pallatanga, 2860 m (KU 217206). *Riama striata*: KU 217206.

Outgroup taxa

Bachia flavescens: AMNH 140925.

Appendix 4

A monophyletic taxonomy

The following classification reflects our TE phylogeny (Fig. 1). Given that *Riama* is polyphyletic, we redefine it, describe a new genus, and resurrect *Oreosaurus*. A paucity of samples precluded the inclusion of five species in our analysis: *R. inanis*, *R. luctuosa*, *R. petrurum*, *R. rhodogaster* and *R. stellae*. Regardless, our assessment includes the examination of all species currently allocated to *Riama* (Appendix 2). Therefore, following the arguments of Grant et al. (2006: 149), we tentatively refer them to a genus. In addition, the recently resurrected *Pantodactylus* (Goicoechea et al., 2016) nests within *Cercosaura*. Therefore, we return it to the synonymy of *Cercosaura*.

Subfamily: Cercosaurinae Gray, 1838 (tribe Cercosaurini of Goicoechea et al., 2016) **sensu n.**

Content: *Anadia* Gray, 1845; *Andinosaura* **gen.n.**; *Cercosaura* Wagner, 1830; *Echinosaura* Boulenger, 1890; *Euspondylus* Tschudi, 1845; *Gelanesaurus* Torres-Carvajal et al., 2016; *Macropholidus* Noble, 1921; *Neusticurus* Duméril and Bibron, 1839; *Oreosaurus* Peters, 1862; *Petracola* Doan and Castoe, 2005; *Pholidobolus* Peters, 1862; *Placosoma* Tschudi, 1847; *Potamites* Doan and Castoe, 2005; *Proctoporus* Tschudi, 1845; *Riama* Gray, 1858.

Comments: The analysis of Torres-Carvajal et al. (2016) recovered both *Echinosaura* and *Proctoporus* as nonmonophyletic genera. Their

analysis also identified three unnamed clades composed of undescribed species from Peru and southern Ecuador. To maintain supraspecific rank equivalency within Cercosaurinae, these three clades await formal nomenclatural recognition as genera (Torres-Carvajal et al., 2016).

Genus: *Riama* Gray, 1858.

Type species: *Riama unicolor* Gray, 1858, by original designation.

Content (16 species): *Riama anatoloros* (Kizirian, 1996); *R. balnearior* (Kizirian, 1996); *R. cashcaensis* (Kizirian and Coloma, 1991); *R. cephalolineata* (García-Pérez and Yustiz, 1995) **comb.n.** (see below); *R. colomaromani* (Kizirian, 1996); *R. columbiana* (Andersson, 1914); *R. inanis* (Doan and Schargel, 2003); *R. labionis* (Kizirian, 1996); *R. meleagris* (Boulenger, 1885); *R. orcesi* (Kizirian, 1995); *R. raneyi* (Kizirian, 1996); *R. simotera* (O'Shaughnessy, 1879); *R. stigmatoral* (Kizirian, 1996); *R. striata* (Peters, 1862); *R. unicolor* Gray, 1858; *R. yumborum* Aguirre-Peñafiel et al., 2014.

Characterization and diagnosis: All unambiguously optimized synapomorphies for this clade are from DNA sequences. Phenotypic synapomorphies are not known. Other characteristics include: (1) head scales smooth; (2) frontoparietal and parietal scales paired; (3) interparietal, frontal and frontonasal scales single; (4) prefrontal scales usually absent (occasionally present in specimens of *R. "Cordillera Occidental"*; present in *R. cephalolineata*, but see comments below); (5) lower eyelid divided into several scales; (6) loreal scale absent or present; (7) scale organs on labials present; (8) anteriormost supraocular and anteriormost superciliary scales unfused (fused in some specimens of *R. "Cordillera Central"*); (9) dorsal surface of the tongue covered in scale-like papillae; (10) nuchal scales smooth in most species (rugose in *R. striata*, and undescribed *R. "Cordillera Central"* and *R. "Cordillera Occidental"*); (11) dorsal body scales rectangular; keeled (low, rounded keel) or striated (shallow or deep furrows), smooth in some specimens of *R. simotera* and *R. meleagris*; (12) ventral body scales smooth (rugose in *R. "Cordillera Occidental"*); (13) limbs pentadactyl; digits clawed; (14) femoral pores in males present, in females absent or present; (15) hemipenial lobes usually narrow, indistinct from hemipenial body (large, distinct from hemipenial body in *R. balnearior*).

Riama differs from *Andinosaura* by (usually) having hemipenial lobes narrow, indistinct from hemipenial body. It differs from *Oreosaurus* by having a narrow band of differentiated granular lateral scales.

Distribution: northern Andes of South America (Colombia, Ecuador, and Venezuela) above 1500 m a.s.l. *Riama* is an exclusively Andean radiation.

Comments: Currently, *Riama* contains 16 described species. The descriptions of four additional species from Colombia (including *R. "Cordillera Occidental"*, *R. "Nariño"* and *R. "Cordillera Central"* from the present analysis) are currently in manuscript form (S.J. Sánchez-Pacheco and D.A. Kizirian, in preparation).

The generic placement of *Proctoporus cephalolineatus* from the Venezuelan Mérida Andes has been uncertain. In the original description, García-Pérez and Yustiz (1995) suggested that it was closely related to *P. achlyens* and *P. shrevei* (both of which were in *Riama*, but now in *Oreosaurus*, see below). However, Doan and Schargel (2003: 73) argued against its assignment to *Proctoporus* s.l. due to the apparent presence of prefrontal scales in the holotype (the only known specimen of this species), while asserting "it most likely belongs to *Euspondylus* or *Pholidobolus*". Consequently, relevant phylogenetic studies and generic classifications (e.g. Doan and Castoe, 2005; Goicoechea et al., 2012) overlooked it. Without comment, Goicoechea et al. (2016) included this species in *Proctoporus* s.s. Doan and Schargel (2003) described *Proctoporus inanis* (prefrontals absent) from the Venezuelan Mérida Andes, and Doan and Castoe (2005) transferred it to *Riama*. However, Rivas et al. (2012) noted its resemblance to *Proctoporus cephalolineatus*, and suggested synonymy. The geographically proximate type localities and similar

levels of individual variation in presence or absence of prefrontals in other cercosaurines (e.g. *Macropholidus huancabambae*, Reeder, 1996; *Proctoporus spinalis*, Köhler and Lehr, 2004; *Proctoporus sucullucu* Doan and Castoe, 2003; *Andinosaura stellae* **comb.n.**, Sánchez-Pacheco, 2010a; and *Riama* “Cordillera Occidental”, herein) are consistent with the hypothesis of conspecificity. However, we retain *R. inanis* as a valid species pending a review. The Andean distribution and resemblance to other species predicts that *R. cephalolineata* **comb.n.** and *R. inanis* belong to *Riama*; this assignment awaits confirmation.

Genus: *Andinosaura* **gen.n.**⁵.

Type species: *Riama crypta* Sánchez-Pacheco et al., 2011.

Content (11 species): *Andinosaura afrania* (Arredondo and Sánchez-Pacheco, 2010) **comb.n.**; *A. aurea* (Sánchez-Pacheco et al., 2012) **comb.n.**; *A. crypta* (Sánchez-Pacheco et al., 2011) **comb.n.**; *A. hyposticta* (Boulenger, 1902) **comb.n.**; *A. kiziriani* (Sánchez-Pacheco et al., 2012) **comb.n.**; *A. laevis* (Boulenger, 1908) **comb.n.**; *A. oculata* (O’Shaughnessy, 1879) **comb.n.**; *A. petrorum* (Kizirian, 1996) **comb.n.**; *A. stellae* (Sánchez-Pacheco, 2010a) **comb.n.**; *A. vespertina* (Kizirian, 1996) **comb.n.**; *A. vieta* (Kizirian, 1996) **comb.n.**

Characterization and diagnosis: All unambiguously optimized synapomorphies for this clade are from DNA sequences. Phenotypic synapomorphies are not known. Other characteristics include: (1) head scales usually smooth (slightly rugose in *A. vieta* and *A. stellae*); (2) frontoparietal and parietal scales paired; (3) interparietal, frontal and frontonasal scales single; (4) prefrontal scales usually absent (occasionally present in specimens of *A. stellae*); (5) lower eyelid divided into several scales; (6) loreal scale absent or present; (7) scale organs on labials present; (8) anteriormost supraocular and anteriormost superciliary scales unfused; (9) dorsal surface of the tongue covered in scale-like papillae; (10) nuchal scales smooth in most species (rugose in *A. stellae* and *A. vieta*); (11) dorsal body scales rectangular; smooth, keeled (low, rounded keel), striated (shallow furrows) or rugose; (12) ventral body scales smooth (rugose in *A. stellae* and *A. vieta*); (13) limbs pentadactyl; digits clawed; (14) femoral pores in males present, in females absent or present; and (15) hemipenial lobes large, distinct from hemipenial body.

Andinosaura differs from *Riama* by having hemipenial lobes large, distinct from hemipenial body. It differs from *Oreosaurus* by having a narrow band of differentiated granular lateral scales.

Distribution: northern Andes of South America (Colombia and Ecuador) above 1100 m a.s.l. *Andinosaura* is an exclusively Andean radiation.

Etymology: *Andinosaura* (gender feminine), formed from the Spanish *Andino* (from the Andes) and the Latin *Sauria* (lizard), in reference to its distribution. The suffix is used commonly for gymnophthalmid genera.

Comment: *Andinosaura* contains nearly half of the species previously referred to the large, polyphyletic genus *Riama* s.l. We include *A. stellae* in this genus on the basis of its distinctive rugose scales covering almost the entire body, a condition also found in *A. vieta*. Although *A. petrorum* occurs sympatrically with *Riama anatóloros* and *R. stigmator* in southern Ecuador, we include this species in *Andinosaura* instead of *Riama* because Doan (2003a) found it to be the sister species of *A. vespertina*, and Sánchez-Pacheco et al. (2012) suggested that it might be closely related to *A. vespertina*, *A. aurea* and *A. kiziriani*.

Genus: *Oreosaurus* Peters, 1862

Type species: *Ecleopos* (*Oreosaurus*) *luctuosus* Peters, 1862; by subsequent designation by Burt and Burt (1931).

Content (five species): *Oreosaurus achlyens* (Uzzell, 1958) **comb.n.**; *O. luctuosus* (Peters, 1862) **comb.n.**; *O. mediarmidi* (Kok and Rivas,

2011) **comb.n.**; *O. rhodogaster* (Rivas et al., 2005) **comb.n.**; *O. shrevei* (Parker, 1935) **comb.n.**

Characterization and diagnosis: All unambiguously optimized synapomorphies for this clade are from DNA sequences. Phenotypic synapomorphies are not known. Other characteristics include: (1) head scales smooth; (2) frontoparietal and parietal scales paired; (3) interparietal, frontal and frontonasal scales single; (4) prefrontal scales usually absent (present in *O. mediarmidi*); (5) lower eyelid divided into several scales; (6) loreal scale usually present (absent in *O. “Venezuela”* and *O. shrevei*); (7) scale organs on labials present; (8) anteriormost supraocular and anteriormost superciliary scales unfused; (9) dorsal surface of the tongue covered in scale-like papillae; (10) nuchal scales keeled or smooth; (11) dorsal body scales hexagonal (or sub-hexagonal) or rectangular; smooth or keeled (prominent keel); (12) ventral body scales smooth; (13) limbs pentadactyl; digits clawed; (14) femoral pores in both sexes present; (15) hemipenial lobes large, distinct from hemipenial body (narrow, indistinct from hemipenial body in *O. “Sierra Nevada”*).

Oreosaurus differs from *Riama* and *Andinosaura* by lacking a narrow band of differentiated granular lateral scales (oval, nongranular scales instead).

Distribution: Sierra Nevada de Santa Marta in northern Colombia, coastal mountain ranges (Cordillera de la Costa, CC), massif of Turimiquire and montane areas of the Península de Paría (Cordillera Oriental—part of the CC) in northern Venezuela, Aripo Northern Range in the Caribbean island of Trinidad, and tepuis from the Chimantá Massif in southeastern Venezuela. Elevation: 650–2242 m a.s.l.

Comments: Peters (1862) erected *Oreosaurus* as a subgenus of *Ecleopos* for his new species *E. (O.) striatus* and *E. (O.) luctuosus* (in sequence). Boulenger (1885) elevated *Oreosaurus* to genus rank. Andersson (1914) synonymized it with *Proctoporus*, and Doan and Castoe (2005) implicitly placed it in the synonymy of *Riama*. Peters (1862) did not designate a type species. Although *O. striatus* was first described, Burt and Burt (1931), without comment (but still a valid action), designated *O. luctuosus* as the type species (Uzzell, 1958: 2; *contra* Peters and Donoso-Barros, 1970 and Kizirian, 1996: 86). A dearth of available material precluded our inclusion of the type species. However, following the arguments of Grant et al. (2006: 299) and Frost et al. (2008: 387), we apply the name *Oreosaurus* to this clade based on the presumed close relationship of *O. luctuosus* to *O. achlyens* and *O. shrevei* (Uzzell, 1958; Doan and Schargel, 2003). *Oreosaurus achlyens* and *O. luctuosus* occur in sympatry at Rancho Grande on the coastal range of Venezuela. In the unlikely event that *O. luctuosus* is not part of this clade, there are no other available generic names (but see below).

We refer *O. rhodogaster* to this genus based on the assertion of Rivas et al. (2005) that *O. shrevei* and *O. rhodogaster* are likely sister species. As such, *Oreosaurus* has five nominal species only, although *O. “Sierra Nevada”* and *O. “Venezuela”* are being described (Sánchez-Pacheco et al. and Rivas et al., unpublished).

Anadia is a large, broadly distributed and morphologically heterogeneous genus (Oftedal, 1974). Despite the inclusion of the tepuian *A. mediarmidi* (herein referred to *Oreosaurus*) and two Andean species from Ecuador, *A. petersi* and *A. rhombifera* (Torres-Carvajal et al., 2016; this study), the relationships of most species of *Anadia* remain enigmatic (Myers et al., 2009; Kok and Rivas, 2011). Our phylogenetic analysis corroborates the nonmonophyly of *Anadia* (Torres-Carvajal et al., 2016), and unexpectedly nests *A. mediarmidi* within *Oreosaurus* (Fig. 1).

It could be construed as more prudent to refrain from resurrecting *Oreosaurus* until additional species of *Anadia* and *Euspondylus* (including generic type species; see below), especially from northern South America (see Kok and Rivas, 2011 and Torres-Carvajal et al., 2016), are included in phylogenetic analyses. However, this solution renders both *Anadia* and *Riama*

⁵This nomenclatural act has been registered in Zoobank: urn:lsid:zoobank.org:act:F228513F-0DDB-4F3F-A771-68A0B5CD902E.

polyphyletic because it overlooks existing evidence of the relationships of these genera (Torres-Carvajal et al., 2016; this study). This solution also ignores empirical knowledge on the allocations of the type species of *Oreosaurus* (*O. luctuosus*; see above) and *Anadia* (*A. ocellata*). Oftedal (1974), based on morphological similarity, considered *A. ocellata* to be closely related to *A. vittata*, *A. rhombifera* and *A. petersi* (i.e. the *A. ocellata* group). Instead, we prefer to propose a taxonomic change as both a better representation of current knowledge of cercosaurine phylogeny and an invitation for refutation (for similar arguments see Grant et al., 2006 and Frost et al., 2008). Thus, we resurrect the available

name *Oreosaurus* from the synonymy of *Riama* to accommodate the species forming this clade plus putatively closely related taxa. The recognition of *Oreosaurus* secures a monophyletic *Riama* and remedies the polyphyly of *Anadia* (Torres-Carvajal et al., 2016; this study). That said, the future discovery that *Anadia marmorata* (type species of *Argalia* Gray, 1846) is imbedded within this clade would render *Oreosaurus* a junior subjective synonymy of *Argalia*. Because *A. marmorata*, *O. achlyens* and *O. luctuosus* occur in sympatry, and given the number of species currently referred to *Anadia* and their morphological diversity, this genus will likely experience additional partitioning.